FINAL REPORT

LOAD DISTRIBUTION ON HIGHWAY BRIDGES BASED ON FIELD TEST DATA

Principal Investigator:
M. Arockiasamy

Research Associate:
Ahmed Amer

Submitted to:
Florida Department of Transportation

Under:
HPR Study No. 0668, WPI 0510668
State Job No. 99500-3512-119, Contract No. B-8431

Monitored by:
Structural Research Center
Florida Department of Transportation
2007 East Dirac Drive
Tallahassee, Florida 32304

Center for Infrastructure and Constructed Facilities
Department of Ocean Engineering
Florida Atlantic University
Boca Raton, Florida 33431

April 1995

TECHNICAL REPORT STANDARD TITLE PAGE

1. Report No.	2. Government Accession No.	3. Receipient's Calalog No.
FL/DOT/RMC/668-8431		

4. Title and Subtitle	5. Report Date
Load Distribution on Highway Bridges Based on Field Test Data	April 1995
	6. Performing Organization Code

7. Authors	8.Performing Organization Report No.
M. Arockiasamy and Ahmed Amer	

9. Performing Organization Name and Address	10. Work Unit No.
Florida Atlantic University Center for Infrastructure and Constructed Facilities Department of Ocean Engineering Boca Raton, Florida 33431	11. Contract or Grant No. WPI 0510668

12. Sponsoring Agency Name and Address	13. Type of Report and Period Covered
Florida Department of Transportation 605 Suwannee Street Tallahassee, Florida 32399-0466	Final Report
	14. Sponsoring Agency Code 99500-3512-119, B-8431

15. Supplementary Notes
Prepared in cooperation with the Federal Highway Administration

16. Abstract

The study presents the load distribution on the more commonly used bridge types in Florida viz., slab-on-girder, solid slab, voided slab and double Tee bridges. The existing analytical and field load distribution methods for different bridge types are reviewed in this study. Grillage analogy is used as an analytical tool to study the various parameters affecting wheel load distribution.

Both analytical and field studies on the wheel load distribution of solid and voided slab, slab-on-AASHTO girders, slab-on-bulb-Tee and double-Tee bridges are presented. In addition to the analytical study, data from field tests performed by Structures Research Center, FDOT, are compared with those based on the grillage analogy, AASHTO and LRFD codes. Several parameters such as span length, bridge width, slab thickness, girder type, edge beam, number of lanes, etc. are considered in the parametric studies.

Simplified formulae for the effective width of solid slab bridges and shear load distribution of slab-on-AASHTO girder bridges are proposed in this study. In general, the bridge rating based on wheel load distribution factors calculated from measured strains seems to give satisfactory results except for bridges with preexisting cracks.

17. Key Words	18. Distribution Statement
wheel load distribution; slab-on-girder; solid slab; voided slab; double Tee bridge; grillage analogy; slab-on-bulb-Tee; field test; LRFD codes; effective width; bridge rating	No restrictions. This document is available to the public through the National Technical Information Service, Springfield, Virginia 22161

19. Security Classif. (of this report)	20. Security Classif. (of this page)	21. No. of Pages	22. Price
Unclassified	Unclassified	182	

Form DOT F 1700.7 (8-89)

UNIT CONVERSION TABLE

To convert from	To	Multiply by
inch	centimeter (cm)	2.54
square inch	square centimeter	6.4516
kip	kiloNewton (kN)	4.44747
kip/sq. in. (ksi)	kN/sq. m (kPa)	6,894.28
kip-foot	kN-meter	1.3556

DISCLAIMER

The opinions, findings and conclusions expressed in this publication are those of the authors who are responsible for the facts and accuracy of the data presented herein. The contents do not necessarily reflect the views or policies of the Florida Department of Transportation or the Federal Highway Administration. This report does not constitute a standard, specification or regulation.

The report is prepared in cooperation with the Florida Department of Transportation and the Federal Highway Administration.

ACKNOWLEDGMENTS

The authors wish to express their sincere thanks to Dr. Mohsen A. Shahawy, Chief Structures Analyst, Dr. Moussa Issa, Structural Analyst and Mr. Adnan El Saad, Research Engineer of Florida Department of Transportation for their excellent suggestions, discussions and constructive criticisms throughout the project. They wish to express their appreciation to Dr. S. E. Dunn, Professor and Chairman, Department of Ocean Engineering, and Dr. C. S. Hartley, Dean, College of Engineering, Florida Atlantic University for their continued interest and encouragement.

The valuable assistance in the preparation of the final report from Mr. Vikas Sinha, Mr. Ming Zhuang, Mr. Sowrirajan Raghavachary and Mr. Sattanathan Ponnuswamy, Graduate Students, Florida Atlantic University, is gratefully acknowledged.

SUMMARY

The study presents the wheel load distribution on the more commonly used bridge types in Florida viz., slab-on-girder, solid slab, voided slab and double Tee bridges. The existing analytical and field load distribution methods for different bridge types are reviewed in this study. Grillage analogy is used as an analytical tool to study the various parameters affecting wheel load distribution.

Both analytical and field studies on the wheel load distribution of solid and voided slab, slab-on-AASHTO girders, slab-on-bulb-Tee and double-Tee bridges are presented. In addition to the analytical study, data from field tests performed by Structures Research Center, FDOT, are compared with those based on grillage analogy, AASHTO and LRFD codes. Several parameters such as span length, bridge width, slab thickness, girder type, edge beam, number of lanes, etc. are considered in the parametric studies.

Simplified formulae for the effective width of solid slab bridges and shear load distribution of slab-on-AASHTO girder bridges are proposed in this study. In general, the bridge rating based on wheel load distribution factors calculated from measured strains seems to give satisfactory results except for bridges with preexisting cracks.

TABLE OF CONTENTS

LIST OF FIGURES

LIST OF TABLES

CHAPTER 1

INTRODUCTION

1.1 INTRODUCTION

Analysis of the response of highway bridges to vehicular live loads is the key element in designing new bridges and evaluating existing bridges for their load-carrying capacities. The American Association of State Highways and Transportation Officials (AASHTO) method of load distribution reduces the complex analysis of a bridge subjected to one or more vehicles to simple analysis of a beam. According to AASHTO method, the maximum load effects in a girder can be obtained by treating a girder as a one dimensional beam subject to a loading, which is obtained by multiplying one line of wheels of the design vehicle by a load fraction (Wheel-Load Distribution Factor). This concept was first introduced by Newmark (1948).

Distribution factors (DFs) are nondimensional measures of load distribution in a bridge. At a given point of a transverse section the distribution factor for a certain response is equal to the ratio of the response at that point to the average response at the cross section containing the point. The AASHTO load distribution factor is defined as S/D, where D, is a constant and has the units of length and S is the girder spacing. The constant D is given by the AASHTO specifications for different bridge types. The AASHTO values for D for this extremely simplified method are based upon research

reported by Newmark (1948). The simplicity of the method, however, does take its toll in accuracy as explained in Chapter 2.

Recent research has produced a substantial amount of information on various bridge types indicating a need for revisions of the current AASHTO bridge specifications. These conservative load distribution factors may be acceptable for the design of new bridges, but are unacceptable for reviewing existing bridges. The conservative load distribution factors that are used to evaluate an old bridge, may give the impression that the bridge is unsafe, while the bridge is safe, if more accurate distribution factors are used.

Within a time span of approximately 30 years, from roughly 1960 to 1990, the science of bridge analysis and design has undergone major changes. Following the advent of the digital computers, the bridge engineers have available today a number of powerful analytical tools in so-called refined methods of analysis, including the following:

1. The grillage analogy method
2. The orthotropic plate method
3. The articulated plate method
4. The finite element method, including finite strip formulation

The results from the above refined methods of analysis should be used to improve the existing simplified approaches. These approaches would aid the designer to compute the distribution factors more efficiently without the need for performing complicated analysis in the design office.

NCHRP project 12-26 (1992) was initiated in the mid-1980s in order to develop comprehensive specification provisions for distribution of wheel loads in highway bridges. The study was performed in two phases: Distribution of wheel loads on beam-and-slab and box girder bridges was considered in Phase I, whereas slab, multi-box beam, and spread box bridges were analyzed in Phase II. Three levels of analysis were considered for each bridge type. The level 3, involves detailed finite element modeling of the bridge deck. Level 2 includes either graphical methods, nomograph and influence surfaces, or simplified computer programs. Level 1 methods provide simple formulae to predict distribution factors. The major part of the NCHRP research project was devoted to the level 1 analysis methods because of its ease of application, established use, and good correlation with the higher levels of analysis in their application to a majority of bridges.

In the NCHRP project, the formulae presented in the current AASHTO specifications were evaluated and alternate formulae developed, that offer improved accuracy and wider range of applicability. These formulae were developed for interior and exterior girder moment and shear load distribution for single or multiple lane loading. The formulae developed in the NCHRP research project form the basis for the proposed LRFD bridge design specifications and commentary.

Interest in field load testing of highway bridges has increased significantly in recent years. The increased interest has resulted in part from large number of older bridges across the country with posted load limits that are below the normal legal truck weights. Field load testing frequently offers a means of illustrating that the safe load capacity of a bridge, or bridge rating, is greater than the capacity determined from standard rating calculations based on the AASHTO method. One method for use of

test results in rating calculations is to calculate wheel-load distribution factors for the girders based on test data. These measured wheel-load distribution factors can be used in bridge-rating calculations in place of those factors defined by AASHTO code.

1.2 METHODOLOGY AND APPROACH

A grillage analysis using plane grid model can be used with minimal computer resources to calculate the response of bridges such as solid slab, voided slab and slab-on-girder bridges. As part of the NCHRP project 12-26 (1992), various modeling techniques were evaluated and it was found that a plane grid model may be used to accurately predict wheel-load distribution factors and the results will be close to those of detailed finite element analysis. Grillage analogy method will be used in this study as the main analytical tool in the case of girder and slab bridges. A major advantage of plane grid analysis is that shear and moment values for girders are directly obtained in contradistinction to moments per unit width in the case of finite element analysis. Also, as the needed computer resources are minimal, it is possible to conduct wide range of parametric studies using the grillage analogy.

Important parameters such as beam spacing, span length, slab thickness, etc., will be identified for every bridge type from the bridge data base available with Florida Department of Transportation. The average properties obtained from the data base will be used in the parametric studies of the beam-and-slab, slab and voided slab bridge types. The data from field tests will be collected and classified to evaluate the current AASHTO specifications, the proposed LRFD specifications and the results from the grillage analogy method.

1.3 OBJECTIVES AND SCOPE

The present study is focused on the more commonly used bridge types in Florida such as slab-on-girder, solid slab, voided slab and double Tee bridges. The objectives of the study are the following:

i) To determine the distribution factors and identify the load distribution main parameters by using grillage analogy method. The different bridge types would consist of solid slab, voided slab, slab-on-AASHTO girders, slab-on-Bulb Tee girders and double Tee beams.

ii) To compare the current AASHTO and the proposed LRFD distribution factors with those based on FDOT field tests, and the grillage analogy method.

iii) To derive simple design formulae for distribution factors, if needed, that would provide a more accurate and realistic alternative to the current design codes.

Chapter 2 reviews the different analytical and field load distribution methods for different bridge types. **Chapter 3** discusses the grillage analogy concepts, the cross sectional properties of different bridge types for grillage analogy idealization, field test procedures and methodologies.

Chapter 4 presents the analytical studies and field test analysis for solid slab and voided slab bridges. **Chapter 5** summarizes the results of the grillage analogy method and field test studies of slab-on-AASHTO girder and slab-on-Bulb Tee girder bridges. **Chapter 6** presents the analysis of double Tee beam bridges and a comparison with the field test results. The summary and conclusions are presented in **Chapter 7**.

CHAPTER 2

LITERATURE REVIEW

2.1 INTRODUCTION

A thorough understanding of wheel load distribution is required to develop a realistic design and rating of the highway bridges. The design specifications of AASHTO are generally simple to use and their wheel-load distribution factors have been shown to be conservative. National Cooperative Highway Research Program (NCHRP) project 12-26 (1992) was initiated in the mid-1980s in order to develop comprehensive specification provisions for distribution of wheel loads in highway bridges. This chapter summarizes the main concepts of the current AASHTO specifications and the proposed LRFD code which is based on NCHRP project.

There is a growing interest in field testing of highway bridges. Load testing is an attractive means for evaluating the strength of the bridges under study, because it can provide a more realistic appraisal of bridge behavior. Load distribution factor based on the field tests will be more practical than those based on analytical studies. This chapter also summarizes the experimental investigations on the distribution factors.

2.2 REVIEW OF AASHTO METHOD

The American Association of State Highways and Transportation Officials (AASHTO) specifications permit a simplified method for obtaining longitudinal moments and shears due to live loads. According to this method, a longitudinal girder, or a strip of unit width in the case of slabs, is isolated from the rest of the structure and treated as one dimensional beam. The beam is subjected to loads comprising one line of wheels of the design vehicle multiplied by a load fraction S/D. S is the girder spacing in the case of slab-on-girder bridges; and D, which has the units of length, is specified to have certain values according to the bridge type. Values of D for various bridges, as given in the AASHTO specifications are reproduced in Table 2.1 (1989).

Table 2.1 Distribution of wheel loads based on AASHTO code

Floor type	One lane	Two or more lanes
Concrete: On prestressed concrete girder	S/7.0 If S exceeds 10 ft., use note f.	S/5.5 If S exceeds 14 ft., use note f
Concrete: On concrete T-beams	S/6.5 If S exceeds 6 ft., use note f.	S/6.0 If S exceeds 10 ft., use note f
Concrete box girders	S/8.0 If S exceeds 12 ft., use note f	S/7.0 If S exceeds 16 ft., use note f

f. In this case the load on each stringer shall be the reaction of the wheel loads, assuming the flooring between the stringers to act as a simple beam.

This AASHTO load distribution concept was first introduced by Newmark (1948). AASHTO wheel-load distribution factors (S/D) were developed by idealizing the bridge as an orthotropic plate in which the longitudinal moment intensity has a continuous distribution in the transverse direction

(Sanders and Ellby 1970). Also, AASHTO distribution factors were developed for non-skewed and simply-supported bridges. After extensive analyses (Newmark 1948 and Sanders and Ellby 1970), it was confirmed that the value of D for a given type of bridge varies within such a narrow margin that a single value can be used for design purposes. This simplicity could be achieved due to the following basic assumptions:

i) The transverse pattern of distribution of a load effect is independent of the longitudinal position of loads.

ii) The transverse distribution patterns of various load effects are similar (moment or shear).

iii) The bridge conforms to a basic form and it does not possess any complicating features such as edge stiffening, skew angle, continuity, etc.

These assumptions were criticized by Bakht and Moses (1988). They mentioned that while the value of distribution factor (DF) for a given response due to a single point load may vary significantly along the span, its value due to several loads varies between much narrower limits and concluded that the first assumption may be realistic. Using rigorous analyses, it can be readily demonstrated that the transverse distribution of responses become more localized, as the number of deflection derivatives to which the response is related increases. For example, the distribution factors for deflection under a concentrated load in a bridge are smaller than those for longitudinal moments, which, in turn, are smaller than those for longitudinal shear. Thus, the second assumption appears to be unrealistic.

Another major shortcoming of the current AASHTO specifications, Zokaie et al (1991), is that the piecemeal changes that have taken place over the last 50 years have led to inconsistencies in the distribution criteria. These include inconsistencies in the following:

i) Consideration of reduction in load intensity for multiple lane loading,

ii) Changes in distribution factors to reflect the changes in the design lane width,

iii) Verification of accuracy of wheel-load distribution factors for various bridge types.

Recent research has produced a substantial amount of information on various bridge types indicating a need for revisions of the current conservative AASHTO bridge specifications. These conservative distribution factors may be acceptable for the design of new bridges, but are unacceptable for reviewing existing bridges. The conservative distribution factors that are used to evaluate an old bridge may give the impression that the bridge is unsafe, while the bridge is safe, if more accurate distribution factors are used.

2.3 REVIEW OF NCHRP PROJECT (PROPOSED LRFD CODE)

National Cooperative Highway Research Program (NCHRP) project 12-26 (1992) was initiated in the mid-1980s in order to develop comprehensive specification provisions for distribution of wheel loads in highway bridges. The study was performed in two phases: Beam-and-slab and box girder bridges were analyzed in Phase I, whereas slab, multi-box beam, and spread box bridges considered in Phase II. Three levels of analysis were considered for each bridge type. The level 3 involves detailed finite element modeling of the bridge deck. Level 2 includes either graphical methods, nomograph and influence surfaces, or simplified computer programs. Level 1 provides simple formulae to predict distribution factors.

Level 3 involves detailed bridge deck analysis. Several finite element computer programs were found useful for different bridge types. For analysis of beam-and slab bridges, the GENDEK-5

computer program is very accurate and can be used to analyze straight and skew bridges. For the analysis of slab bridges, The MUPDI program was found to be the most accurate and practical method for nonskewed prismatic bridges. It is recommended that this level of analysis should be used for highly irregular bridges or truck load configuration.

Level 2 involves use of nomograph, designed charts, and plane grid analysis. The plane grid analysis (grillage analogy) was the most useful method due to its flexibility to analyze different truck types. It was concluded, if the grillage analogy model is generated with care, and the loads are placed in their correct locations, the results will be close to those of detailed finite element analysis. Level 1 analysis involves the use of simplified formulae for calculation of wheel load distribution factors. This method has some limitations, but is very simple and effective.

The major part of the NCHRP research project was devoted to the level 1 analysis methods, because of its ease of application, established use, and good correlation with the higher levels of analyses in their application to a majority of bridges.

A limited parametric study conducted as part of this research showed that variations in the truck axle configuration or truck weight do not significantly affect the wheel-load distribution factors. The variations of wheel load distribution factors with different axle configurations were below 1% in most cases.

In the NCHRP project, the formulae presented in the current AASHTO specifications were evaluated and alternate formulae developed, that offer improved accuracy and wider range of applicability. These formulae were developed for interior and exterior girder moment and shear load

distribution for single or multiple lane loading. The formulae developed in NCHRP research project form the basis for the proposed LRFD new specifications.

2.4 REVIEW OF OTHER ANALYTICAL STUDIES

Advanced computer technology has become available in recent years, which allows detailed finite element analysis of bridge decks. However, many computer programs exist, which employ different formulations and techniques. It is important that the computer methodology and formulation that produce the most accurate results, should be used to calculate the load distribution factors.

Hays et al (1986) idealized the bridge superstructure using plate elements and plane or space frame members with the centroid of the girders coinciding with the centroid of the concrete slab. Based on this idealization, a computer program SALOD was developed to compute flexural load distribution factors for a variety of girder-slab bridges under specific vehicular loading. A series of field tests was conducted to validate the modeling techniques used in developing SALOD program. In general, it was confirmed that the SALOD program is a useful tool for predicting the moment in bridges for purposes of analysis and design.

Imbsen and Nutt (1978) imposed rigid links between the idealized concrete slab, which was modeled as plate elements, and steel beams, which were modeled as space frame members, to accommodate the eccentricity of the beams. However, Bishara (1984) modeled the bridge superstructure using plate elements, the girder flanges by space frame members, and the girder web using plate elements.

Tarhini et al (1992) modeled a typical steel I-girder bridge using ICES STRUDL II three dimensional finite element analysis to develop realistic wheel load distribution factors. The concrete slab was modeled using an isotropic, eight-node brick element, with three degrees of freedom at each node. The girder flanges and the web were modeled using three-dimensional, quadrilateral, four-node plate element with five degrees of freedom at each node. Three linear springs were inserted at the interface nodes and spring stiffnesses were selected to permit the concrete slab to move relative to the girders and simulate the noncomposite action. Based on a study of various parameters affecting the wheel load distribution, a formula was developed to predict the wheel load distribution in steel I-girder bridges as a function of girder spacing and span length.

2.4 REVIEW OF STUDIES BASED ON THE FIELD TESTS

The interest in field load testing of highway bridges has increased significantly in the recent years. Tiedman et al (1993) tested a 0.4-scale bridge model in FHWA laboratory. The prototype bridge is continuous over two spans with each span equal to 140 ft. A single axle of an AASHTO HS-20 truck was simulated with a pair of concentrated loads. Reactions, moments, displacements, and rotations due to axle loading were analyzed and compared with those calculated using finite element method, AASHTO code and NCHRP method. The results of the study show that finite element analysis most accurately predicted the bridge behavior under the truck axle loading.

Stallings and Yoo (1993) performed a series of diagnostic tests on three short-span, two-lane, steel-girder bridges. Tests were performed with stationary and moving test trucks placed on bridges one at a time and side by side. Wheel load distribution factors were calculated from the stationary-

truck test. The calculated girder strains using AASHTO were consistently larger than measured values. This conservatism was attributed to the inaccuracies of the assumptions made in a simplified bridge analysis using AASHTO wheel-load distribution factors. Based on the results, the use of measured wheel-load distribution factors does not ensure more accurate values for distribution factors.

Warren and Malvar (1993) investigated the lateral distribution of wheel loads in a navy pier deck. An initial finite element-parametric study was carried out to determine more appropriate values for effective-widths. In-service pier tests were conducted to corroborate the numerical predictions. From those analyses and test results, a one-third scale laboratory model using an effective width of 10 ft. was designed, constructed, and tested. Analyses and test results confirmed that effective-width values for reinforced concrete slabs in the navy pier deck can often be doubled over current AASHTO allowable values. For the navy pier-deck designs where large truck-mounted cranes dominate load requirements, increasing the allowable slab thickness by a factor of two will result in higher load capacity, longer spans, and less construction materials.

CHAPTER 3

METHODS OF ANALYSIS FOR EVALUATING LOAD DISTRIBUTION

3.1 INTRODUCTION

This chapter presents the basic concepts of the grillage analogy method which will be used in calculating the wheel-load distribution factors. The stiffnesses of plane / space frame members, and the appropriate cross-sectional properties of different bridge structural elements idealized in the grillage analogy are summarized in this chapter. The AASHTO and LRFD load distribution factor equations will be presented in the following chapters for each bridge type. The basic procedure for field load testing and the methodology for computing the load distribution based on field test data is summarized in section 3.6.

3.2 GRILLAGE ANALOGY METHOD

3.2.1 Introduction

The grillage analogy is used for calculating wheel load distribution factors. It is an economical and simple method that can be fully automated using a microcomputer. The published literature by Cope and Clark (1984), and Bakht and Jaeger (1986) show results from the grillage analogy as applied to bridge structures.

The grillage analogy method has the following merits:

(a) It can be used even in cases where the bridge exhibits complex features such as heavy skew, edge stiffening, isolated and random locations of supporting piers, etc.

(b) Unlike a plane frame, this analogy incorporates torsional rigidity of the bridge superstructure.

(c) The grillage idealization has no restriction on the number of transverse beams in the analysis.

3.2.2. Grillage Analogy Concept

The grillage analogy is essentially an assembly of one-dimensional beams, which is subjected to loads acting in the direction perpendicular to the plane of the assembly. The deformation characteristics of a rectangular element of an isotropic plate subjected to out-of-plane load can be represented by an equivalent frame work model with a distribution of stiffness that represents as accurately as possible the properties of the real structure. The rectangular model consists of an assembly of four side and two diagonal beams. This idealization is shown in Figure 3.1 and the expressions for the properties of the various beams are as follows:

$$
\begin{aligned}
I_x &= \left(L_y - \frac{\nu L_x^2}{L_y}\right)\frac{t^3}{24(1-\nu^2)} \\
I_y &= \left(L_x - \frac{\nu L_y^2}{L_x}\right)\frac{t^3}{24(1-\nu^2)} \\
J_x &= \left(\frac{EL_y(1-3\nu)}{G}\right)\frac{t^3}{24(1-\nu^2)} \qquad \text{.....(3. 1)} \\
J_y &= \left(\frac{EL_x(1-3\nu)}{G}\right)\frac{t^3}{24(1-\nu^2)}
\end{aligned}
$$

$$I_d = \left(\frac{\nu(L_x^2 + L_y^2)^{1.5}}{L_x L_y} \right) \frac{t^3}{24(1-\nu^2)}$$

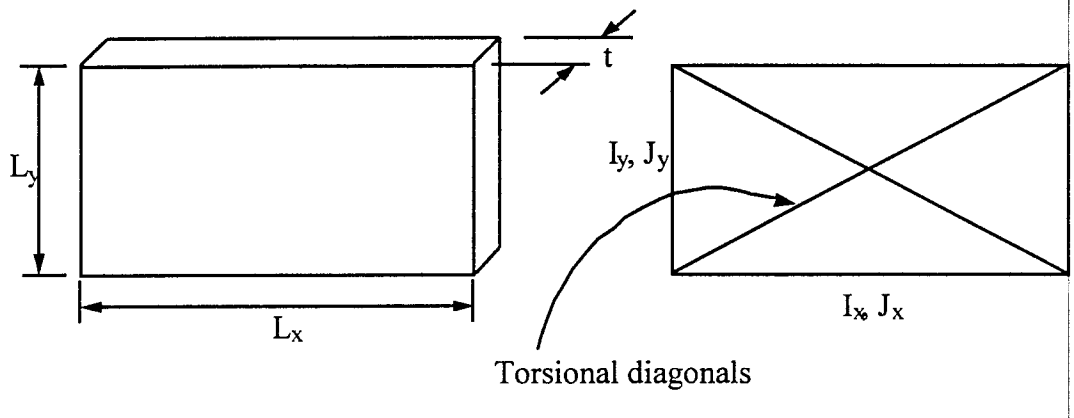

Figure 3.1 Grillage idealization of slab element

where I and J refer to the second moment of area and torsional inertia respectively, and ν is the Poisson's ratio of the material of the plate. By making the Poisson's ratio zero, the diagonal beams can be eliminated, and the grillage reduced to an orthogonal assembly of beams. The expressions for various beam properties appropriate to the different types of bridge girders, corresponding to zero Poisson's ratio are given in later sections. The matrix displacement method is used in the analysis of the bridge structure idealized with longitudinal and transverse beams. The stiffness equations of typical planar and space frame elements used in the analysis are presented below.

3.2.2.1 Stiffness of plane frame member

Figure 3.2a shows a typical plane frame element with two translational and one rotational degrees of freedom at each node. The member stiffness matrix for the plane frame member accounting for axial, flexural and shear strains is shown in Eqn. 3.2.

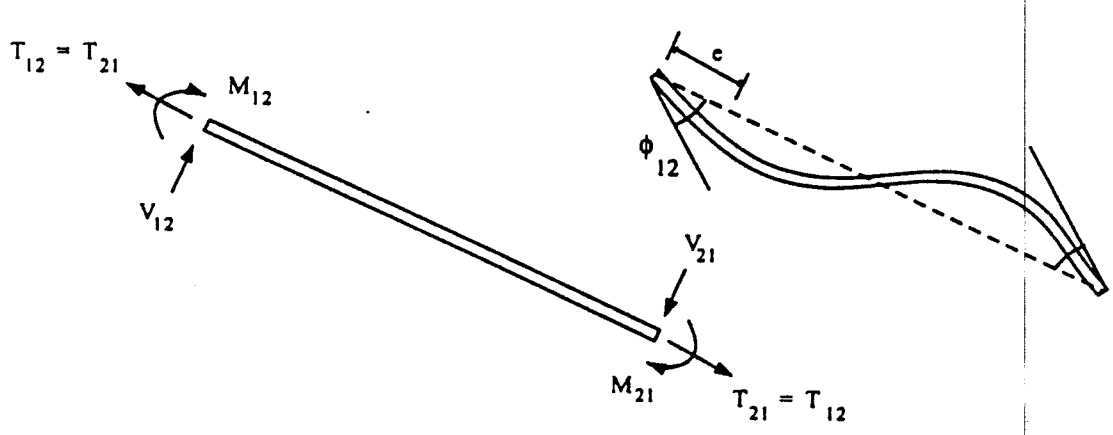

Figure 3.2a Typical plane frame element [Harrison, 1973]

$$\begin{bmatrix} T_{12} \\ M_{12} \\ M_{21} \end{bmatrix} = \begin{bmatrix} \frac{EA}{L} & 0 & 0 \\ 0 & \frac{n+3}{n+12}\cdot\frac{4EI}{L} & \frac{n-6}{n+12}\cdot\frac{2EI}{L} \\ 0 & \frac{n-6}{n+12}\cdot\frac{2EI}{L} & \frac{n+3}{n+12}\cdot\frac{4EI}{L} \end{bmatrix} \cdot \begin{bmatrix} e \\ \phi_{12} \\ \phi_{21} \end{bmatrix} \qquad \text{..... (3. 2)}$$

$$\text{where} \quad n = \frac{\beta AGL^2}{EI}$$

3.2.2.2 Stiffness of space frame member

Figure 3.2b shows a typical space frame element with six stress resultants at each end - three forces, two bending moments and a twisting moment. These resultants are not independent but are related to each other by six member equilibrium equations. The six independent stress

resultants in a space frame member are related to the corresponding member deformations as shown in Eqn. 3.3.

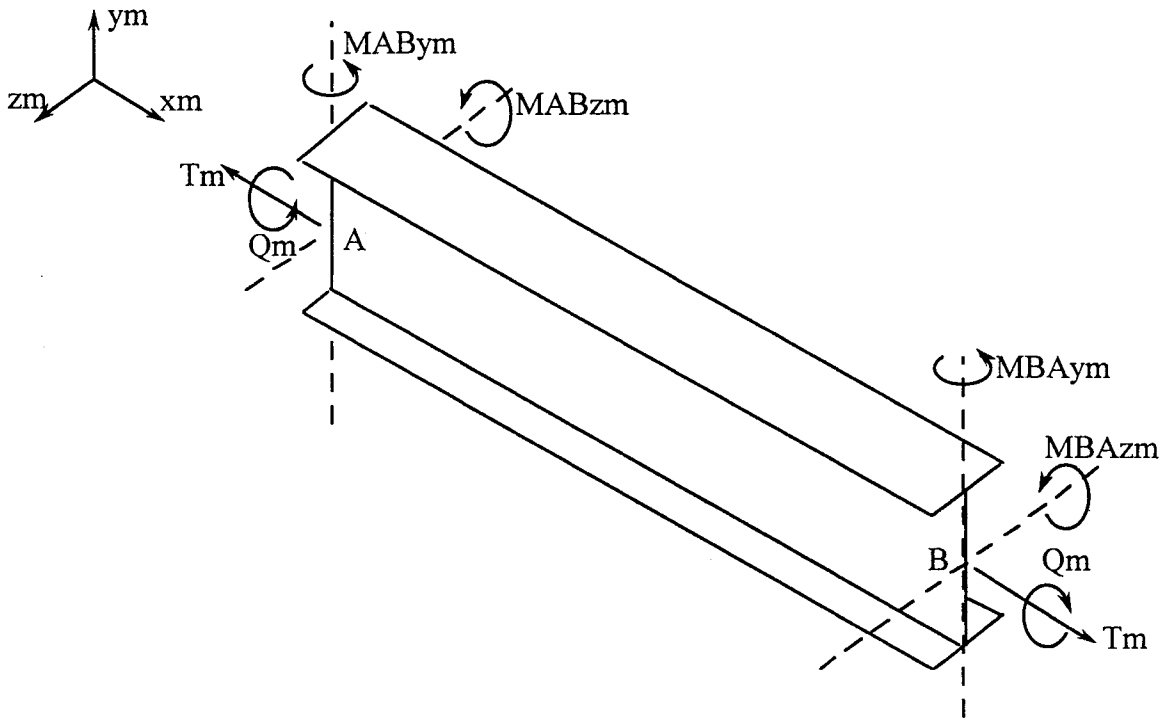

Figure 3.2b Typical space frame element [Harrison, 1973]

$$\begin{bmatrix} T_m \\ MAB_{zm} \\ MBA_{zm} \\ MAB_{ym} \\ MBA_{ym} \\ Q_m \end{bmatrix} = \begin{bmatrix} \frac{EA}{L} & 0 & 0 & 0 & 0 & 0 \\ 0 & \frac{4EI_z}{L} & \frac{2EI_z}{L} & 0 & 0 & 0 \\ 0 & \frac{2EI_z}{L} & \frac{4EI_z}{L} & 0 & 0 & 0 \\ 0 & 0 & 0 & \frac{4EI_z}{L} & \frac{2EI_z}{L} & 0 \\ 0 & 0 & 0 & \frac{2EI_z}{L} & \frac{4EI_z}{L} & 0 \\ 0 & 0 & 0 & 0 & 0 & \frac{GI_x}{L} \end{bmatrix} \begin{bmatrix} e \\ \phi AB_z \\ \phi BA_z \\ \phi AB_y \\ \phi BA_y \\ \theta \end{bmatrix} \quad \ldots\ldots (3.3)$$

3.3 BRIDGE TYPES

The scope of this study includes solid slabs, voided slabs, I-girder (AASHTO types and Bulb Tee types) and double-T beams. These are *shallow superstructures* in the sense that load distribution takes place mainly through bending and torsion in the longitudinal and transverse directions, with deflections due to shear being negligible. Shallow superstructures are well suited for analysis using the grillage analogy method. The section properties and mesh design used in the analyses are discussed in the following three sections:

3.3.1 Solid Slab

Solid slab bridges are used for spans up to 45 ft. (13.725 m). The idealized mesh for grillage analysis is shown in Figure 3.3a. The properties of the grillage members for solid slab elements are given below:

$$I_x = \frac{L_y t^3}{24} \qquad \text{.....(3.4)}$$

$$I_y = \frac{L_x t^3}{24} \qquad \text{.....(3.5)}$$

$$J_x = \left(\frac{E}{G}\right)\frac{L_y t^3}{24} \qquad \text{.....(3.6)}$$

$$J_y = \left(\frac{E}{G}\right)\frac{L_x t^3}{24} \qquad \text{.....(3.7)}$$

where

E = modulus of elasticity

G = shear modulus

I_x = the moment of inertia in the longitudinal direction

I_y = the moment of inertia in the transverse direction

J_x = the torsional inertia in the longitudinal direction

J_y = the torsional inertia in the transverse direction.

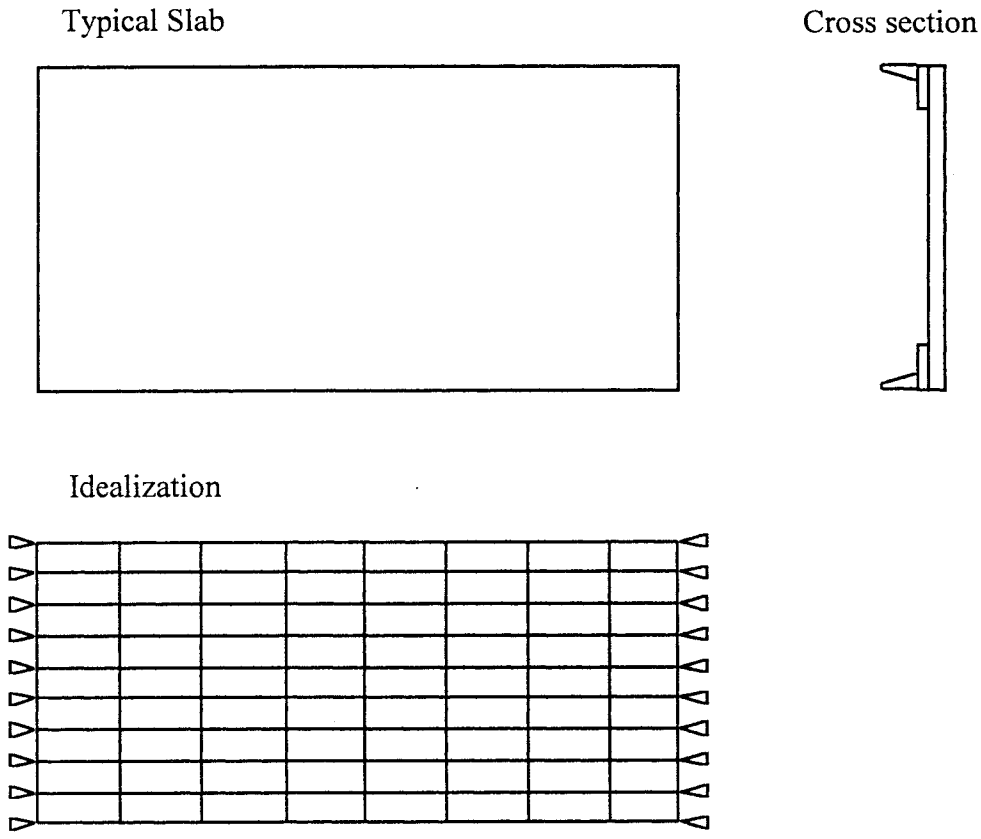

Figure 3.3a Solid slab - grillage idealization

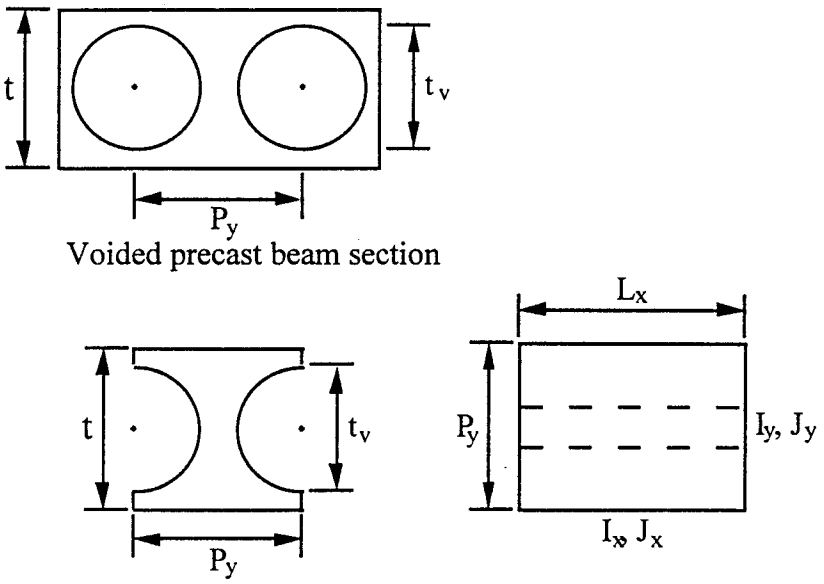

Figure 3.3b Grillage idealization of voided slab element

3.3.2 Voided Slab

Voided slab bridges are used for spans upto 50 ft. (15.2 m). Grillage idealization of voided slab bridges is similar to that of solid slab bridges, differing only in the properties of the grillage members and the necessary placement of the longitudinal grillage members coincidental with void centerlines. An idealized voided slab element is shown in Figure 3.3b. The properties of the grillage members for voided slab bridges are given below:

$$I_x = \frac{P_y t^3}{12} + \frac{\pi t^4}{64} \qquad \text{.....(3. 8)}$$

$$I_y = \frac{L_y t^3}{12}\left[1 - \left(\frac{t_v}{t}\right)^4\right] \qquad \text{.....(3. 9)}$$

$$J_x = \frac{L_y t^3}{6}\left[1 - 0.85\left(\frac{t_v}{t}\right)^4\right] \qquad \text{.....(3. 10)}$$

$$J_y = \frac{L_x t^3}{6}\left[1 - 0.85\left(\frac{t_v}{t}\right)^4\right] \qquad .....(3.11)$$

where

P_y = the center to center distance of the circular voids

t_v = the diameter of the circular voids.

3.3.3 Slab-on-Girder

AASHTO girder bridges can be used for spans up to 100 ft. (30.5 m) and Bulb Tee girder bridges can be used up to 150 ft. (45.72 m) depending on the type. To idealize a slab and girder bridge the longitudinal members of the grillage are positioned to coincide with the actual girders. These girders are given the properties of the girders plus the associated portion of the slab. The transverse grillage beams represent appropriate portions of the deck slab. An idealized element and typical assembly of beams are shown in Figures 3.4 and 3.5 respectively.

The properties of the grillage members for slab and girder elements are given below:

$$I_x = \frac{L_y t^3}{12} \qquad .....(3.12)$$

$$I_y = \frac{L_x t^3}{12} \qquad .....(3.13)$$

$$J_x = J_g + \left(\frac{E}{G}\right)\frac{L_y t^3}{6} \qquad .....(3.14)$$

$$J_y = \left(\frac{E}{G}\right)\frac{L_x t^3}{12} \qquad .....(3.15)$$

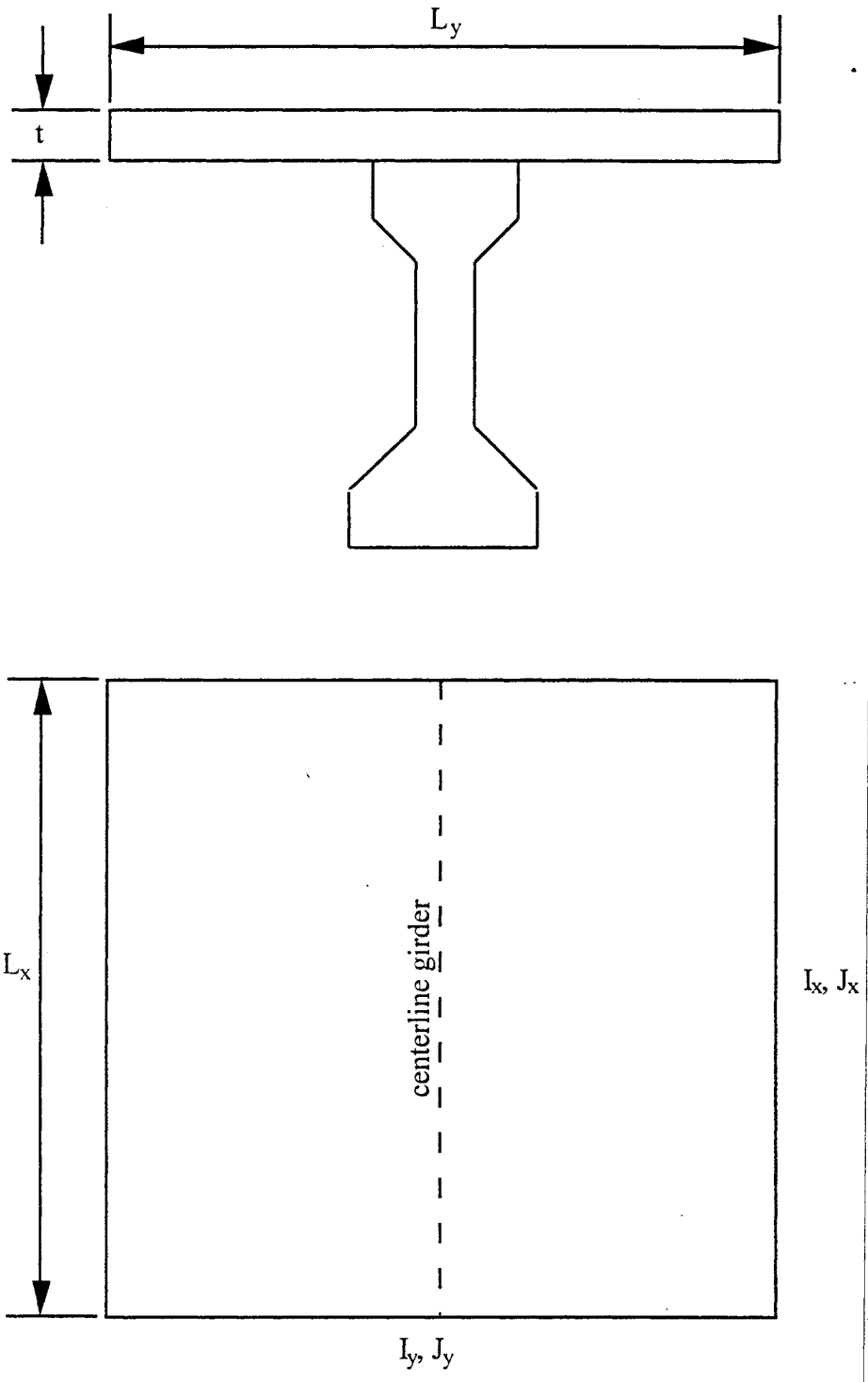

Figure 3.4 Grillage idealization of slab & girder element

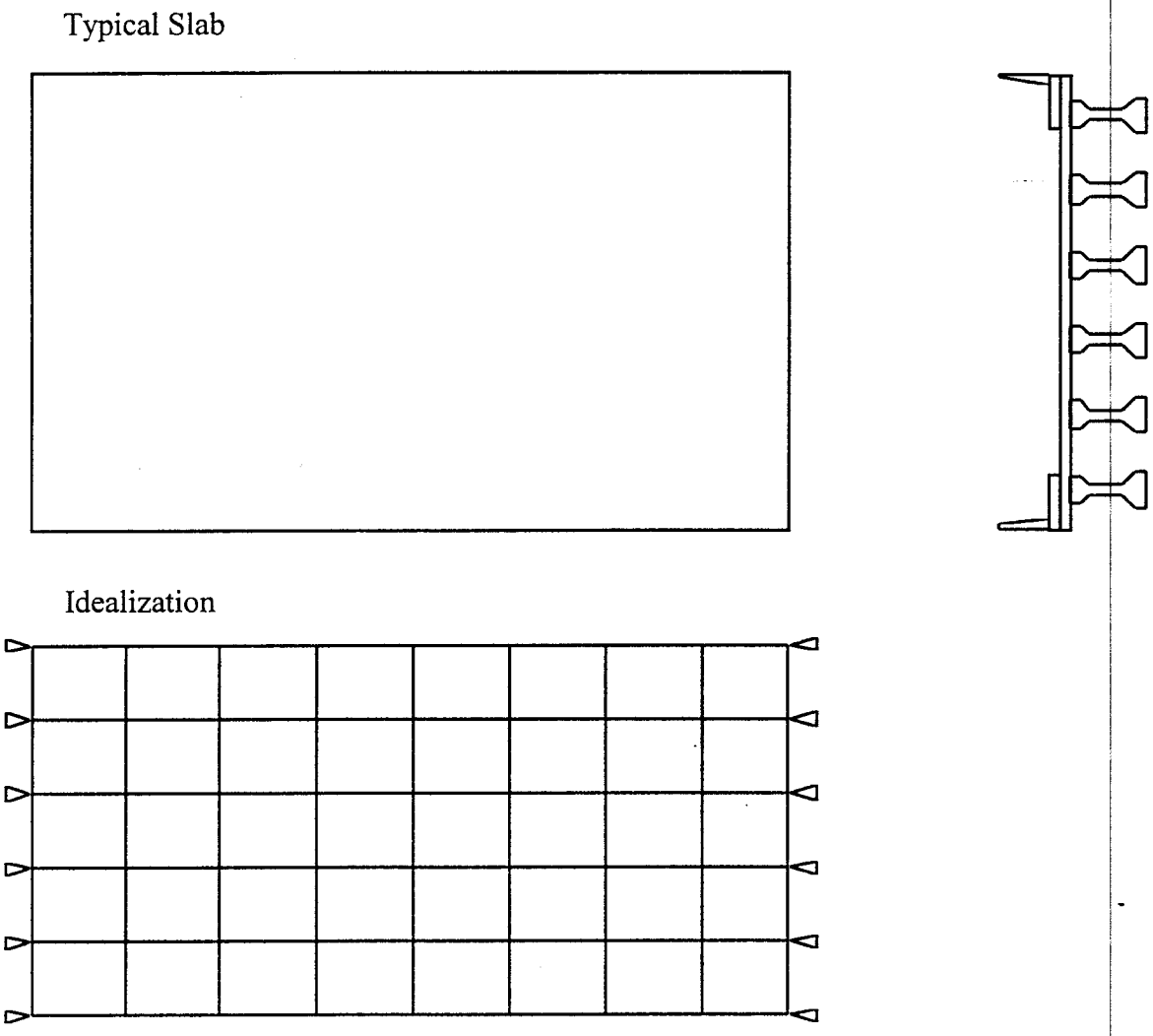

Figure 3.5 Slab and girder - grillage idealization

where

J_g = the girder torsional inertia.

For the analysis of AASHTO girders, the torsional inertias are calculated by dividing the beam into a number of rectangles and adding the torsional inertias of the individual rectangles as

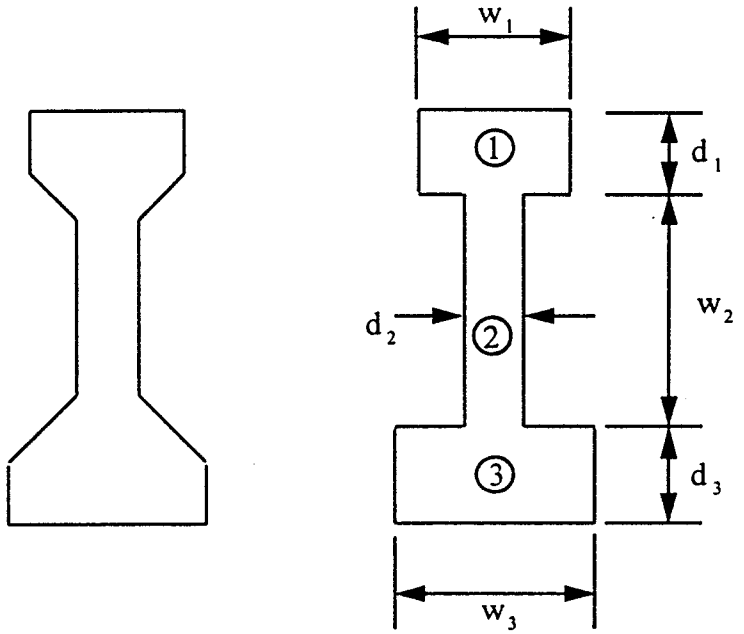

Figure 3.6 Idealization for calculating torsional inertia

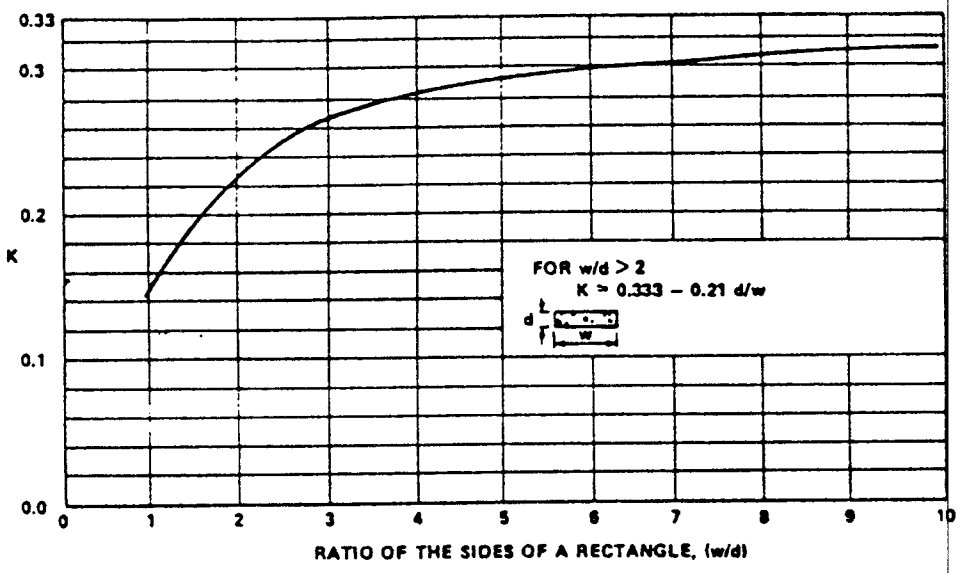

Figure 3.7 Values of the torsion coefficient [Bakht and Jaeger, 1985]

shown in Figure 3.6 and given by:

$$J_g = \sum_{n=1}^{3} K_n w_n d_n^3 \qquad \text{.....(4. 17)}$$

where

w = the larger side of each rectangle

d = the smaller side of each rectangle

K = the torsional coefficient determined from Figure 3.7 [Bakht and Jaeger,1985].

3.3.4 T-Beam and Double-T Girders

T-Beams and Double-T girder bridges can be used for spans upto 65 ft. (19.8 m), depending on the type. To idealize a T-Beam bridge, the longitudinal members of the grillage are positioned to coincide with the center line of the T-Beams (center of the webs). The member in the grillage analogy are assigned the properties of the T-Beams. The transverse grillage beams represent appropriate portions of the top flange of the T-Beams. An idealized element and typical assembly of beams are shown in Figures 3.8 and 3.9 respectively.

Idealization

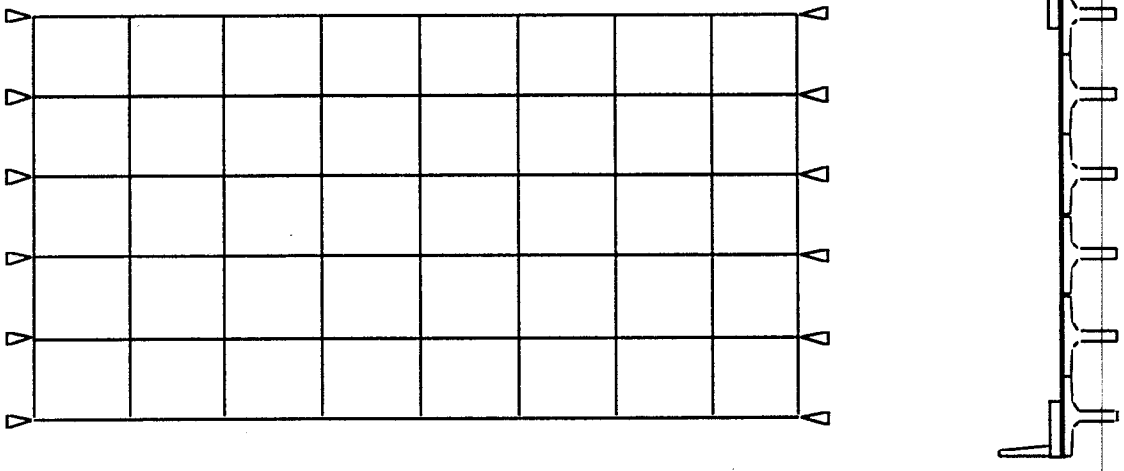

Figure 3.8 T-Beam - grillage idealization

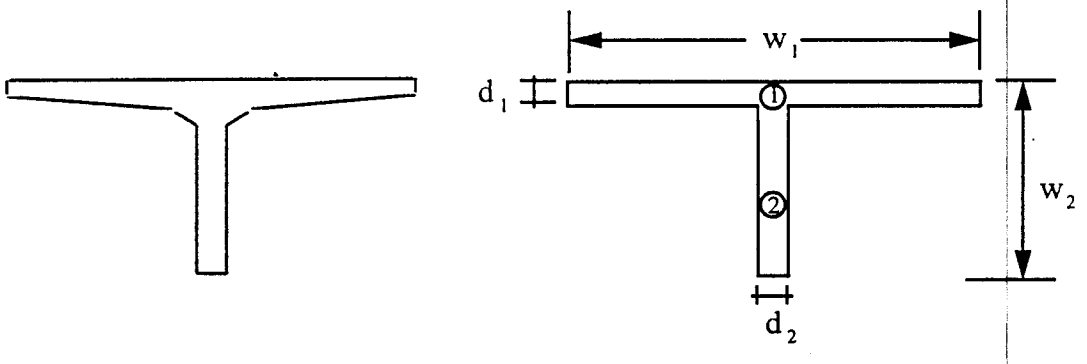

Figure 3.9 Idealization for calculating torsional inertia

The properties of the grillage members of the T-Beam elements are similar to those of AASHTO girders, as illustrated in the previous section, and are given below:

$$I_x = \frac{L_y t^3}{12} \qquad \text{.....(3. 17)}$$

$$I_y = \frac{L_x t^3}{12} \qquad \text{.....(3. 18)}$$

$$J_x = J_g + \left(\frac{E}{G}\right)\frac{L_y t^3}{6} \qquad \text{.....(3. 19)}$$

$$J_y = \left(\frac{E}{G}\right)\frac{L_x t^3}{12} \qquad \text{.....(3. 20)}$$

where

J_g = the girder torsional inertia.

The torsional inertias of the T-Beams are calculated by dividing the beam into a number of rectangles and adding the torsional inertias of the individual rectangles as shown in Figure 3.9 and given by

$$J_g = \sum_{n=1}^{3} K_n w_n d_n^3 \qquad \text{.....(3. 21)}$$

where

w = the larger side of each rectangle

d = the smaller side of each rectangle

K = the torsional coefficient determined from Figure 3.7 [Bakht and Jaeger,1985].

The Double-T beam can be idealized as an equivalent T-beam without compromising the accuracy of the analysis results. There are two approaches to idealize a Double-T cross-section into a T-Beam cross-section; in the first approach, the Double-T section can be cut between the two Ts (flange) to result in two T-Beam cross-sections; in the second approach, a single T can be built-up keeping the same area, moment of inertia and depth of centroid as that of the given Double-T beam. Figure 3.10 shows the idealization of a Double-T girder into a T-Beam.

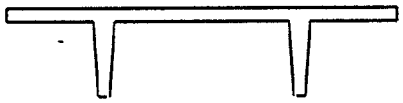

(a) Double-T Girder

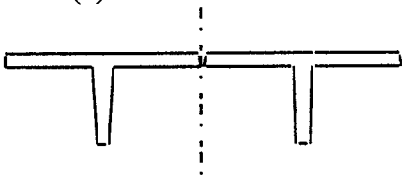

(b) Idealization of a Double-T into two T-Beams

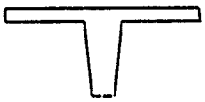

(a) Combining the two webs of Double-T beam into a single T-Beam

Figure 3.10 Idealizations of Double-T girder into T-Beam

3.4 LOADS

By definition, the grillage analogy can accommodate loads perpendicular to the grid. Live and dead loads are considered in developing the computer program, but only live load is considered in calculating the wheel load distribution factors.

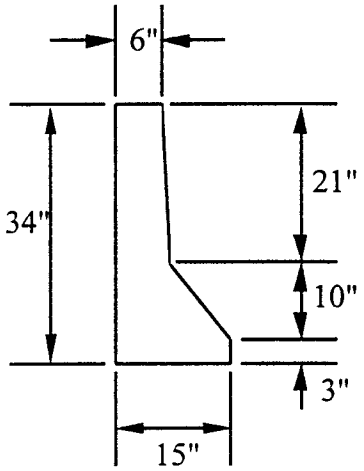

Figure 3.11 Standard parapet

3.4.1 Dead Loads

The dead load consists of the physical weight of the structure. This includes the bridge deck, girders, edge beams or sidewalks, parapet, and overlay.

Edge beams (sidewalks) and parapets can also be included in the weight of the structure. The edge beam dimensions can be defined by the user and a standard parapet used as shown in Figure 3.11. The edge-stiffening that is provided by the presence of edge beams and/or parapets is taken into account by adjusting Eqns. 3.4 through 3.15. In general:

$$EI_{TOTAL} = EI_b + EI \qquad .....(3.22)$$

where

EI_b = the stiffness provided by the edge beam and/or parapet.

Overlays can also be added to the dead load of the structure. The user has the options of using asphalt (144 lb/ft^3), concrete(150 lb/ft^3), other, or none.

3.4.2 Live Loads

The live load configurations available to the user consists of traditional AASHTO H and HS type loads shown in Figures 3.12. The position of the trucks on the bridge would be specified with respect to both the longitudinal and transverse directions. The trucks on the bridge may be placed in the longitudinal direction by defining the position of the center of the rear wheel. The center line of the truck could also be specified with respect to edge of the bridge.

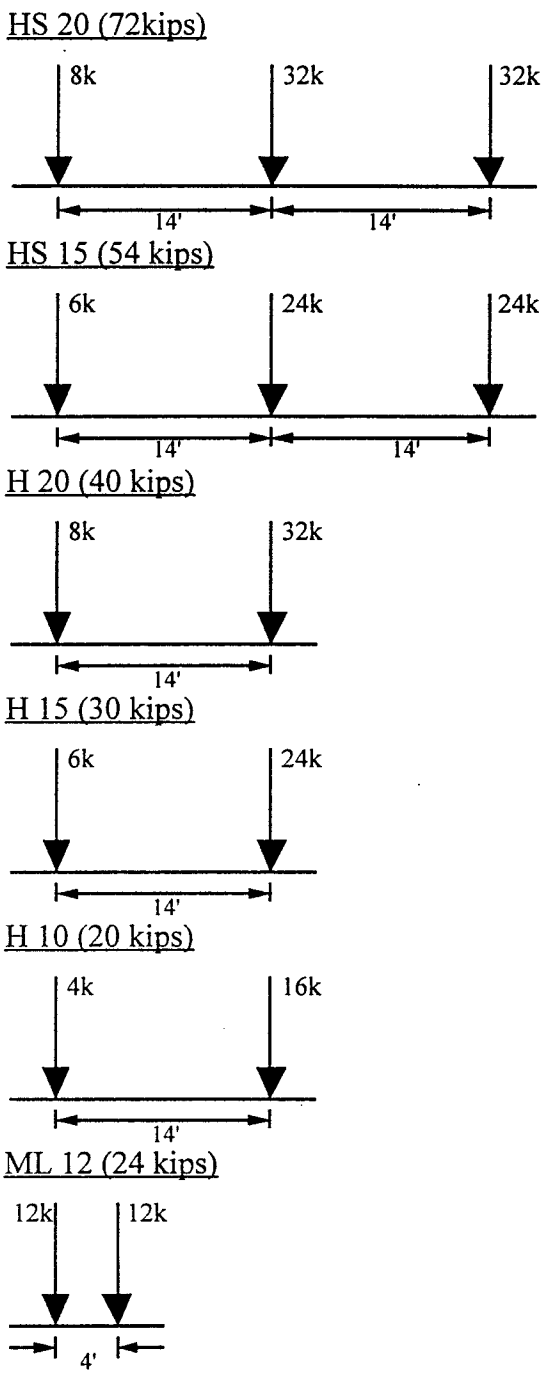

Figure 3.12 AASHTO live load configurations

3.5 LOAD DISTRIBUTION FACTORS BASED ON FIELD TESTS

Field load testing frequently offers a means of determining whether the load capacity of a bridge is greater than the capacity determined from standard rating calculation based on the AASHTO method. In some cases the field tests indicate a higher load capacity, because the AASHTO wheel load distribution factors used in standard rating calculations tends to overestimate the loads carried by the individual girders. Examples of how field tests have been used to assess various aspects of bridge behavior are given by Bakht and Csagoly (1980), Bakht and Jaeger (1990) and others.

Florida Department of Transportation (FDOT) has been testing many bridges to check their strength and establish bridge ratings. The strength of bridge elements is generally determined by first placing strain or deflection transducer gages at the bridge critical locations along the elements, and then incrementally loading them to induce maximum effects. The data collected can then be analyzed and used to establish the strength of each component as well as the **load distribution factors**.

The FDOT's bridge load testing system consists of two test vehicles, a mobile data acquisition system and a mobile machine shop. The two test vehicles have been designed to deliver the ultimate live loads specified by AASHTO code. Each vehicle is a specially designed tractor-trailer combination, weighing in excess of 200 kips when fully loaded with concrete blocks. Detailed dimensions of the test vehicles are shown in Figure 3.13. Each vehicle can carry maximum of 72 concrete blocks, each weighing approximately 2,150 pounds. Incremental loading

is achieved by adding blocks with a self-contained hydraulic crane mounted on each truck. Figs. 3.14 and 3.15 show the wheel loads for each load increment.

Once a bridge is identified for load testing, a site survey and an analysis of existing plans and inspection reports give further information on the feasibility of such a test. Details of instrumentation and loading locations are then established. The next step is to mobilize testing equipment and personnel to the bridge site.

The test vehicles are initially loaded with a number of concrete blocks, established from the preliminary analysis of the existing structure. The vehicles are then driven and placed on the critical locations of the bridge, while the data acquisition system monitors the instrumentation during loading. The data is immediately analyzed, displayed and compared to the theoretical prediction to ensure the safety of the bridge, equipment and testing personnel. After each load step, if the results compare favorably with the theoretical prediction, additional blocks are added to the vehicles and the test repeated until the ultimate AASHTO load is achieved. The data gathered can then be analyzed and a report of the findings prepared. Bridges that carry both vehicles without apparent distress are considered structurally safe.

Data from some bridge test reports will be used for load distribution analyses. The typical report contains transverse strain distributions in the maximum bending moment section for several loading stages. The typical report also contains the applied moment vs. strain curves for several loading stages.

Measured Distribution Factors

One method for use of test results in rating calculations is to use test data to calculate wheel-load distribution factors. This measured wheel-load distribution factor can be used in bridge-rating calculations in place of wheel load distribution defined by AASHTO. AASHTO (Guide specifications 1989) has also presented a refined bridge-rating methodology in which measured wheel-load distribution factors can be used.

Goshen et al. (1986) assumed that the distribution factor for a girder was equal to the ratio of the strain at the girder to the sum of all the bottom-flange strains. O'Connor and Pritchard (1985) measured the total bending moment applied to a multigirder bridge by using a weighted sum of the bottom-flange strains.

In the present study, the measured strains would be multiplied by the section modulus times elastic modulus to calculate the measured moments. The ACI equation was used to calculate the elastic modulus of concrete based on f'_c = 5000 psi. The measured moment distribution will be used to calculate the measured wheel-load distribution factors. The measured wheel-load distribution factors will be compared with AASHTO , LRFD and grillage analysis wheel load distribution factors.

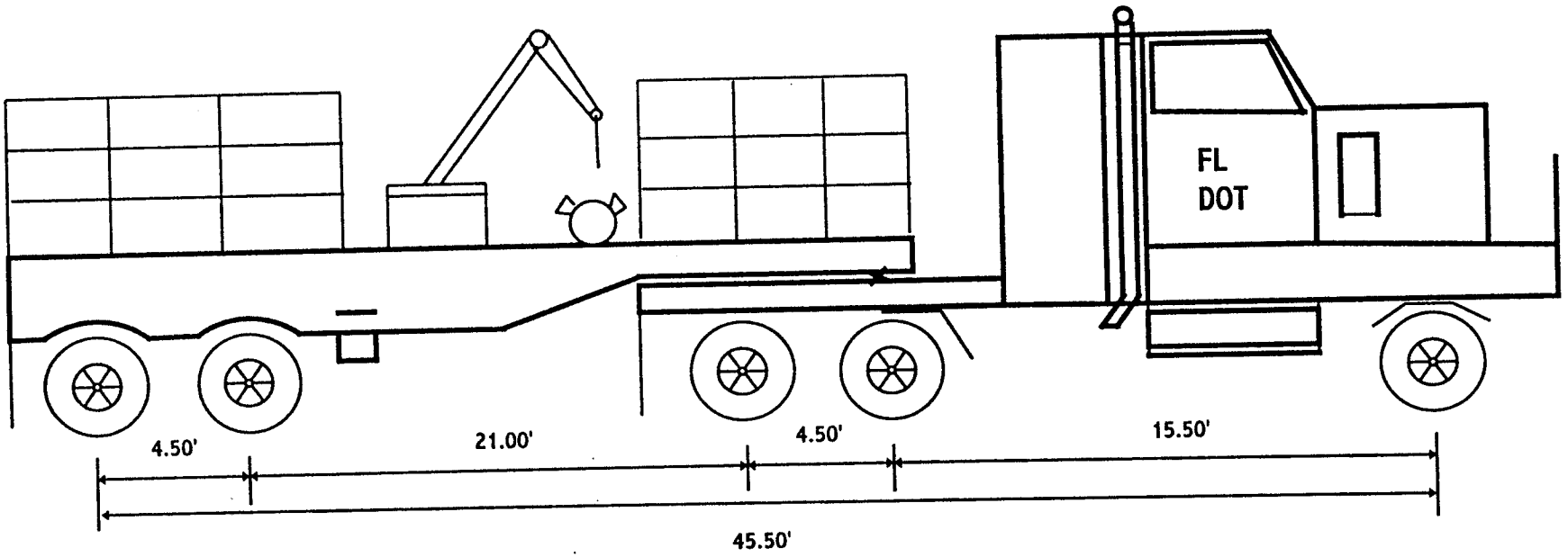

Fig. 3.13 Typical FDOT test vehicle

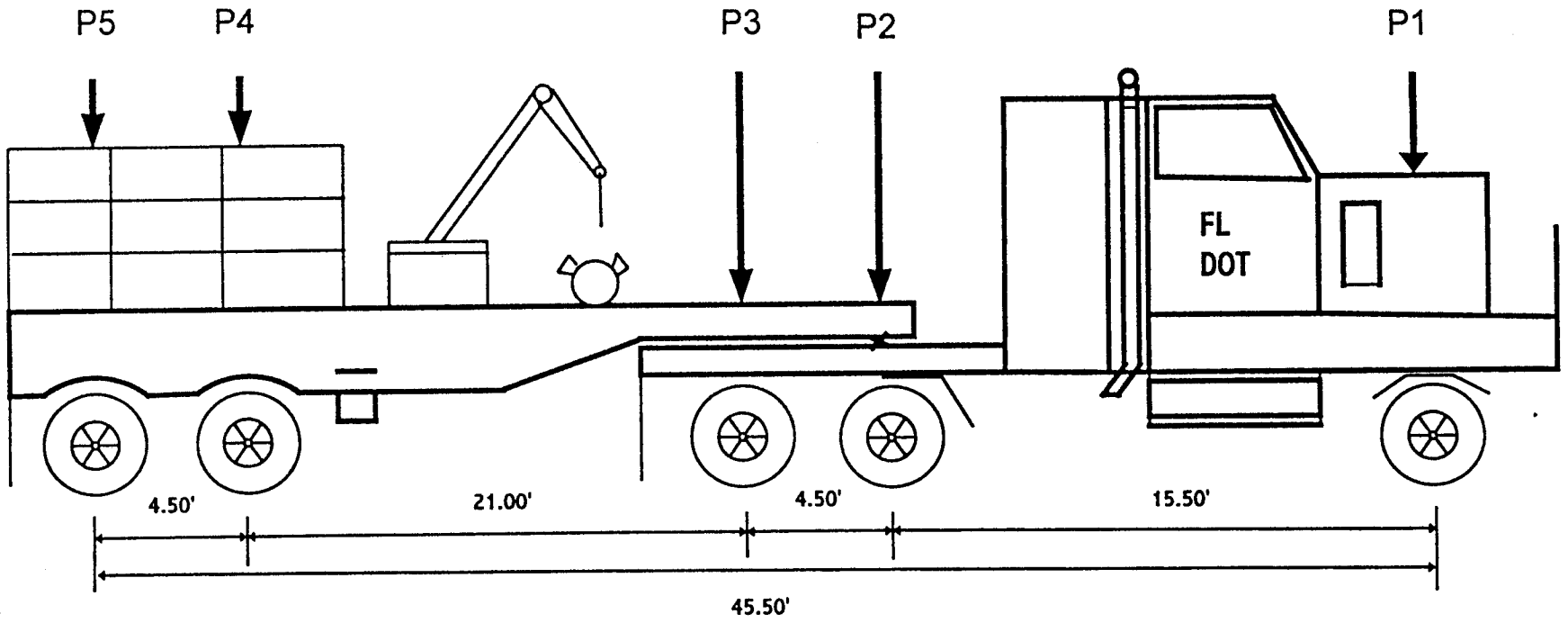

# A Block	P5	P4	P3	P2	P1
24	30.61	30.61	11.01	11.01	11.26
30	35.48	35.48	11.68	11.68	11.26
36	41.78	41.78	11.95	11.95	11.26
42	46.60	46.60	12.67	12.67	11.26

Fig. 3.14 Typical truck loads for spans less than 55 ft. vehicle

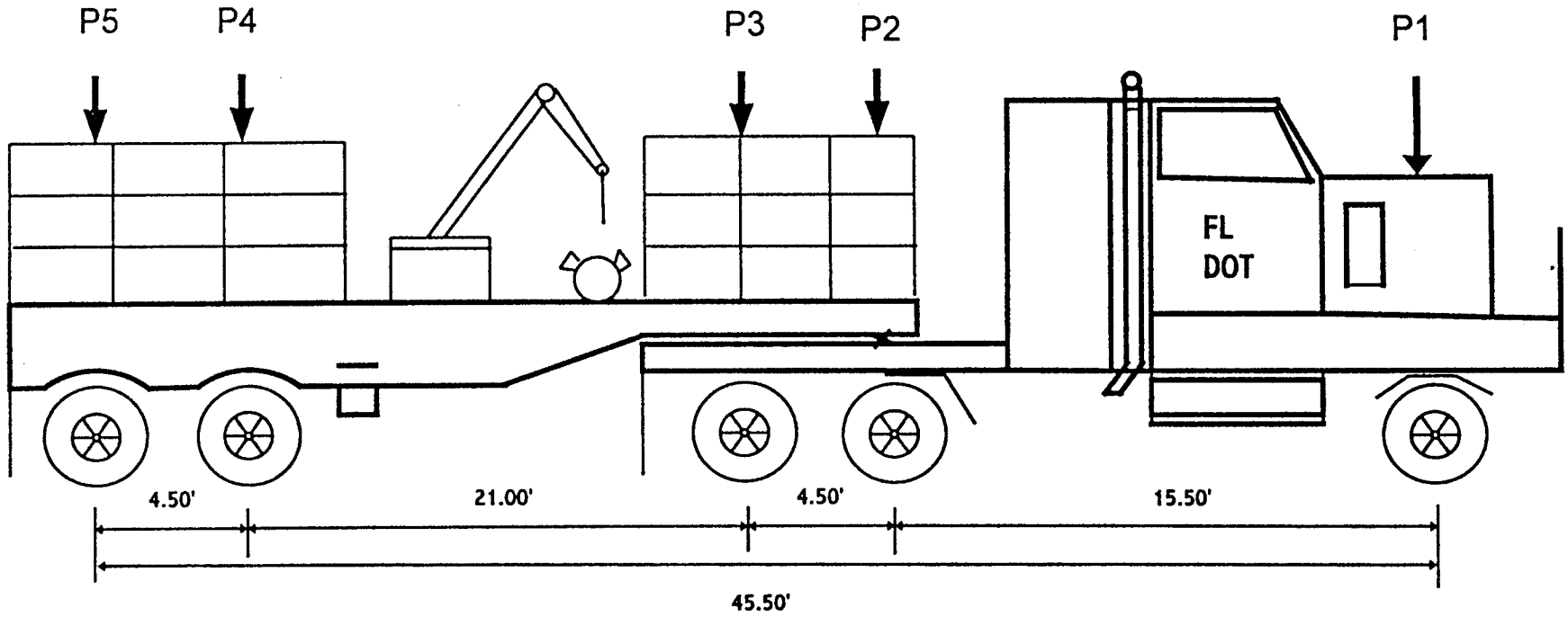

# A Block	P5	P4	P3	P2	P1
24	22.40	22.40	18.66	18.66	11.49
36	29.21	29.21	24.95	24.95	11.66
48	36.03	36.03	28.23	28.23	11.83
72	49.66	49.66	37.80	37.80	12.17

Fig. 3.15 Typical truck loads for spans larger than 55 ft.

CHAPTER 4

LOAD DISTRIBUTION ANALYSES OF SOLID AND VOIDED SLAB BRIDGES

4.1 INTRODUCTION

The slab bridges are solid or voided sections that span between supports in the longitudinal direction, i.e., traffic direction. The slab bridges are practical for shorter spans up to 45 ft. for voided sections and up to 30 ft. for solid sections (Heins and Lawrie, 1984). They also offer a minimal structure depth for which structure opening and vertical clearance are significant. In addition to the above advantage, slab bridges are commonly used for its low construction costs.

Wheel load distribution on slab bridges based on both grillage analogy method and field tests performed by Florida Department of Transportation (FDOT) is presented in this chapter. The objectives of the analyses are the following:

i) Determine the effective width using grillage analogy method and study the effects of span length, bridge width, slab thickness, edge beam and other parameters on wheel load distribution.

ii) Verify the current AASHTO and the proposed LRFD load distribution factors using solid and voided slab bridge field tests.

iii) Derive simple design criteria for load distribution that would provide more accurate alternative to current designs.

4.2 METHOD OF ANALYSIS

The AASHTO procedure to calculate the flexural distribution factors is generally used for bridge design by DOT's and tends to be overly conservative particularly for analyzing and rating of existing bridges, which may cause unnecessary rerouting of vehicles in certain circumstances (Warren and Malvar, 1993). The current AASHTO approach is to calculate an effective width E, over which the concentrated wheel load (half truck load) is assumed to be uniformly distributed (AASHTO specification, 1989)

$$\mathbf{E = 4.0 + 0.06\,S\ (feet)\ (E < 7\,ft)} \qquad \mathbf{(4.1)}$$

where S = span length, in feet. A larger value of E means to more efficient distribution of the load. Slab thickness and flexural reinforcement are then determined from an equivalent strip of width 2E carrying the total truck load. The AASHTO equation is based substantially on Westergaard theory for slabs (Westergaard, 1930). The AASHTO equation considers span length as the only parameter and neglect other important parameters such as bridge width, edge beams, etc.

The proposed LRFD approach is similar to AASHTO method, but considers more parameters such as bridge width and number of lanes. The LRFD approach is based on NCHRP project 12-26 entitled, "Distribution of Wheel Loads on Highway Bridges", which was performed in two phases by

The proposed LRFD approach is similar to AASHTO method, but considers more parameters such as bridge width and number of lanes. The LRFD approach is based on NCHRP project 12-26 entitled, "Distribution of Wheel Loads on Highway Bridges", which was performed in two phases by Imbsen & Associates, Inc.(1989). The proposed LRFD approach for slab bridges was based on limited number of analytical studies. The LRFD effective width of longitudinal strip per lane for both shear and moment with one lane, i.e., two lines of wheels, loaded may be determined as follows:

$$E = 10.0 + 5.0\sqrt{L_1 W_1} \tag{4.2}$$

The effective width per lane for more than one lane loaded, may be determined as

$$E = 84.0 + 1.44\sqrt{L_1 W_1} \leq \frac{W}{N_L} \tag{4.3}$$

where

E = Effective width over which truck load is assumed to be uniformly distributed, in. (This definition of E will be used throughout this chapter),

L_1= Modified span length taken equal to the lesser of the actual span or 60.0 ft., (ft. units),

W_1= Modified edge to edge width of bridge taken equal to the lesser of the actual width or 60.0 ft., (ft. units),

W = Physical edge to edge width of bridge, ft.,

N_L= Number of design lanes.

In addition to the analytical study, data from field tests performed by Structures Research Center, FDOT, are used to verify the results from the analytical study.

4.2.1 Effective Width Calculation

A load distribution factor may be calculated from the distribution of the moments determined from the grillage analyses and field tests. The sum of moments or the total area under the moment distribution curve is equivalent to externally applied moment due to the concentrated loads (including the edge beam moments). The effective width, E is equal to the ratio of total area under the moment curve to the maximum moment. The distribution factor is taken as the reciprocal of the effective width.

4.3 SOLID SLAB BRIDGE: PARAMETRIC STUDY

Several parameters affect the load distribution of solid slab bridges. Span length, bridge width, slab thickness, edge beam and number of lanes are the main parameters which are considered in this section. Figure 4.1 shows the typical slab bridge cross section which is used in the analysis. The typical slab bridge has a span length of 21 ft. with a width equal to 30 ft. and the slab thickness of 12 inch.

4.3.1 Discretization of Slab Bridge Using Grillage Analogy

The size of the beam element was varied to choose the appropriate element size for this study. The typical slab bridge shown in Figure 4.1 was divided into elements in the longitudinal and transverse directions as shown in Figure 4.2. The length X, and the width Y, were varied as shown in Table 4.1. The values of X were chosen as 2.625, 3.5 and 5.25 ft. whereas the Y values were approximately 1.5, 2.0 and 3.0 ft. Table 4.1 summarizes the different cases analyzed using grillage analogy to establish the appropriate discretization of the slab bridge. Five cases were analyzed using grillage analogy and the results shown in Figure 4.3. The effective width, E, is independent of the length X and width Y. The width Y, had relatively more influence than the length X in the mesh discretization. The effective width E, changed by only one percent when the width Y is doubled. Based on this study, the values of X and Y were kept equal to 2.625 and 3.056 ft. respectively throughout the analyses.

Table 4.1 Discretization of the slab bridge: summary of cases

Case no.	Number of divisions in longitudinal direction	Length X, ft.	Number of divisions in transverse direction	Width Y, ft.
1	8	2.625	11	3.056
2	6	3.500	11	3.056
3	4	5.250	11	3.056
4	6	3.500	15	2.115
5	6	3.500	20	1.528

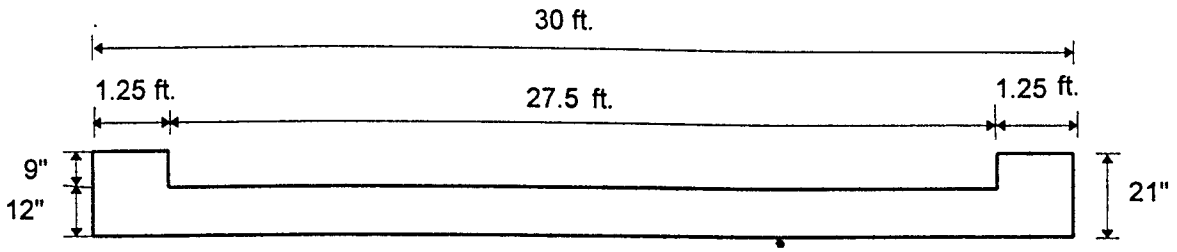

Fig. 4.1 Typical solid slab bridge cross-section

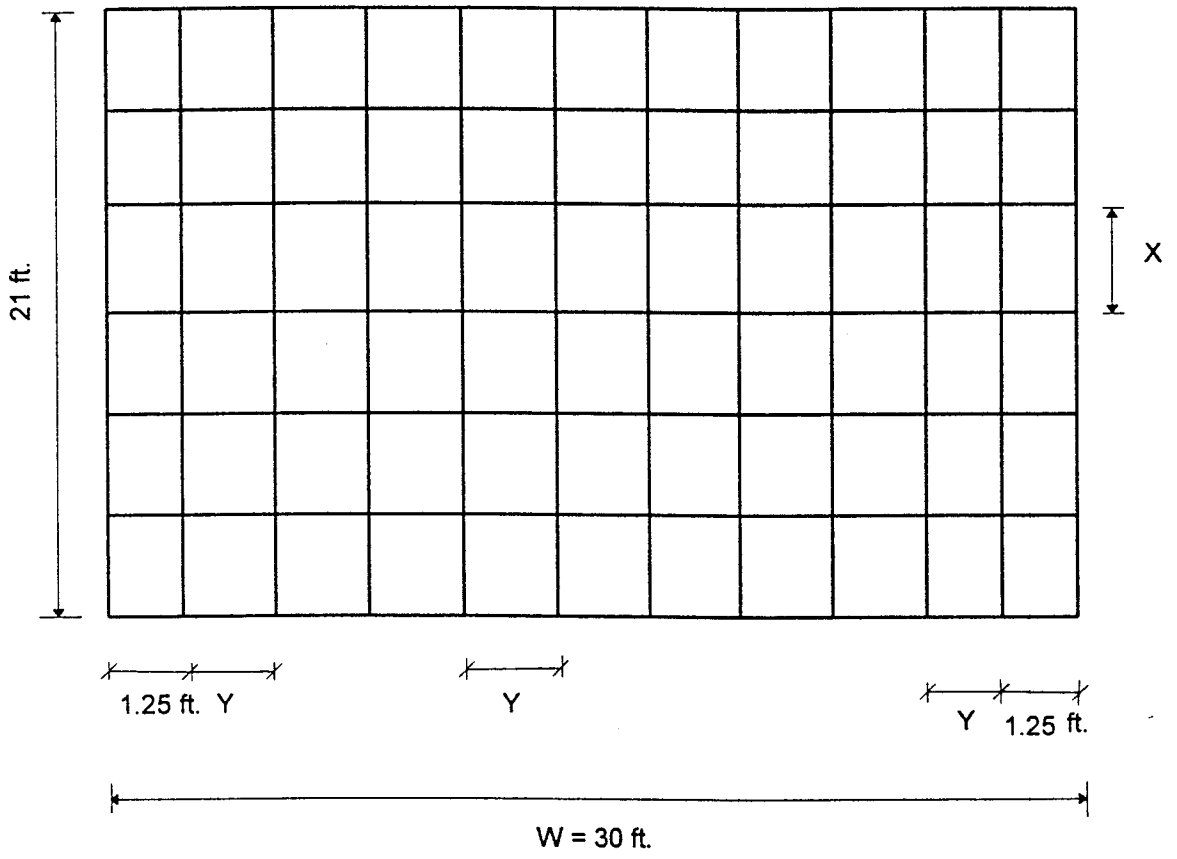

Fig. 4.2 Typical solid slab bridge discretization

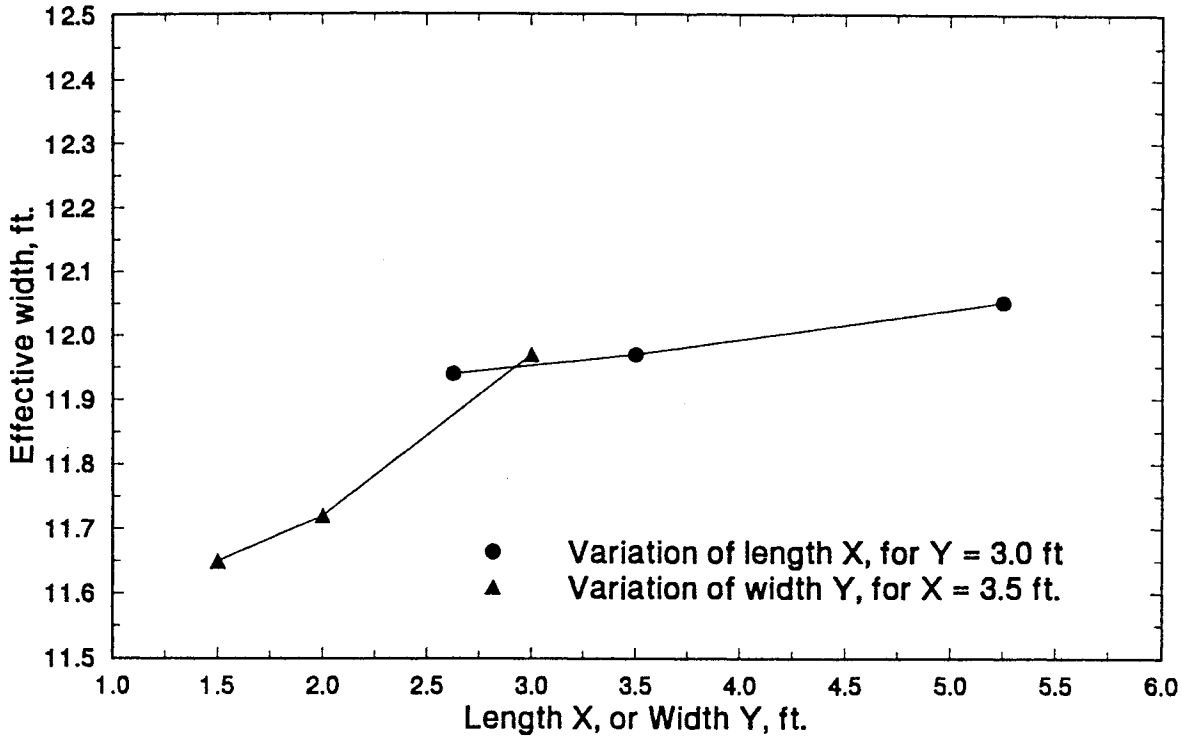

Fig. 4.3 Effective width vs. length / width of element used in discretization

4.3.2 Truck Load Position

The AASHTO HS-20 truck was used in this parametric study. The truck position in the longitudinal direction (span direction) was located to so as to obtain the maximum bending moments. For slab bridges with relatively short spans, the maximum bending moment occurs when only one axle of the truck is at the midspan. For a two lane slab bridge, it was found that the maximum bending moment occurs when the two lanes are loaded as shown in Figure 4.4b. For one lane bridges, the truck was positioned at the center line as shown in Figure 4.4c.

4.3.3 Parametric Studies

Table 4.2 summarizes the cases in which several parameters such as span length, bridge width, slab thickness , edge beam, etc. were considered. Twenty seven cases were investigated using grillage analogy to establish the main parameters affecting the effective width of the solid slab.

4.3.3.1 Span length

Span length is one of the main factors in load distribution in slab bridges. Solid slab bridges with spans from 15 ft. up to 40 ft. (Table 4.2) were investigated in this study. The slab thickness was 12 in. for spans less or equal 24 ft. and 20 in. for the other spans. Figure 4.5 shows the bending moment distribution for typical bridge with different span lengths. The bending moment increases with the increase in the span length and the moment distribution tends to be

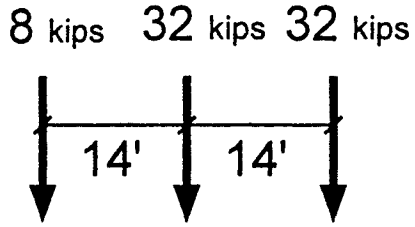

(a) AASHTO HS-20 Truck

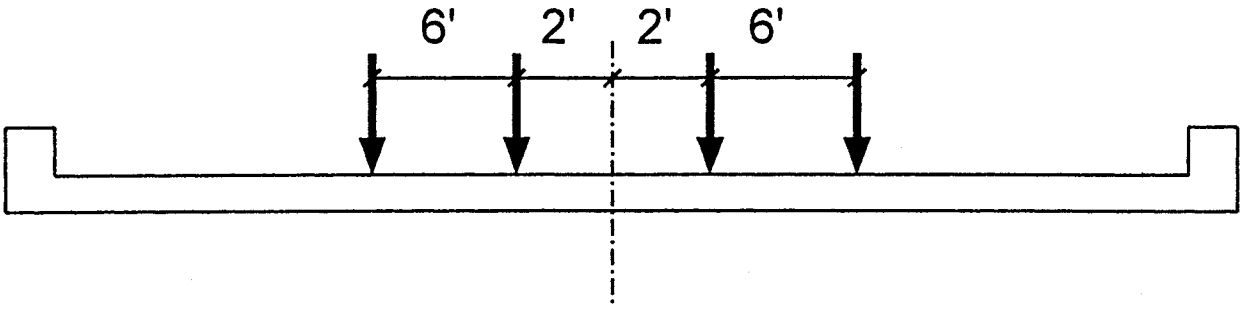

(b) Two lanes load position

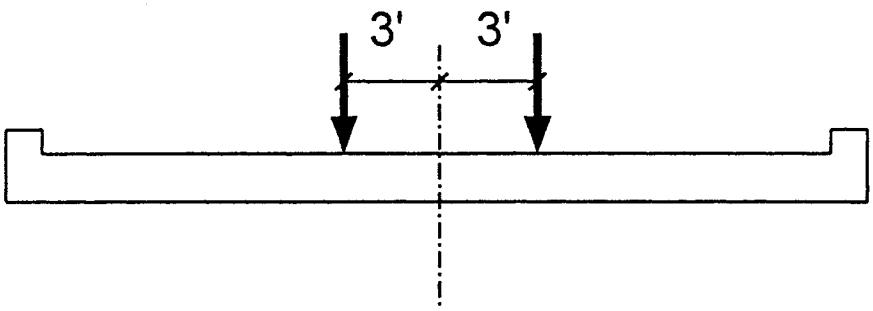

(c) One lane load position

Fig. 4.4 Typical truck load positions for solid slab bridges

more uniform for longer spans, i.e., larger effective width. These bending moment distributions were used to calculate the solid slab effective widths.

Table 4.2 Summary of parametric study cases

Parameter	Span length, ft.	Bridge width, ft.	Slab thickness, in.	Comments
Span length (6 cases)	15 18 21 24 30 40	30 30 30 30 30 30	12 12 12 12 20 20	With edge beam, two lanes
Bridge width (4 cases)	21 21 21 21	26 30 34 38	12 12 12 12	With edge beam, two lanes
Slab thickness (3 cases)	21 21 21	30 30 30	10 12 14	With edge beam, two lanes
Without edge beam (4 cases)	15 18 21 24	30 30 30 30	12 12 12 12	
One lane (4 cases)	15 18 21 24	15 15 15 15	12 12 12 12	
Edge beam depth (3 cases)	21 21 21	30 30 30	12 12 12	Edge beam depth = 6, 12 and 18 in.
Edge beam width (3 cases)	21 21 21	30 30 30	12 12 12	Edge beam width = 1.25, 2 and 3 ft.

Figure 4.6 shows that the effective width increases with increasing span and it is clear that the span is an important parameter in slab bridge load distribution. The effective widths calculated using grillage analogy are larger than those calculated using AASHTO and LRFD codes as shown in Figure 4.6. This means that both AASHTO and LRFD codes give conservative estimate of effective width, E for solid slab bridges. The difference in the estimation of effective width increases with a corresponding increase in the span.

4.3.3.2 Bridge width

The bridge width for the typical bridge was varied between 26 ft and 38 ft as shown in Table 4.2. AASHTO code does not consider the bridge width as a parameter in effective width calculations, while the bridge width is the second main parameter used in the proposed LRFD equation for effective width, E. Figure 4.7 shows insignificant changes in effective width with increase in the bridge width for the same span. Based on this limited study, it seems that the bridge width can be neglected as a parameter in calculating the effective widths of solid slab bridges.

4.3.3.3 Slab thickness

The slab thickness is not considered as a parameter in the current AASHTO specifications or the proposed LRFD code for calculating the effective width. For a typical bridge, the variation of slab thickness between 10 in. and 14 in. has only very little effect in the effective width as

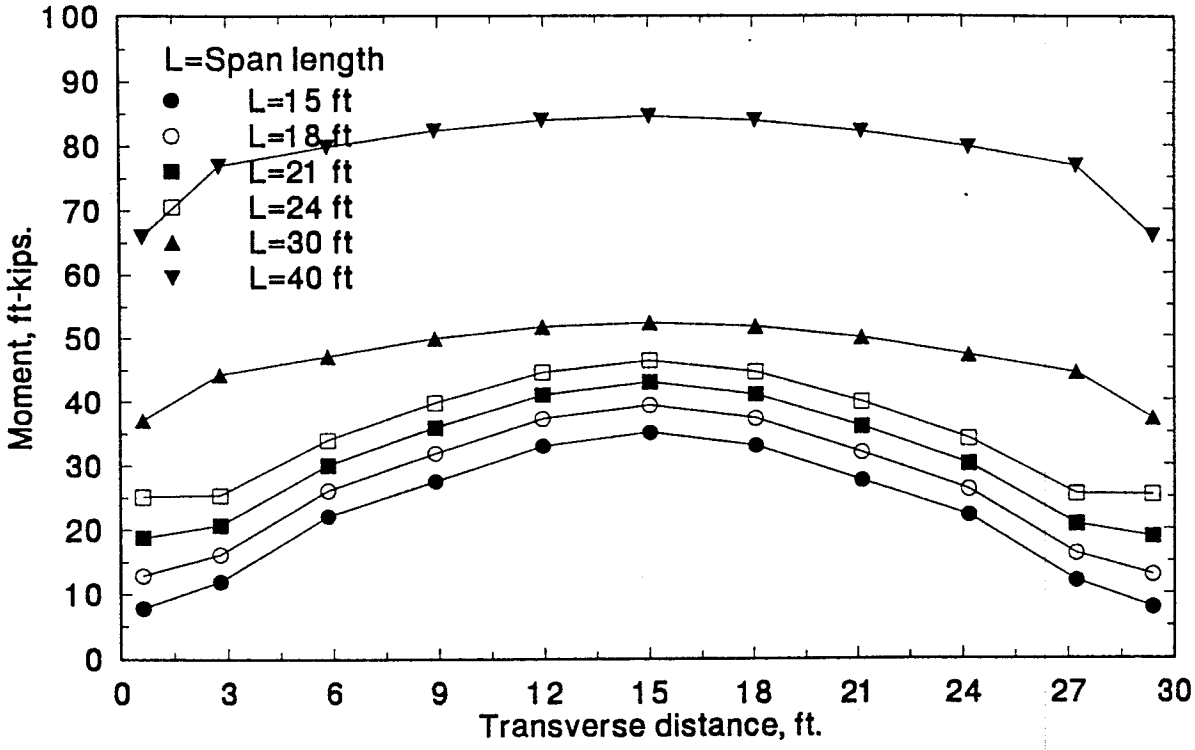

Fig. 4.5 Bending moment distributions for a typical solid slab bridge (different spans)

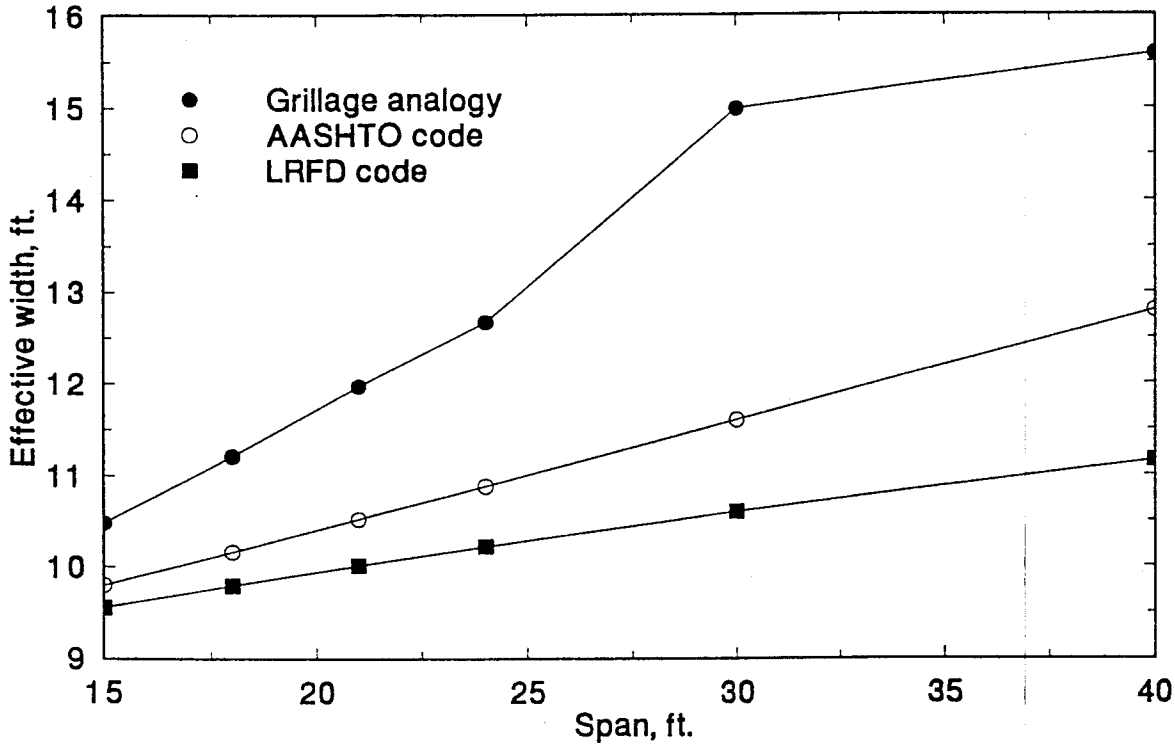

Fig. 4.6 Effective width variation with span length for solid slab bridges

shown in Figure 4.8. This confirms the approaches adopted by AASHTO and LRFD codes in neglecting the thickness as a parameter in effective width calculation.

4.3.3.4 Edge beam

AASHTO code requires that an edge beam should be provided for longitudinally reinforced slabs (main reinforcement parallel to traffic). The edge beam can be one of the following three types:

i) A slab section additionally reinforced,

ii) A beam integral with the slab and deeper than the slab,

iii) An integral reinforced section of slab and curb.

The edge beam of a slab bridge with simple span should be designed for a live load moment of 0.10 PS, where P = wheel load in pounds and S = span length in feet (AASHTO, 1989). One interpretation of this requirement of AASHTO could be that approximately 40% of the live load moment caused by one line of wheels (maximum moment for one line of wheel load in short spans is approximately 0.25 PS) should be added to other computed moments for the width selected for the edge beam. The width of edge beam as required by AASHTO specifications, should not exceed 3 ft.

The proposed LRFD code requires that the edge beams shall be assumed to support one lane of wheels, and where appropriate, a tributary portion of the design lane load (LRFD section 4.6.2.1.4a).

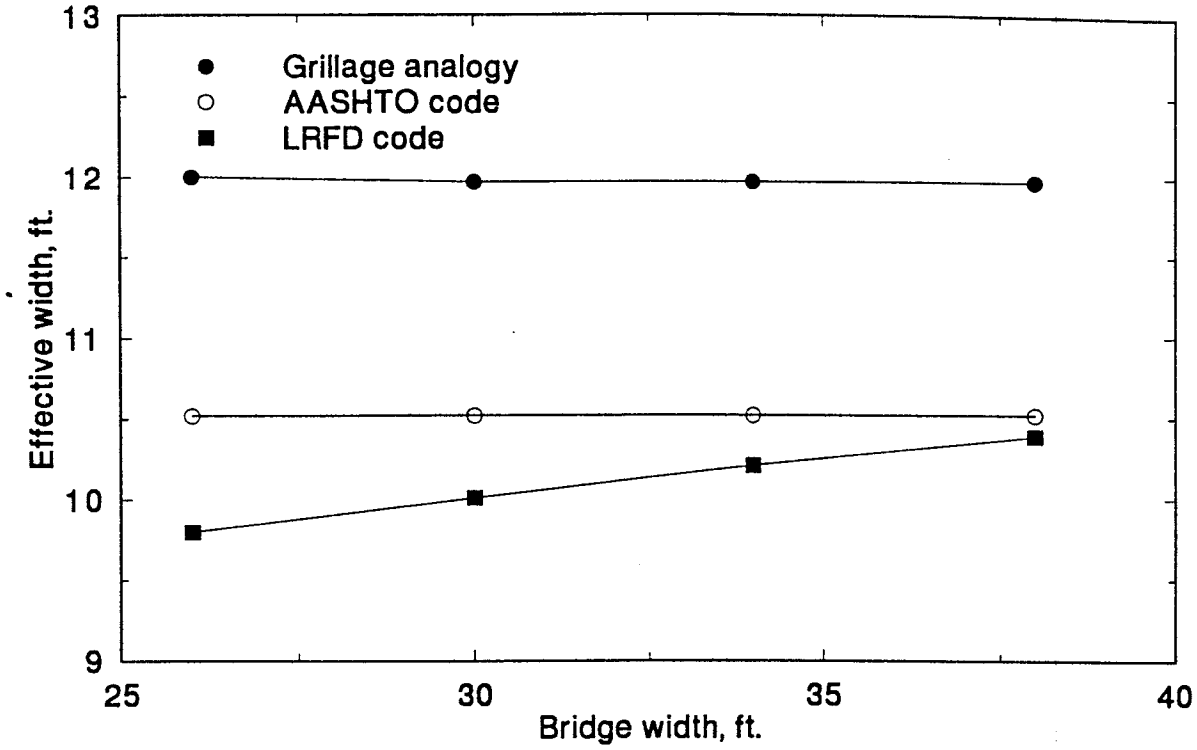

Fig. 4.7 Effective width variation with bridge width for solid slab bridges

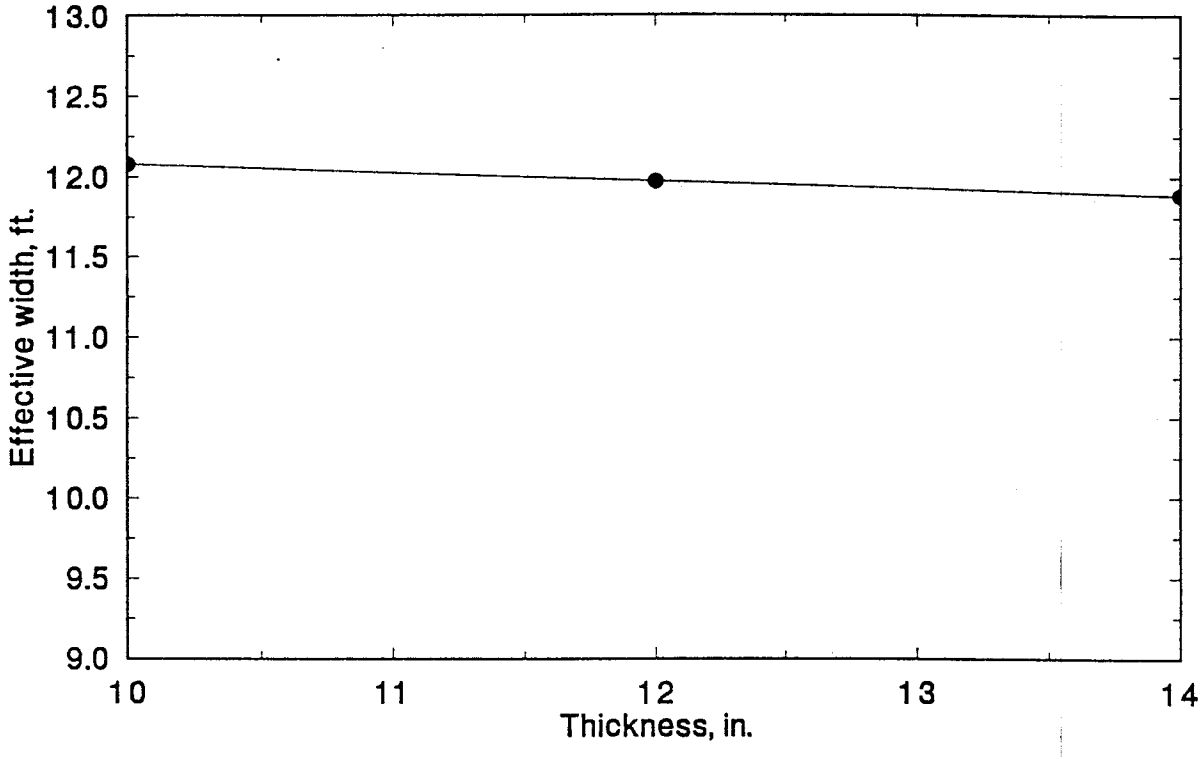

Fig. 4.8 Effective width variation with slab thickness for solid slab bridges

Although edge beam is a very important parameter in load distribution, it is neglected in both AASHTO and LRFD effective width calculations. Figures 4.9 and 4.10 show the bending moment distribution for different edge beam depths and widths respectively. The edge beam moment increases with increase in moment of inertia, i.e. increasing edge beam depth or width. As the edge beam moment increases, the maximum moment in the slab decreases and consequently the effective width, E increases as shown in Figures 4.11 and 4.12 respectively. The edge beam depth significantly affects the value of E as shown in Figure 4.11. Slab bridges without edge beams or with hidden edge beams have greater maximum moment than similar slab bridge with edge beam (Figure 4.13) and the resulting effective width is smaller as shown in Figure 4.14.

These results suggest that the edge beam size should be taken into account in wheel load distribution. Neither current AASHTO code nor the proposed LRFD code considers the edge beam inertia in the effective width equation. Table 4.3 summarizes the edge beam moments calculated using grillage analogy method for different edge beam sizes and compares them with AASHTO code requirements.

4.3.3.5 One lane slab bridges

One lane slab bridges are commonly used in highway intersection and exits. The current AASHTO code has one load distribution formula for both one lane and multilane bridges. The

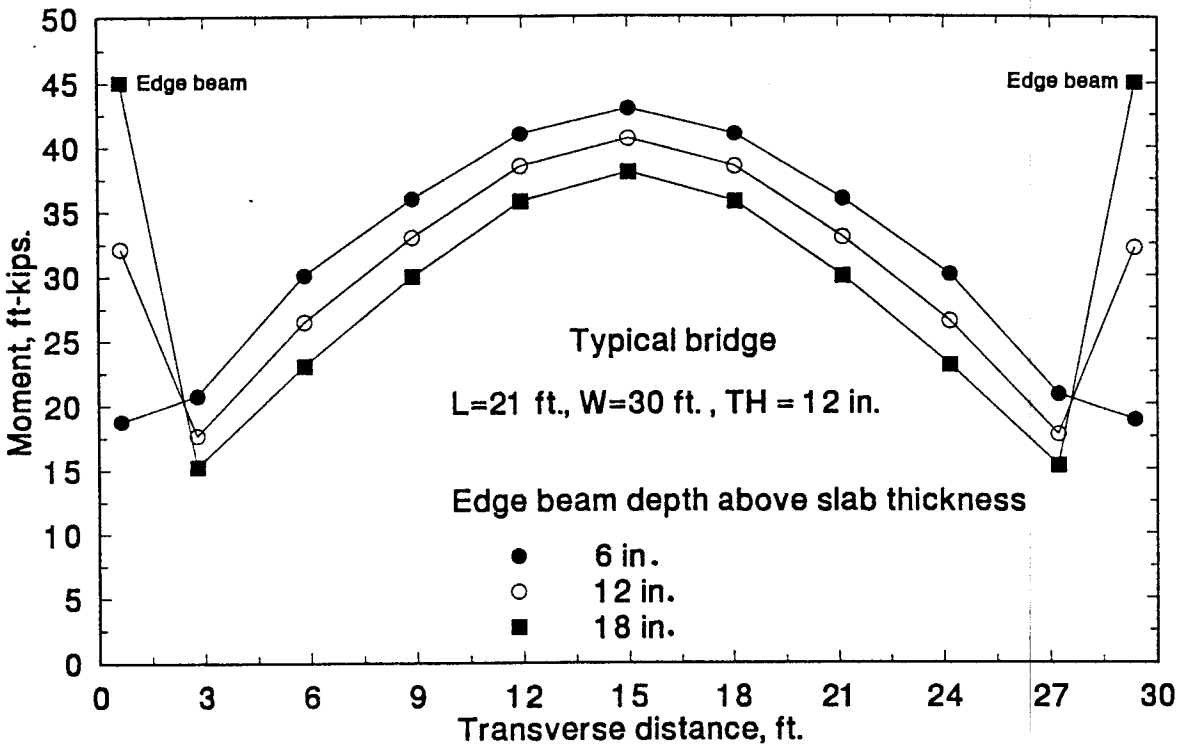

Fig. 4.9 Bending moment distributions for different edge beam depths

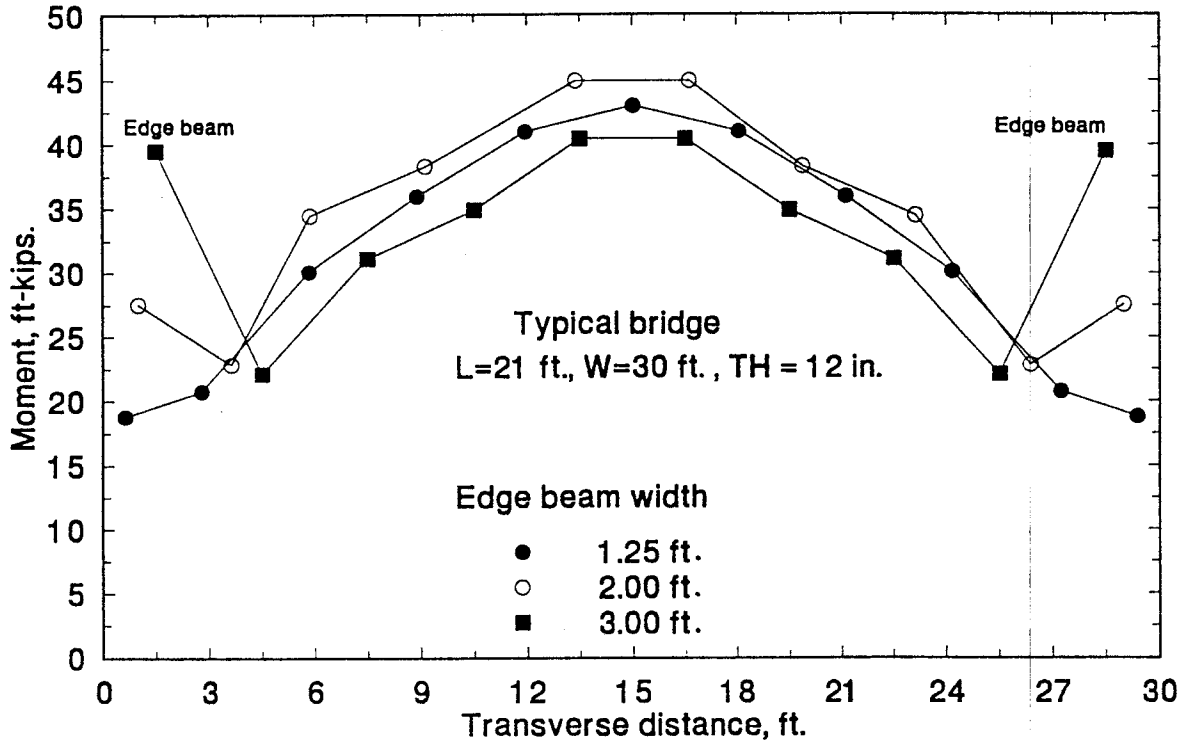

Fig. 4.10 Bending moment distributions for different edge beam widths

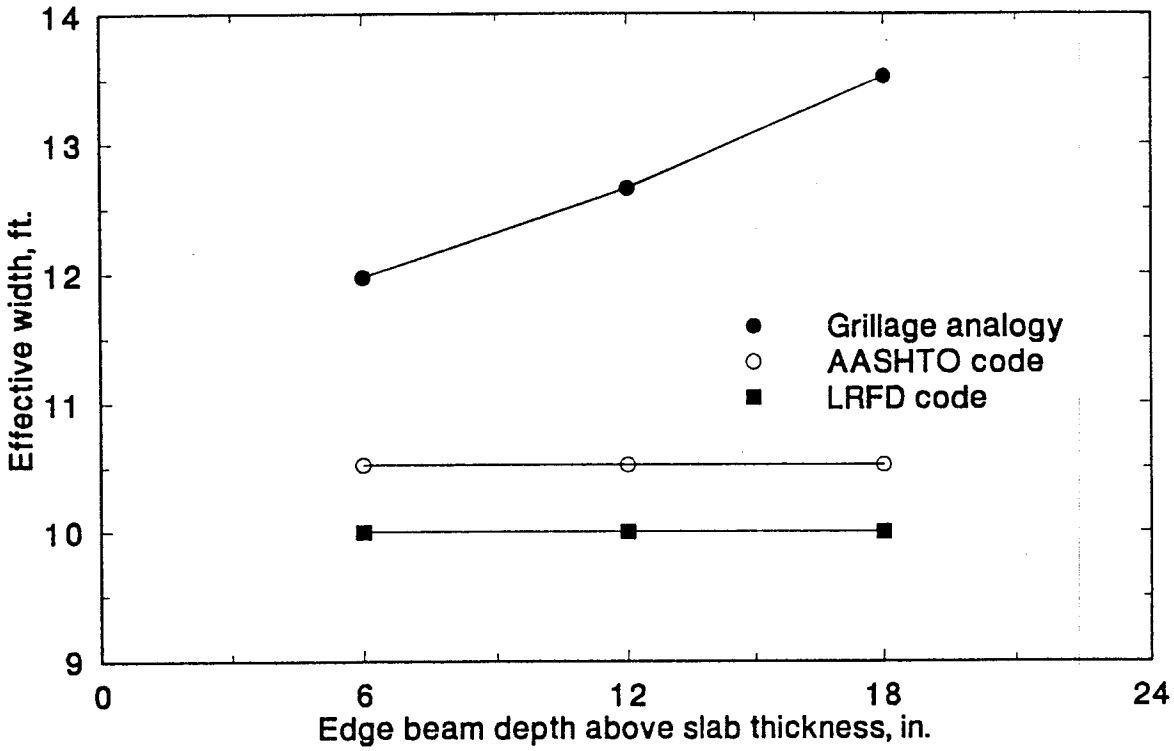

Fig. 4.11 Effective width variation for different edge beam depths

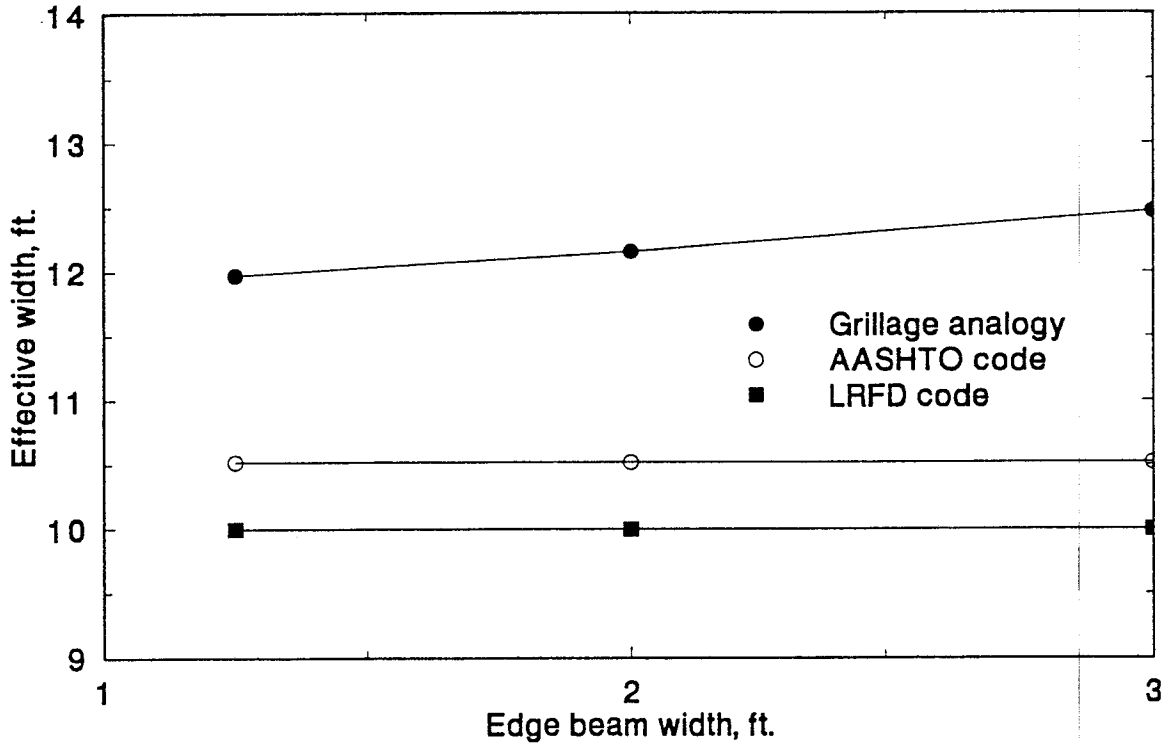

Fig. 4.12 Effective width variation for different edge beam widths

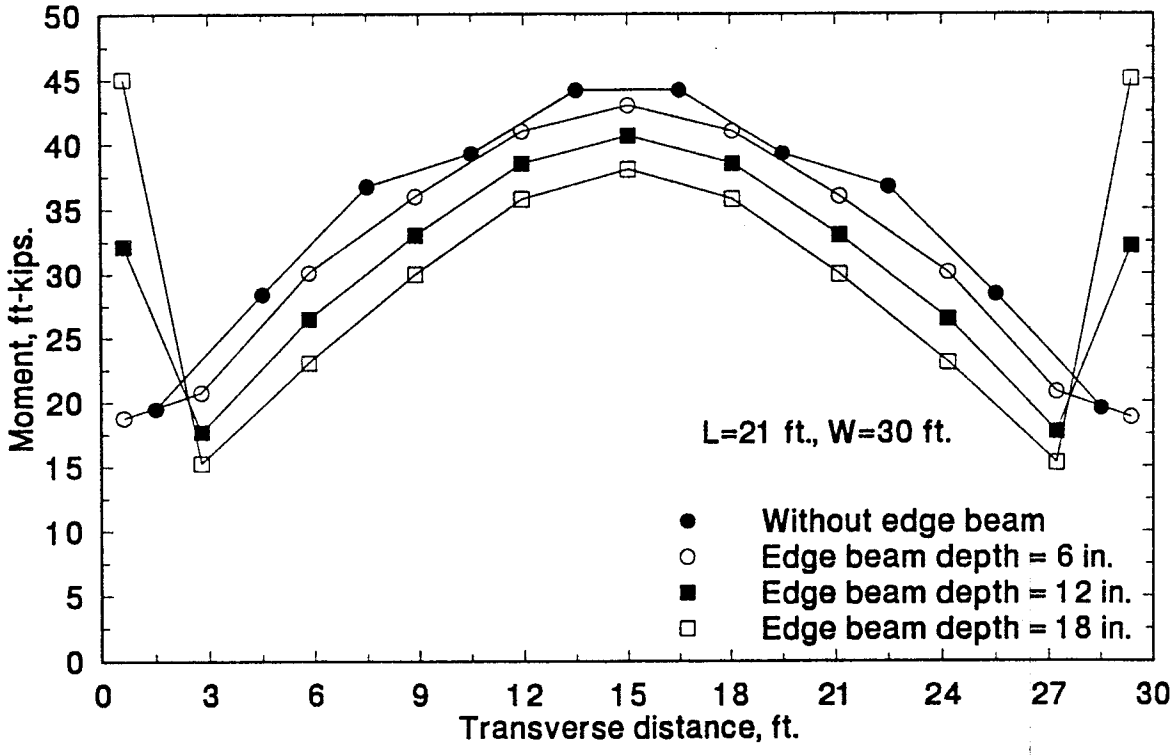

Fig. 4.13 Bending moment distributions for solid slab bridges with and without edge beams

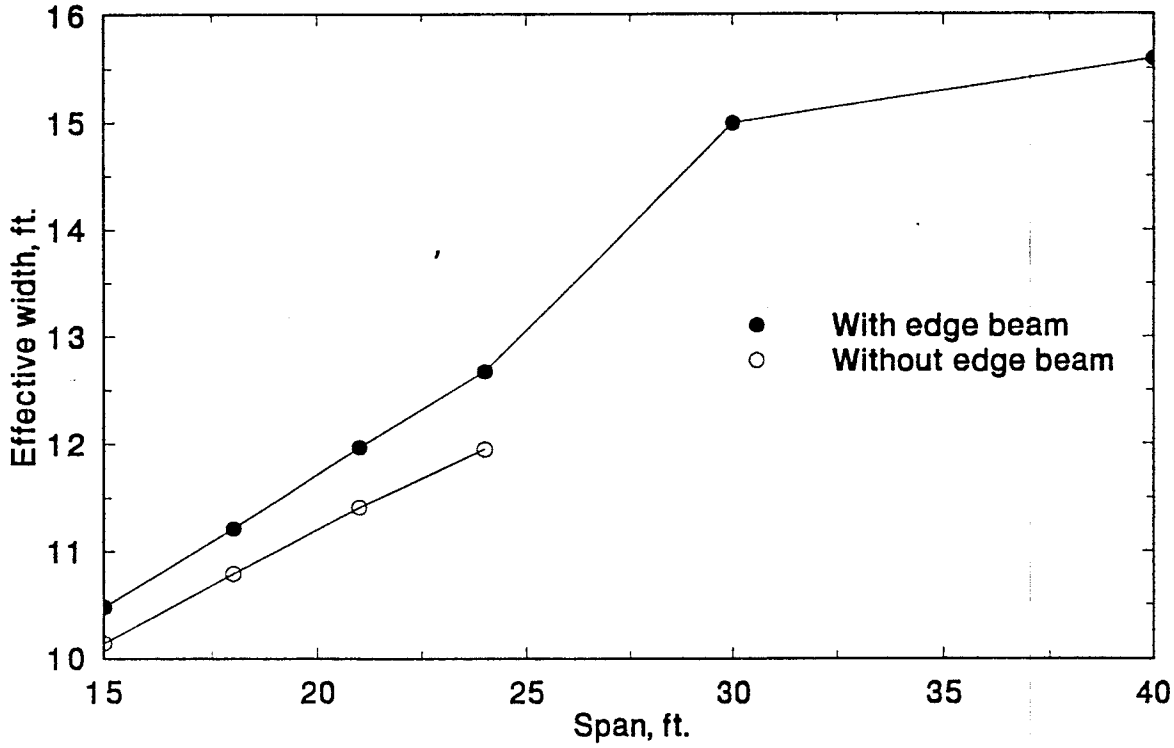

Fig. 4.14 Effective width variation for solid slab bridges with or without edge beams

Table 4.3 Summary of edge beam moments

Case		Grillage analogy method		AASHTO
Width, ft	Depth, in.	Moment, Kip-ft.	% of PS	
1.25	6.0	19.16	6.0	33.6
1.25	12.0	32.13	9.6	33.6
1.25	18.0	45.01	13.4	33.6
2.0	6.0	27.54	8.2	33.6
3.0	6.0	39.50	11.8	33.6

proposed LRFD code introduces different effective width equations for one lane and multi-lane bridges. The effective width, E for all one lane bridges investigated using grillage analogy was taken equal to the physical width, W because all the calculated values were more than the physical width. This means that E, from grillage analogy is equal 15 ft. for all spans and this value is higher than the AASHTO and LRFD code specified conservative values.

4.3.4 Proposed Simplified Effective Width for Solid Slab Bridges

Based on the solid slab parametric studies, the span length and the edge beam depth are the main parameters, which significantly affect the effective width calculations. For solid slab bridges without edge beams or with hidden edge beams (Fig. 4.15), the following equation based on the least square fit of the grillage analogy results for the effective width could be used for spans upto 40 ft. and slab thickness upto 14 in.:

$$E = 6.89 + 0.23\,L \qquad (4.4)$$

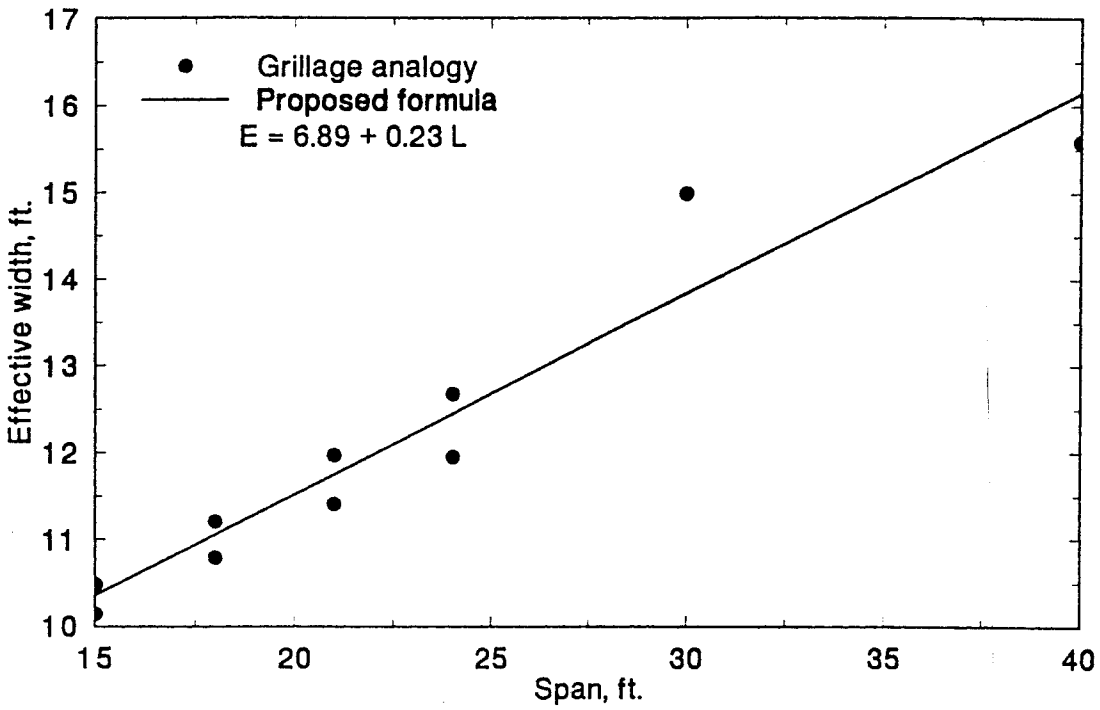

Fig. 4.15 Effective width variation based on the grillage analogy and the proposed formula

where

E = Effective width over which truck load is assumed to be uniformly distributed, ft.

L = Span length, ft.

The effect of edge beam depth above the slab thickness can be taken into consideration by multiplying the above equation by a factor C_{edge} given by

$$C_{edge} = 1.0 + 0.0125 (d_1 - 6.0) \quad (4.5)$$

where d_1 = Edge beam width above the slab thickness, in.

4.4 SOLID SLAB BRIDGE FIELD TESTS

Florida Department of Transportation (FDOT) have tested many solid slab bridges to check their strength and establish bridge ratings. The bridge structural elements are instrumented by placing strain or deflection transducer gages at the bridge deck critical locations, and then incrementally loaded to induce maximum effects. The data collected are then analyzed and used to establish the strength of each component as well as the load distribution.

The test vehicles are initially loaded with a number of concrete blocks of known weights, established from the preliminary analysis of the existing structure. The vehicles are then driven and placed on the critical locations of the bridge, while the data acquisition system monitors the strains and deflections during loading. After each load step, if the measured strains compare favorably with the theoretical prediction, additional blocks are added to the vehicles and the test

repeated until the ultimate AASHTO load is achieved. The data gathered can then be analyzed and a report on the bridge prepared.

Data from some solid slab bridge test reports would be used for load distribution analyses. The typical report contains transverse strain distributions in the maximum bending moment section for several loading stages. It also contains the applied moment vs. strain curves for several loading stages.

One method for use of test results in rating calculations is to use data to calculate wheel-load distribution factors, i.e. effective width, E. The measured effective width can be used in bridge-rating calculations in place of effective width defined by AASHTO.

In the present study, the measured strains will be multiplied by the slab section modulus and the elastic modulus to calculate the measured moments. The ACI equation was used to calculate the elastic modulus of concrete which is determined based on f'_c = 5000 psi. The measured bending moment distribution is used to calculate the measured effective width, which is compared with those based on AASHTO, LRFD and grillage analysis.

4.4.1 Palm Beach County Bridge (# 930086)

The bridge is located on S.R. 98 in Palm Beach County (Palm Beach, Florida). It consists of three simply supported spans with span lengths of 15 feet each. The overall length of the bridge is 45 ft. and the total width is 26 ft., 24 ft. curb to curb as shown in Figure 4.16. The

bridge is a concrete flat slab with 12 in. slab thickness, supported by concrete piles and concrete caps. Prior to load testing, an inspection of the bridge was conducted. The slabs, piles and pile caps along the entire length of the bridge appeared to be in good condition.

The measured strain distribution along the bridge width is shown in Figure 4.17 for different loading stages for combined loads on the left and right lanes. The maximum strain in the transverse direction could be seen to be at a distance of 6 ft. from the bridge center line. Figure 4.18 shows the moment intensities along the transverse direction calculated from the measured strains for the maximum load and those calculated using grillage analogy. Table 4.4 summarizes the effective widths calculated from measured strains and those from grillage analogy, AASHTO code, LRFD code and the proposed formula for bridges # 930086, # 380058 and # 740030. The measured effective width, E was equal to 10.14 ft. which is within 15% of the grillage analogy effective width. Both effective widths calculated from grillage analogy and measured strains are higher than the AASHTO and LRFD values. The effective widths based on the AASHTO and LRFD codes are more conservative. Effective width based on the proposed formula was within 6% of the effective width based on the measured strains.

4.4.2 Taylor County Bridge (# 380058)

The bridge is located on U.S. 27, in Taylor County (District II, Florida). It consists of two simply supported spans with span lengths of 15.25 ft. each. The overall length of the bridge is 30 ft. and the total width is 35 ft., 30 ft. curb to curb as shown in Figure 4.19. The bridge is a

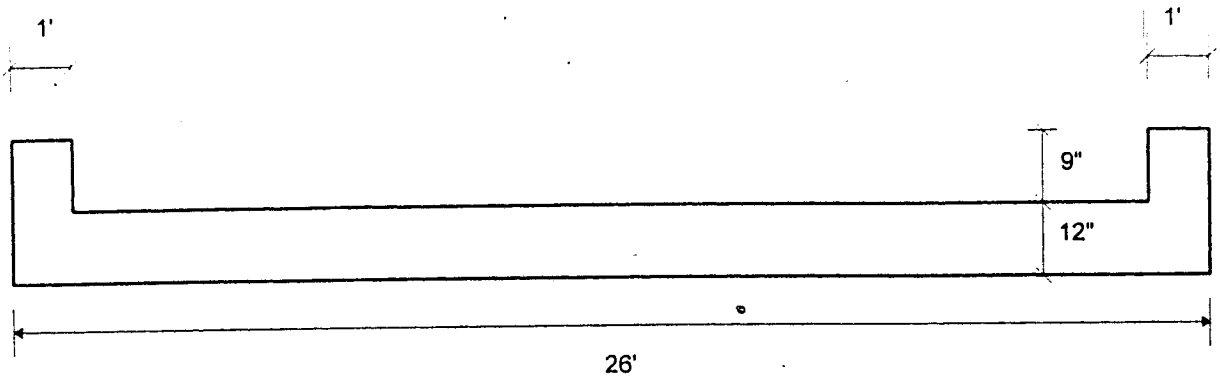

Fig. 4.16 Typical cross-section of solid slab bridge # 930086

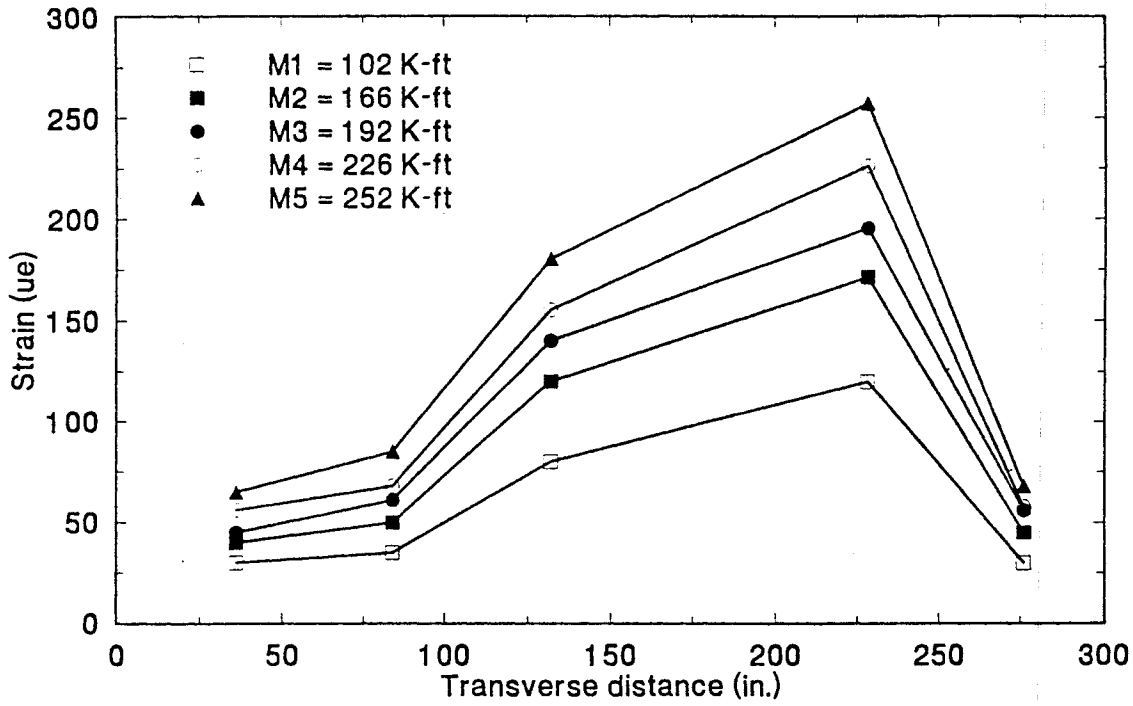

Fig. 4.17 Measured strain distributions for different applied loads (solid slab bridge # 930086)

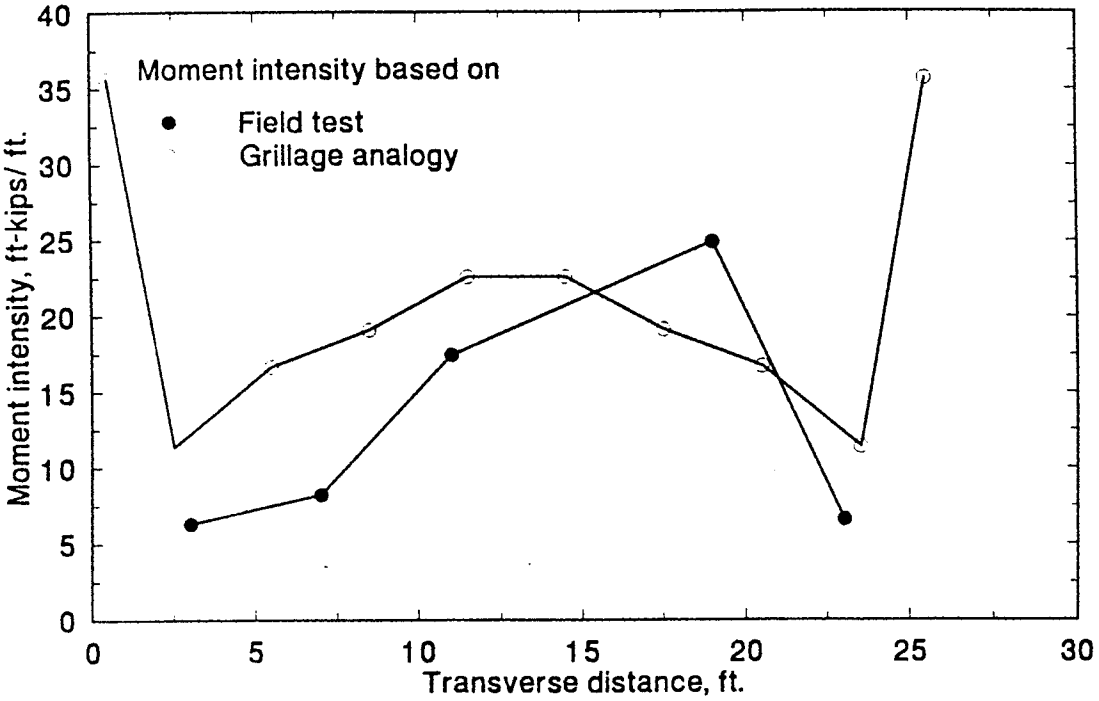

Fig. 4.18 Bending moment intensities based on field test and grillage analogy (solid slab bridge # 930086)

Comparisons between similar solid and voided slab bridges were made to examine the assumption that both solid and voided slab bridges have the same effective width. The grillage analogy method was used in the comparisons. The grillage analogy program for voided slab bridges has six standard sections shown in Figure 4.25 as data base.

Two comparisons were made using the grillage analogy method. In the first case, the span length and bridge width were 21 ft. and 30 ft. respectively. The solid slab thickness equal to 15 in. and voided slab element type No. 1 with slab thickness equal to 15 ft. were used in the first comparison. Both bridges were subjected to AASHTO HS-20 truck loadings. The second comparison is similar to the first except the span length was 30 ft. and the slab thickness 18 in. Figures 4.26 and 4.27 show the bending moments of both solid and voided slab bridges for the first and second comparison respectively. It is clear that the maximum bending moment for solid slab is smaller than that for voided slab, which means the solid slab has larger effective width than voided slab bridges. The difference in effective widths of solid and voided slab bridges may be attributed to the relative vertical movements between the voided slab precast units. This can be observed from the presence of longitudinal cracks in the bridge. Table 4.5 summarizes the effective widths for solid and voided slab bridges. The voided slab effective widths were smaller by about 15 percent than the recommended values in the AASHTO and proposed LRFD codes. Both AASHTO and LRFD gives relatively smaller maximum bending moment for voided slab bridges than that from grillage analogy.

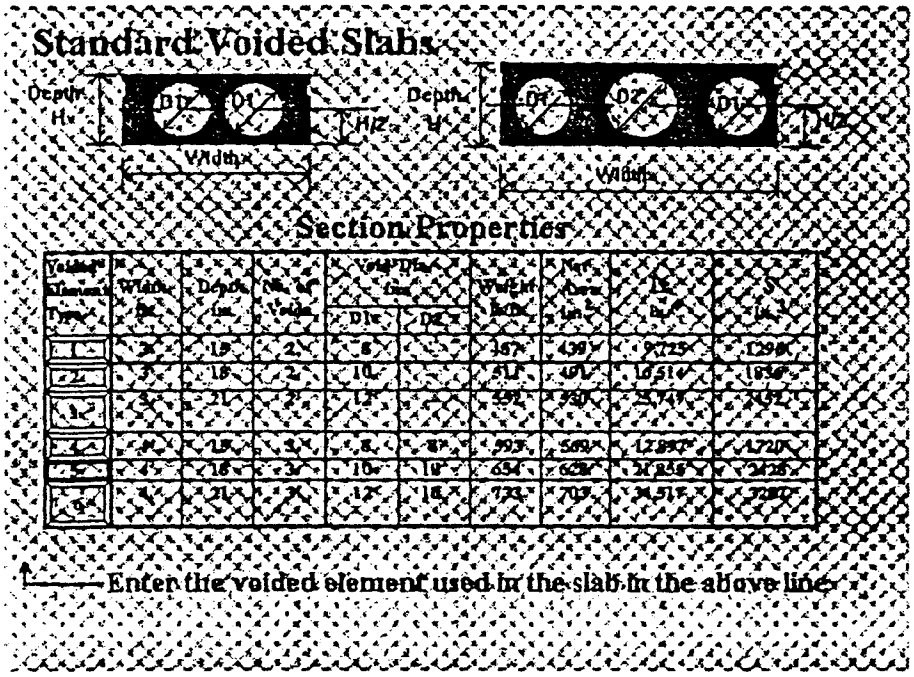

Fig. 4.25 Standard voided slab sections

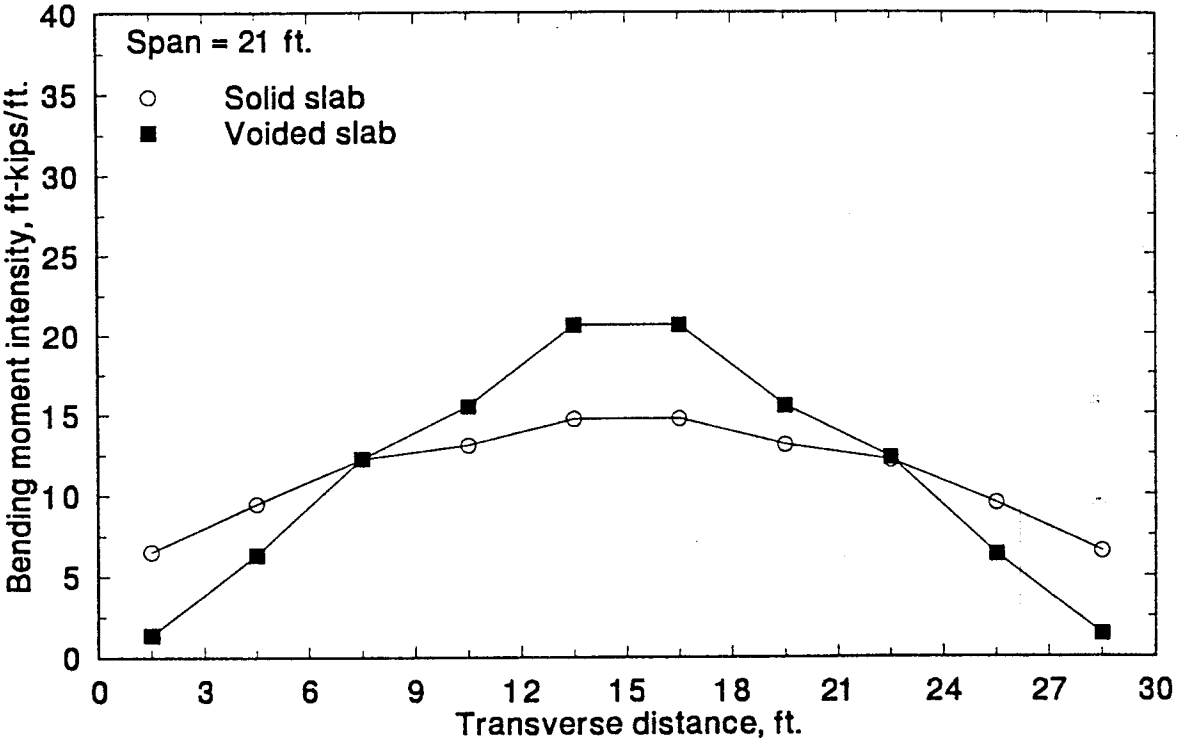

Fig. 4.26 Bending moment intensities for identical solid and voided slab bridges (L = 21 ft.)

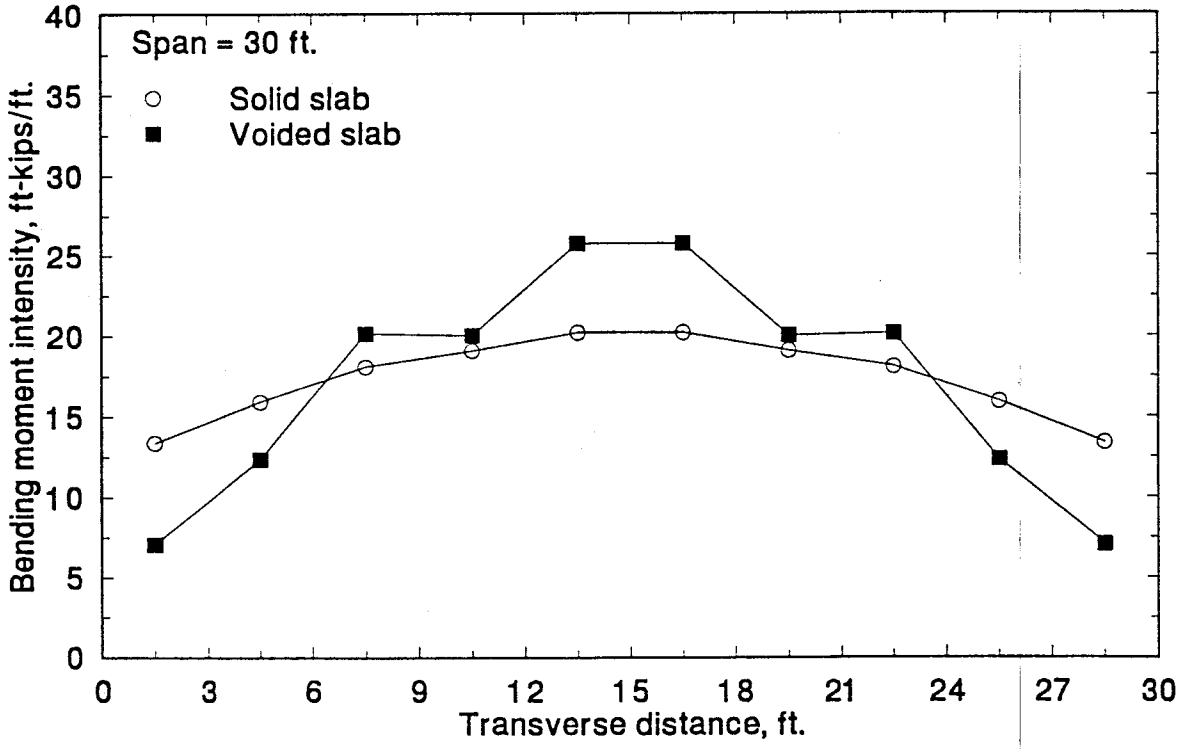

Fig. 4.27 Bending moment intensities for identical solid and voided slab bridges (L = 30 ft.)

Table 4.6 Effective width comparison for solid and voided slab bridges

	Case 1	Case 2
Solid slab	11.41	12.65
Voided Slab	8.17	9.93
AASHTO code	10.52	11.6
LRFD code	10.01	10.6

4.6 VOIDED SLAB BRIDGE FIELD TESTS

Florida Department of Transportation (FDOT) have tested many voided slab bridges to check the strength and establish bridge ratings. The bridge elements are instrumented by placing strain or deflection transducer gages at the bridge critical locations, and then incrementally loaded to induce maximum effects. The data collected are then analyzed and used to establish the strength of each component as well as the load distribution.

Data from certain voided slab bridge test reports are used for load distribution analyses. The typical report contains transverse strain distributions in the maximum bending moment section for several load stages. The typical report also contains the applied moment vs. strain curves for different load stages.

One method for use of test results in rating calculations is to use the test data to calculate wheel load distribution factors, i.e. effective width, E. The measured effective width can be used in bridge rating calculations in place of effective width defined by AASHTO. AASHTO (Guide specifications 1989) has also presented a refined bridge rating methodology in which measured wheel load distribution factors can be used. The measured strains are multiplied by the voided slab section modulus and elastic modulus to calculate the measured moments. The ACI equation was used to calculate the elastic modulus of concrete based on f'_c = 5000 psi. The measured moment distributions are used to calculate the measured effective width and compared with those based on AASHTO and the proposed LRFD codes.

4.6.1 Collier County Bridge (# 030170)

The bridge is located over Macilvan Bay in Collier County (Bartow, Florida). It consists of five simply supported spans with span lengths of 40 ft. each. The overall length of the bridge is 200 ft. and the total width is 34 ft. 8 in., 24 ft. curb to curb. Each span consists of eight 4 ft. wide voided slab units tied together in the transverse direction as shown in Fig. 4.28. The bridge deck thickness is 15 in. and supported by concrete piles and caps. Prior to load testing, an inspection of the bridge was conducted. Several damages were observed in the side walks, piles and bent caps.

The measured strain distribution along the bridge width is shown in Figure 4.29 for different load stages. The maximum strain in the transverse direction was observed at a distance

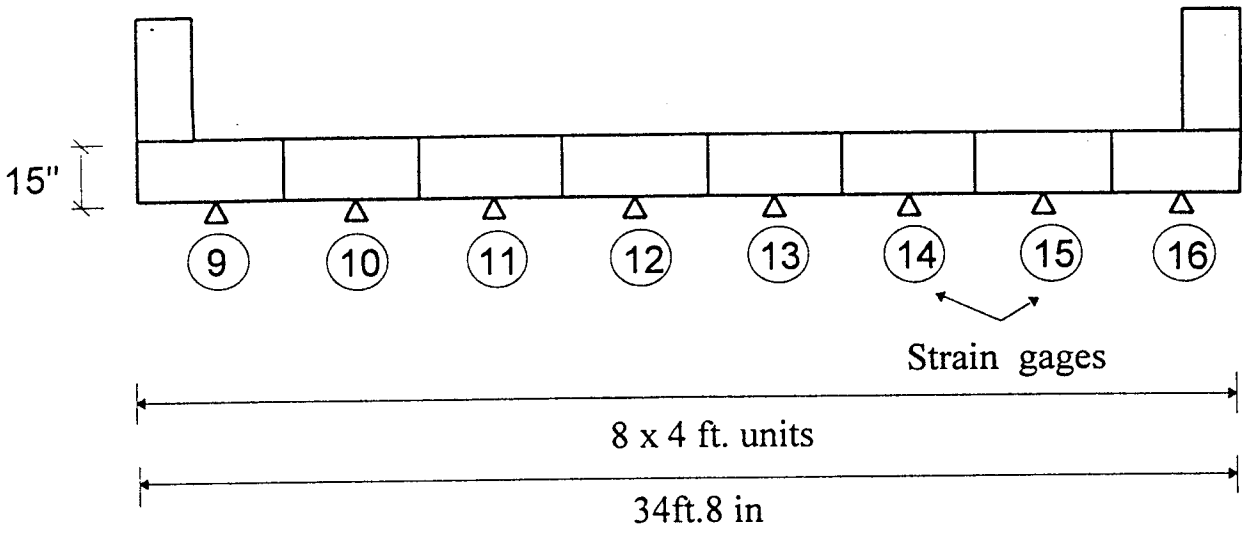

Fig. 4.28 Typical cross-section of voided slab bridge # 030170

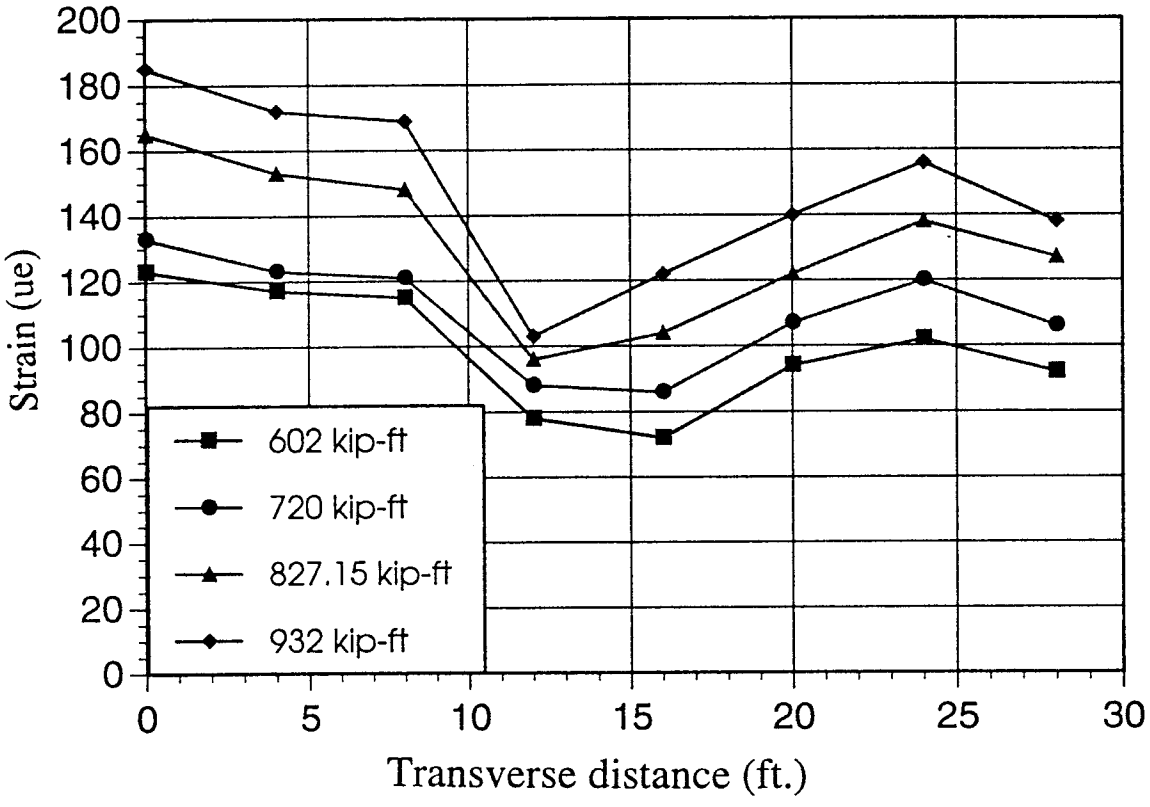

Fig. 4.29 Measured strain distributions for different applied loads (voided slab bridge #030170)

of 2 ft. from the bridge edge. Figure 4.30 shows the moment intensities along the transverse direction calculated from the measured strains for the maximum load and those calculated using grillage analogy. It is clear that the predicted values from the grillage analogy do not compare well with the measured values. This may be due to the relative vertical movement between the precast voided slab units caused by insufficient transverse prestress. The inaccurate prediction may also be due to the observed cracks and damages in the bridge, which needs nonlinear finite element analysis for accurate prediction of the bending moments. Table 4.7 summarizes the effective widths based on the measured strain, AASHTO code, LRFD code and proposed equation (It is derived for solid slab and it may be applicable for voided slab) for bridge numbers 030170, 720435 and 890135. Effective width calculated from measured strains is slightly smaller than AASHTO and slightly larger than LRFD values.

4.6.2 Duval County Bridge (#720435)

The bridge is located over Cedar Creek on San Juan Avenue, in Duval County (Jacksonville, Florida). It consists of eight simply supported spans with span lengths of 42.0 ft. each. The overall length of the bridge is 336 ft and the total width is 65 ft. 8 in., 52 ft. curb to curb as shown in Figure 4.31. The bridge is made of voided slab units, each unit is 4 ft. wide and 18 in thickness. Prior to load testing, an inspection of the bridge was conducted. The slabs, piles and pile caps along the entire length of the bridge appeared to be in good condition.

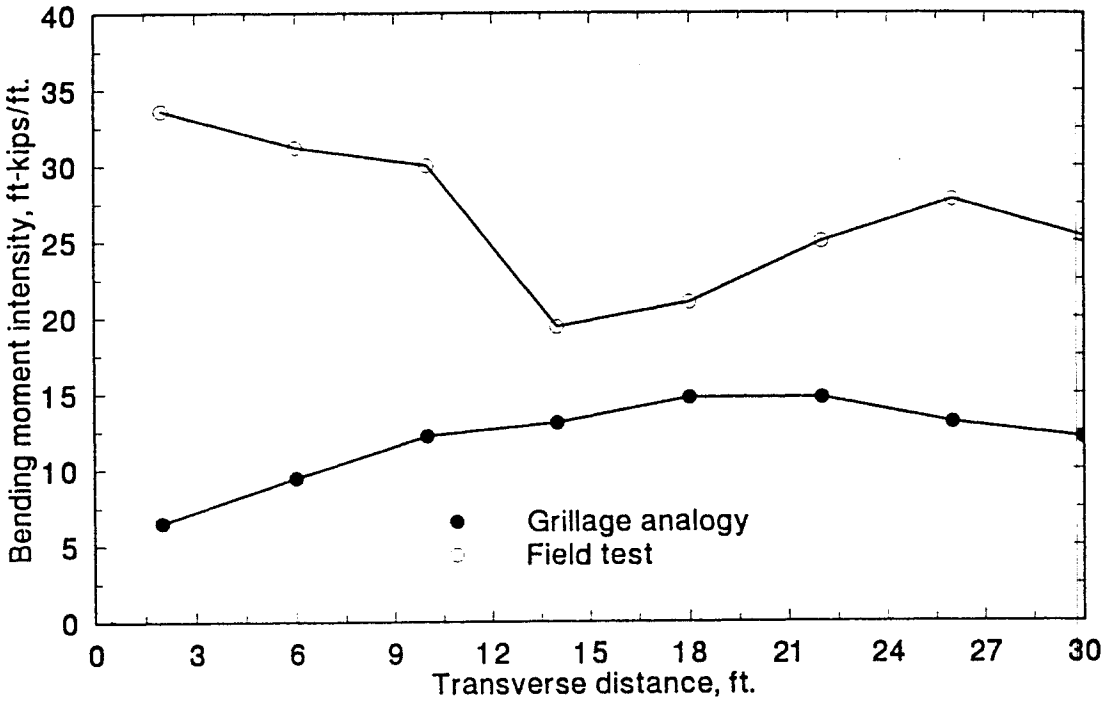

Fig. 4.30 Bending moment intensities based on field test and grillage analogy (voided slab bridge # 030170)

The measured strain distribution along the bridge width is shown in Figure 4.32 for different load stages. The maximum strain in the transverse direction was observed at a distance of 11 ft. from the bridge centerline. Figure 4.33 shows the moment intensities along the transverse direction calculated from the measured strains for the maximum load and those calculated using grillage analogy. Effective widths calculated based on measured strains are higher (20%) than those based on AASHTO and LRFD codes (Table 4.7).

4.6.3 Martin County Bridge (#890135)

The bridge is located on S.R. 710 west, in Martin County (Stuart, Florida). It consists of one simply supported span. The overall length of the bridge is 40 ft. and the total width is 41.5 ft., 38 ft. curb to curb. The bridge is made of ten voided slab units, 4 ft. wide with 18 in. reinforced joint (Fig. 4.34). The superstructure is supported by concrete bents and bent caps with a slab thickness of 18 in. The slabs, piles and pile caps along the entire length of the bridge appeared to be in good condition. There are some longitudinal cracks in the asphalt due to the voided slab units. Also, there are some concrete spalling at R.C joint.

The measured strain distribution along the bridge width is shown in Figure 4.35 for different load stages. The maximum strain in the transverse direction was observed at a distance of 3.25 ft. from the bridge centerline. Table 4.7 summarizes the results of the effective widths based on measured strains, AASHTO and LRFD. The measured effective width, E is higher than those calculated based on AASHTO and LRFD codes.

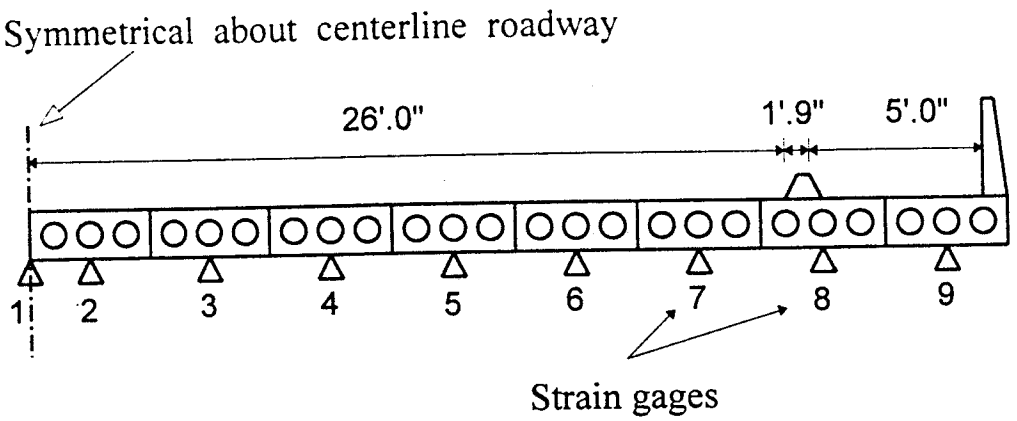

Fig. 4.31 Typical cross-section of voided slab bridge # 720435

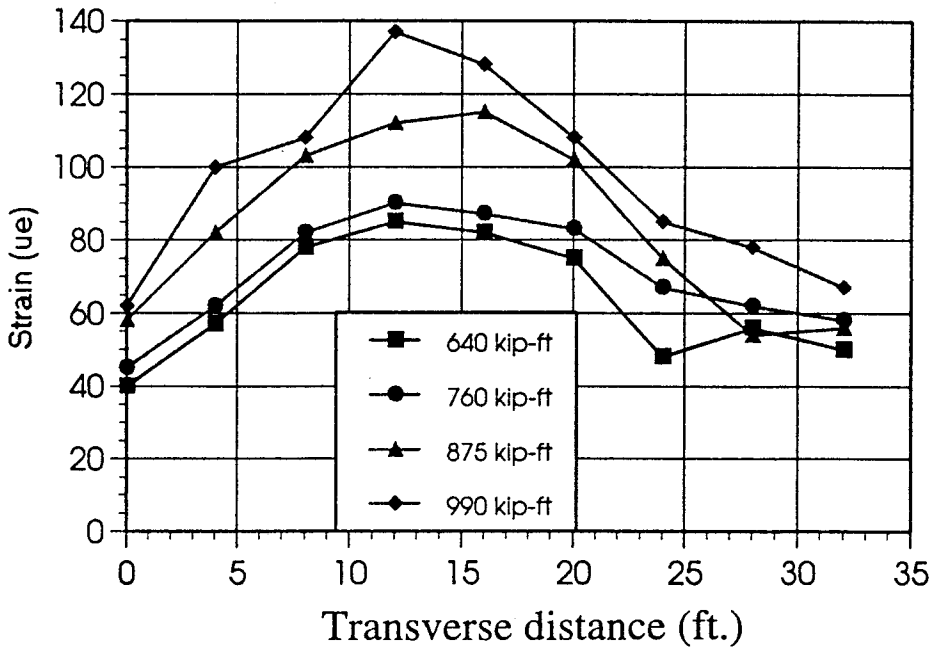

Fig. 4.32 Measured strain distributions for different applied loads (voided slab bridge # 720435)

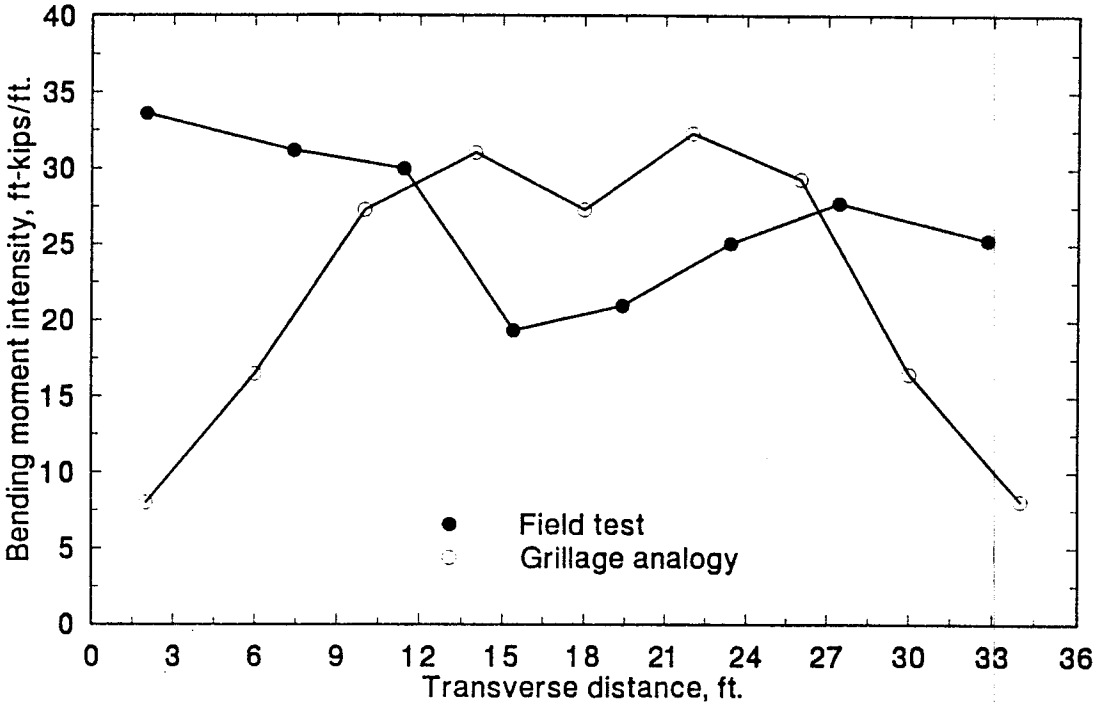

Fig. 4.33 Bending moment intensities based on field test and grillage analogy (voided slab bridge # 720435)

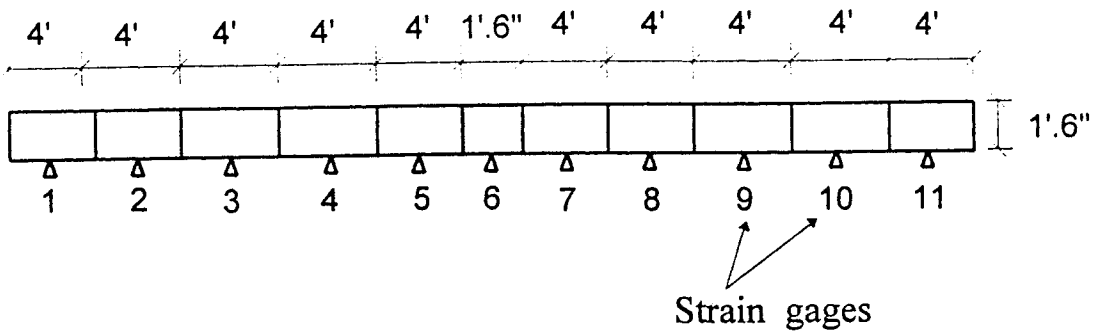

Fig. 4.34 Typical cross-section of voided slab bridge # 890135

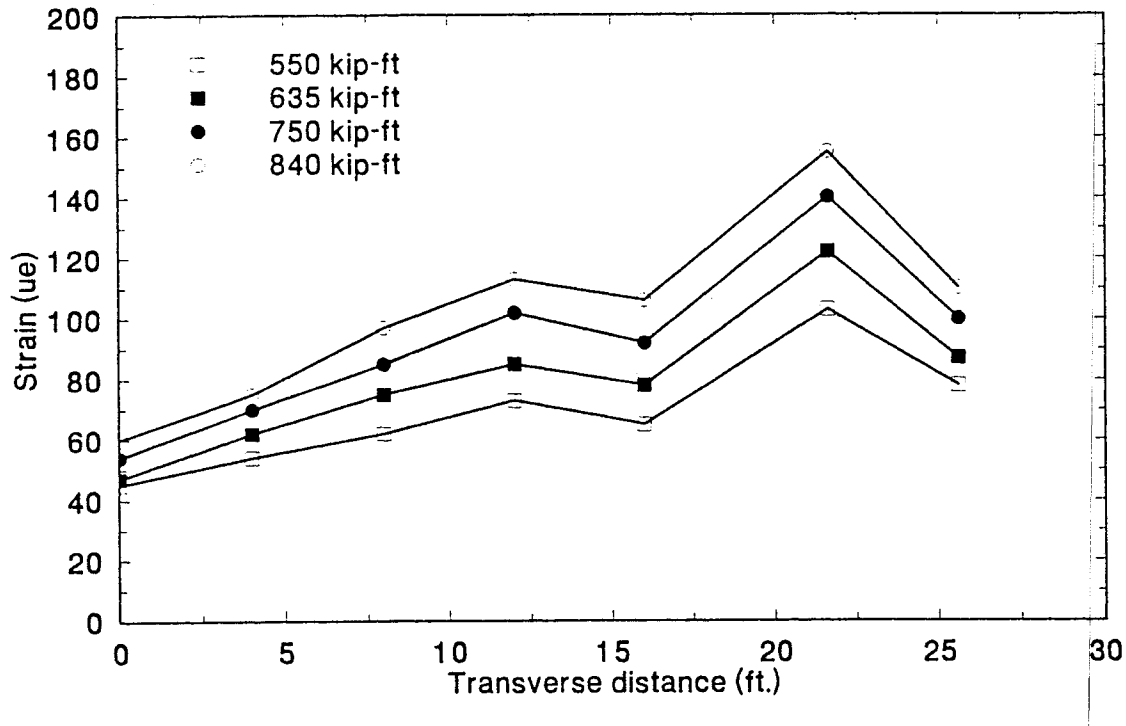

Fig. 4.35 Measured strain distributions for different applied loads (voided slab bridge # 890135)

Table 4.7 Summary of effective width, E for the voided slab field tests

Bridge	Measured strains	AASHTO code	LRFD code	Proposed formula
#030170	12.30	12.8	11.46	16.09
#720435	15.63	13.04	13.3	16.55
#890135	13.3	12.8	11.89	16.55

CHAPTER 5

LOAD DISTRIBUTION ANALYSES OF SLAB-ON-GIRDER BRIDGES

5.1 INTRODUCTION

The slab-on-girder bridges are the most common type of bridges throughout the United States. The precast concrete girders such as standard precast AASHTO I-girders and precast bulb-Tee sections are efficient and very economical. The precast concrete girders are often used with a cast-in-place deck to form the riding surface. The major restrictions to precast girder construction are the limitations in the length and weight. The slab-on-girder bridges are practical for spans up to 120 ft. for AASHTO I-girders whereas the bulb-Tee girders are ideal for spans up to 150 ft.

Analyses performed during design of slab-on-girder bridges are commonly based on the AASHTO wheel load distribution factors. There is a substantial amount of literature that illustrates the conservatism in using the AASHTO wheel load distribution factors (Heins and Lawrie, ,1984 and Warren and Malvar, 1993). This led the NCHRP to develop and propose the LRFD simplified load distribution factors. However, advances in computing technology have facilitated the use of refined analysis methods. In some cases, it is desirable to perform a more advanced structural analysis. This is especially true, when an evaluation of the load capacity of an existing bridge is

being made. Analysis based on grillage analogy is very common and it has been shown to give results very nearly the same as more advanced finite element analyses.

Truck load distributions of slab-on-girder bridges based on grillage analogy and field tests performed by Florida Department of Transportation (FDOT) are investigated in this chapter. The objectives of this investigation are:

i) Determine the load distribution using grillage analogy and study the effects of girder spacing, span length, bridge width, slab thickness, exterior and interior beams and other parameters on truck load distribution,

ii) Verify the current AASHTO and the proposed LRFD load distribution factors using several slab-on-girder bridge field tests,

iii) Derive simple empirical design criteria for load distribution that would provide more accurate alternative to current designs.

5.2 METHOD OF ANALYSIS

The AASHTO procedure to calculate the flexural distribution factors is generally used for bridge design by DOT's and tends to be overly conservative particularly for analysis and rating of existing bridges. The current AASHTO method of load distribution reduces the complex analysis of a bridge subjected to one or more vehicle to the simple analysis of a beam. According to this method, the maximum moment in a girder can be obtained by treating a girder as a one-dimensional beam subjected to a loading, which is obtained by multiplying one line of wheels of the design

vehicle by a load fraction (S/D) where S is average beam spacing in ft. The quantity D in the AASHTO specifications for concrete floor on prestressed concrete girders is 7 for one lane bridges and 5.5 for multi-lane bridges. If S exceeds 10 ft. for one lane bridges and 14 ft. for multi-lane bridges, the load in each girder shall be the reaction of the wheel loads, assuming the flooring between the girders to act as a simple beam. The AASHTO equation is based substantially on the research carried out by Newmark (1948). The AASHTO equation considers spacing as the only parameter and neglects the other important parameters.

The proposed LRFD approach is similar to AASHTO method, but considers more parameters such as span length, bridge width, slab thickness and number of lanes. The LRFD approach is based on NCHRP project 12-26 entitled, "Distribution of Wheel Loads on Highway Bridges", which was performed in two phases by Imbsen and Associates, Inc. The proposed LRFD approach for slab-on-girder bridges gives different distribution factors for bending and shear. The distribution of live loads on precast concrete AASHTO I and bulb-Tee section is categorized under the same category as "K" in the LRFD. The LRFD distribution of live load moment in interior beams per lane is given as

One Design Lane Loaded

$$g = 0.5\,[\,0.12 + (\frac{S}{2.5})^{0.4}\,(\frac{S}{L})^{0.3}\,(\frac{K_g}{12.0\,L\,t_s^{3}})^{0.1}\,] \qquad \textbf{(5.1)}$$

Two or More Design Lanes Loaded

$$g = 0.5\,[\,0.15 + (\frac{S}{3.0})^{0.6}\,(\frac{S}{L})^{0.2}\,(\frac{K_g}{12.0\,L\,t_s^3})^{0.1}\,] \qquad \textbf{(5.2)}$$

where

S = Spacing of supporting beams ($3.5 < S < 16.0$), ft.

L = Span length ($20 < L < 240$), ft.

t_s = Depth of concrete slab ($4 < t_s < 12$), in.

K_g = Longitudinal stiffness parameter.

$= n\,(I + A\,e_g^2)$

n = Modular ratio between beam and deck materials.

I = Inertia of the beam, in^4.

A = Area of the beam, in^2.

e_g = Distance between the centers of gravity of the basic beam and deck, in.

The live load moment for exterior beams may be determined by applying the lane fraction, $g_{exterior}$.

$$g_{exterior} = e\ g_{interior} \qquad \textbf{(5.3)}$$

where

$$e = \frac{7 + d_e}{9.1} \geq 1.0$$

where

d_e = Distance between the center of exterior beam and the interior edge of curb or traffic barrier ($-1.0 < d_e < 5.5$), ft.

The proposed LRFD distribution of live load per lane for shear in interior beams is given as

One Design Lane Loaded

$$g = 0.36 + \frac{S}{25.0} \qquad (5.4)$$

Two or More Design Lanes Loaded

$$g = 0.5\,[\,0.4 + \frac{S}{6.0} - (\frac{S}{25})^{0.2}\,] \qquad (5.5)$$

The live load flexural shear for exterior beams may be determined by applying the lane fraction, $g_{exterior}$.

$$g_{exterior} = e\ g_{interior} \qquad (5.6)$$

where

$$e = \frac{6 + d_e}{10.0}$$

Both analytical and field studies on the truck load distribution of slab-on-girder bridges are presented in this chapter. Grillage analogy explained in Chapter 3 is used to study the various

parameters affecting load distribution and suggest which parameters must be considered. In addition to the analytical study, data from field tests performed by Structures Research Center, FDOT, are used to verify the results from the analytical study.

5.2.1 Load Distribution Factor

A load distribution factor may be calculated from the moments of each girder determined from grillage analyses or field tests. The sum of internal moments is equivalent to externally applied moment due to the concentrated loads. The distribution factor, DF is equal to the ratio of maximum girder moment obtained from grillage analysis or field test to the maximum moment in the bridge idealized as a one-dimensional beam subjected to one set of wheels.

5.2.2 Distribution Patterns of Different Responses

If the bending moment diagrams for all longitudinal girders have exactly the same shapes, then the distribution factor for moments remains constant along the span and for a given longitudinal beam, the distribution factor for moments is the same as that for shears. However, even very small differences in the shapes of the bending moment diagrams have a significant influence on the differences between the distribution factors for different responses. Responses corresponding to higher derivatives of deflection have a steeper distribution than those corresponding to lower derivatives. The difference between the distribution factor for moments and shears can sometimes become so large that special attention has to be given for shear distribution factors.

5.3 SLAB-ON-AASHTO GIRDER FLEXURAL LOAD DISTRIBUTION FACTORS: PARAMETRIC STUDIES

It is important to understand the effect of various parameters on flexural load distribution. Several parameters affect the load distribution of slab-on-girder bridges. Girder spacing, span length, bridge width, girder type, and number of lanes are the main parameters which are considered in this section. Bridge parameters are varied one at a time in a typical bridge. Variation of wheel load distribution factors with each parameter shows the relative importance of the parameters. Figure 5.1 shows the typical slab-on girder bridge cross section used in the analysis. The typical slab-on-girder bridge has a span length equal to 90 ft. with a bridge width of 54 ft. It has prestressed AASHTO girders type IV with a slab thickness of 7 in. The concrete strengths of both the girder and slab were taken equal to 5000 psi.

Grillage Analysis

The typical slab-on-girder bridge shown in Figure 5.1 is divided into elements in the longitudinal and transverse directions as shown in Figure 5.2. The eight longitudinal elements coincided with each girder center line. In this study, each girder was divided into eight elements. Elements in the transverse direction were chosen along the longitudinal nodes as shown in Figure 5.2.

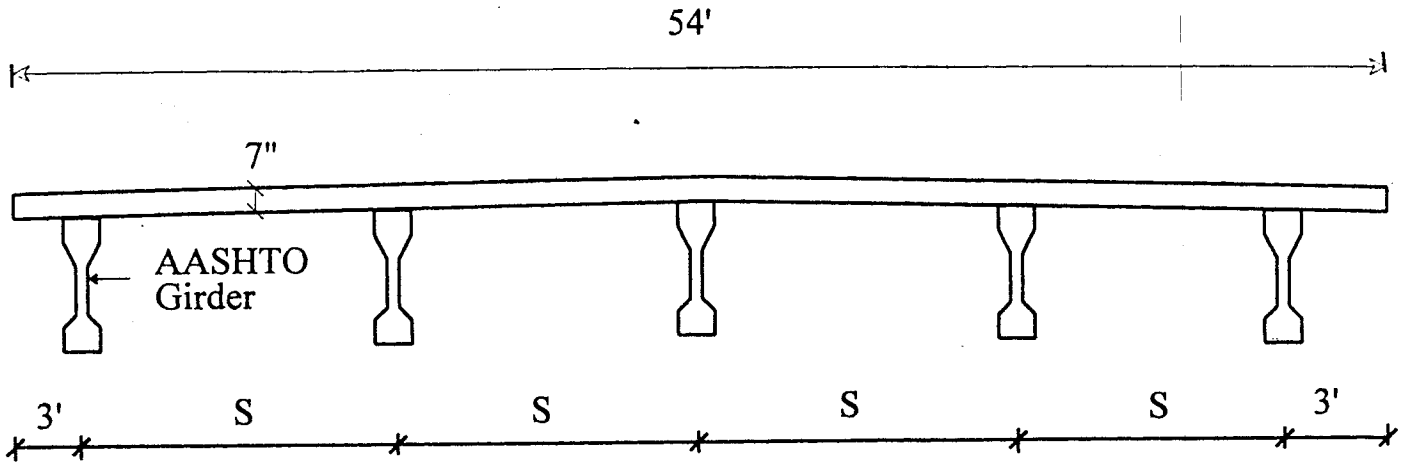

Fig. 5.1 Typical slab-on-girder bridge cross-section

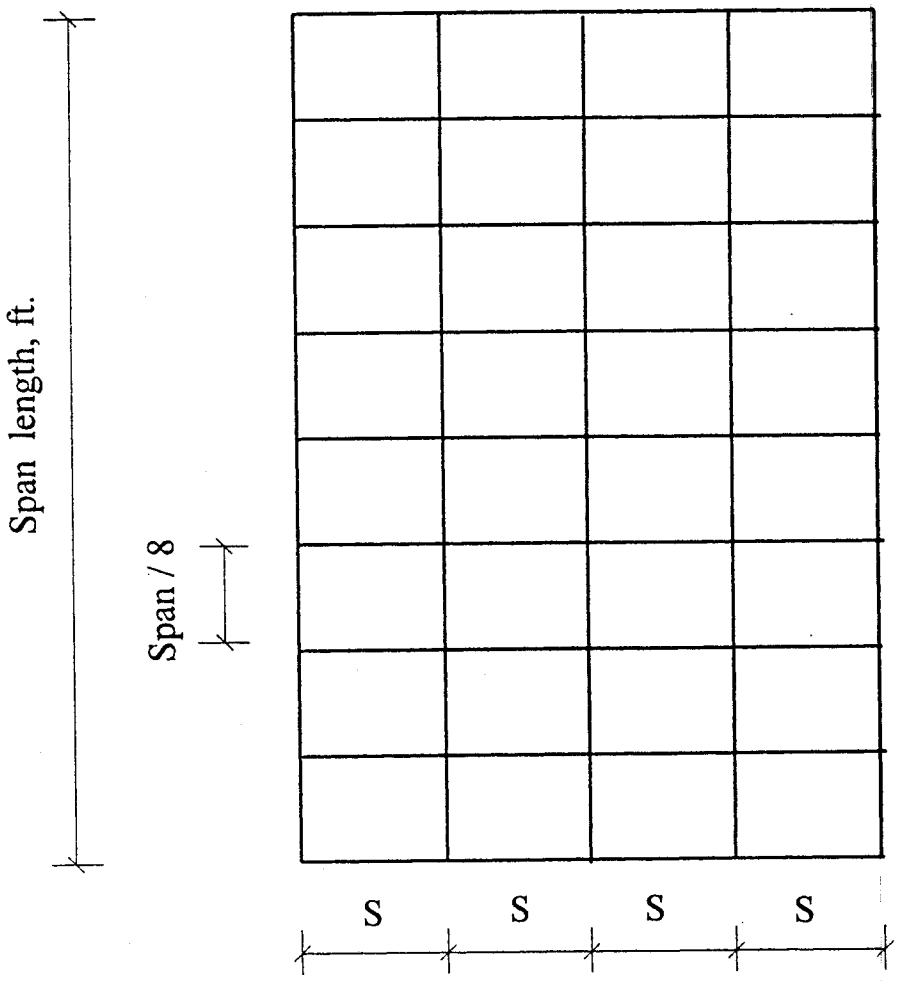

Fig. 5.2 Typical grillage mesh of slab-on-girder bridge

Truck Load Position

The AASHTO HS-20 truck was used in this parametric study. The truck position in the longitudinal direction (span direction) was located to produce the maximum bending moments. To get the maximum bending moments in the bridges, two, three or four trucks were positioned in the transverse direction. The transverse distance between each truck varied from 4 to 6 ft. and in the most cases, it was selected to be 4 ft. For exterior girders, the first axle of the first truck was at 3 ft. from the bridge edge,i.e., exactly over the exterior girder as shown in Fig. 5.3. For interior girders, several positions were tried to obtain the maximum moments.

Table 5.1 summarizes sixty four cases to study the flexural distribution factors of AASHTO girders. The parameters include girder spacing, span length, bridge width, girder type, etc.

5.3.1 Girder Spacing

Girder spacing is an important factor in load distribution of slab-on-girder bridges and it is the only parameter considered in the current AASHTO code. The spacing between AASHTO girders was varied between 5 ft. and 10 ft. for three lane bridges and between 6 ft. and 12 ft. for four lane bridges as shown in Table 5.1.

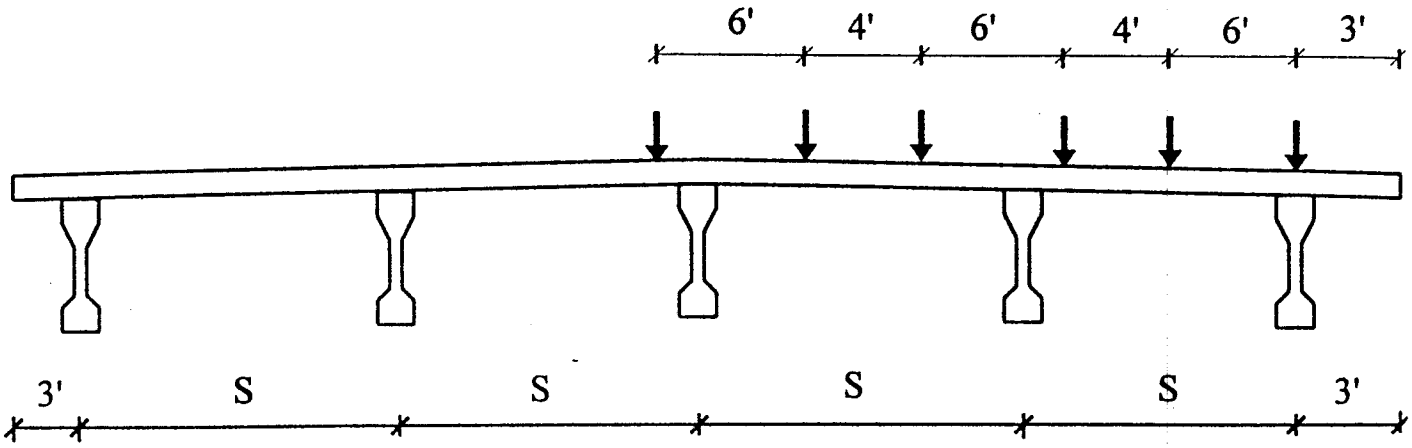

Fig. 5.3 Typical truck load position for the exterior girders

Table 5.1 Slab-on-girder bridges for AASHTO girders: study cases

Parameter	Spacing, ft.	Span length, ft.	Bridge width, ft.	Girder type	Load cases
Spacing (8 cases)	6.0 8.0 9.6 12.0	90 90 90 90	54 54 54 54	IV IV IV IV	3 trucks and 4 trucks
Bridge width (8 cases)	5.0 6.0 7.5 10.0	90 90 90 90	36 36 36 36	IV IV IV IV	2 trucks and 3 trucks
Span length (32 cases)	6.0 8.0 9.6 12.0	50 50 50 50	54 54 54 54	IV IV IV IV	3 trucks and 4 trucks
	6.0 8.0 9.6 12.0	70 70 70 70	54 54 54 54	IV IV IV IV	
	6.0 8.0 9.6 12.0	80 80 80 80	54 54 54 54	IV IV IV IV	
	6.0 8.0 9.6 12.0	100 100 100 100	54 54 54 54	IV IV IV IV	
Girder type (16 cases)	6.0 8.0 9.6 12.0	100 100 100 100	54 54 54 54	V V V V	3 trucks and 4 trucks
	6.0 8.0 9.6 12.0	100 100 100 100	54 54 54 54	VI VI VI VI	

Figures 5.4a and 5.4b show that the distribution factor, DF increases with increasing girder spacing for interior and exterior girders respectively. The DF for interior girders is more dependent on girder spacing, S than the exterior girders. The DF calculated using grillage analogy ranges from 1.18 to 2.24 for interior girders and from 1.14 to 1.85 for exterior girders. In general, the girder spacing is a very important factor in determining wheel load distribution.

The current AASHTO distribution factors are the same for interior and exterior girders. Figures 5.4a and 5.4b show that the AASHTO distribution factors are smaller than those calculated using grillage analogy for interior girders (3 to 8 percent) and larger for exterior girders (-5 to 18 percent). When the value of d_e in Eqn. 5.3 is taken equal to about 2 ft., the LRFD distribution factors are the same for interior and exterior girders. The LRFD distribution factors are smaller (up to 20 percent) than those calculated using grillage analogy for interior girders particularly for larger spacing (S=12 ft.). It is shown in Fig. 5.4 that the distribution factors based on LRFD code are within 4 percent of those calculated using grillage analogy for smaller spacings (S= 5 ft.).

5.3.2 Span Length

Span length is one of the main factors in load distribution of slab-on-girder bridges. The current AASHTO code ignores span length effect on load distribution, while the proposed LRFD code considers the span length as an important factor in wheel load distribution. Slab-on-

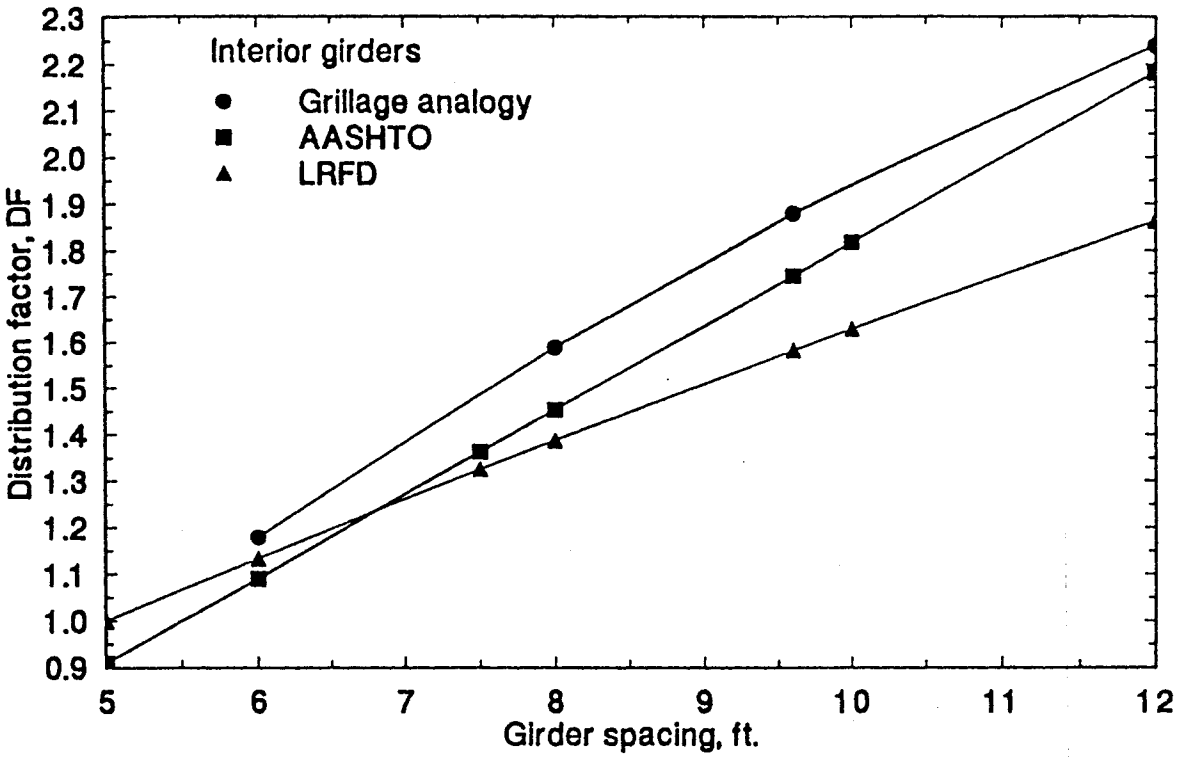

Fig. 5.4 Effect of girder spacing variations on load distribution of slab-on-girder bridges

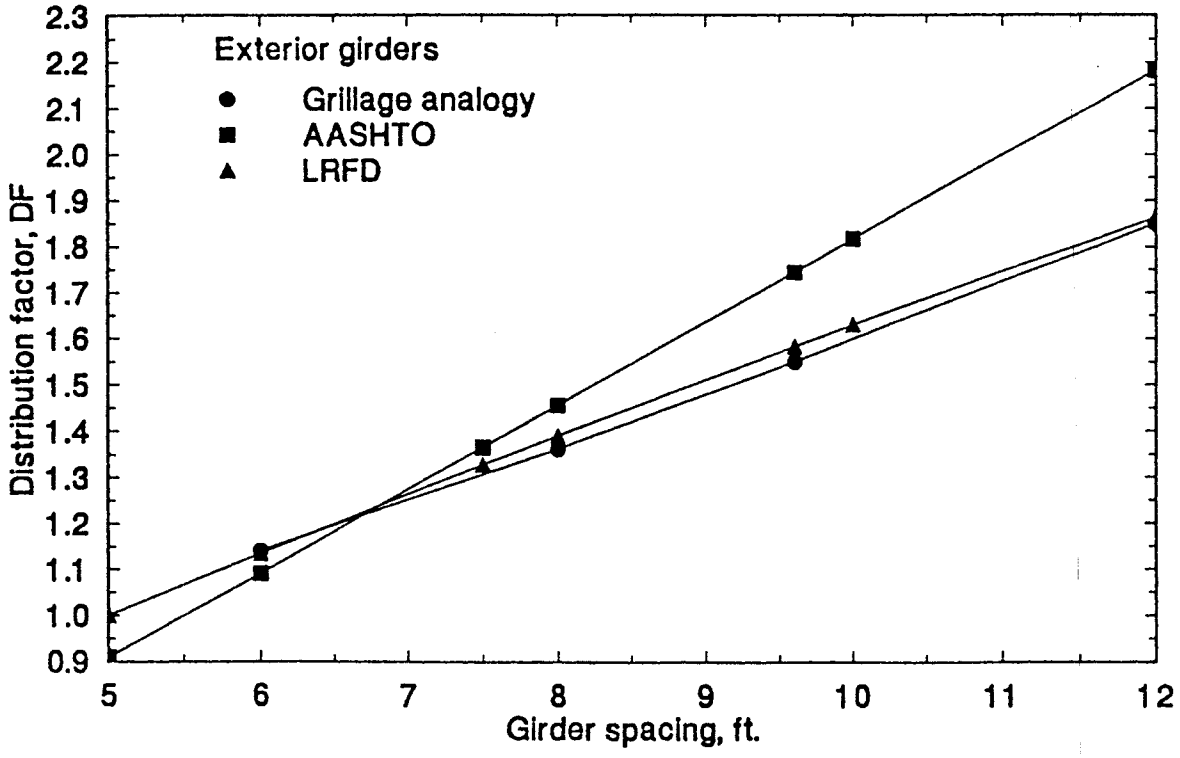

Fig. 5.4 Effect of girder spacing variations on load distribution of slab-on-girder bridges

AASHTO girder bridges with spans from 50 ft. up to 100 ft. are investigated in this section. The slab thickness was 7 in. for all the bridges.

Four AASHTO HS-20 trucks were positioned in the transverse direction to calculate the maximum bending moment in the interior girders, while three HS-20 trucks were positioned to calculate the maximum bending moment for exterior girders. Figures 5.5 and 5.6 show the bending moment distributions for a typical bridge (type IV AASHTO girder and bridge width = 54 ft.) with different span lengths for interior and exterior girders respectively. The bending moment increases with the increase in the span length and the moment distribution tends to be more uniform for shorter spans. These bending moment distributions were used to calculate the distribution factors as explained in section 5.2.1.

Figures 5.7 and 5.8 show the changes in load distribution factors with increasing span for interior and exterior girders respectively. The load distribution factors of the interior girders decrease with increasing span (1% to 5%) and the load distribution factors of exterior girders increase with span increase (10% to 11%). It is clear that the load distribution factor for exterior girder is more dependent on span length than the interior girders. The distribution factor calculated using grillage analogy is slightly larger (7%) than the distribution factor based on AASHTO specifications as shown in Figures 5.9 and 5.10 for interior and exterior girders respectively. This means that AASHTO code gives slightly unsafe estimate of distribution factor, DF. Figure 5.10 shows that the LRFD load distribution factors are inaccurate for shorter

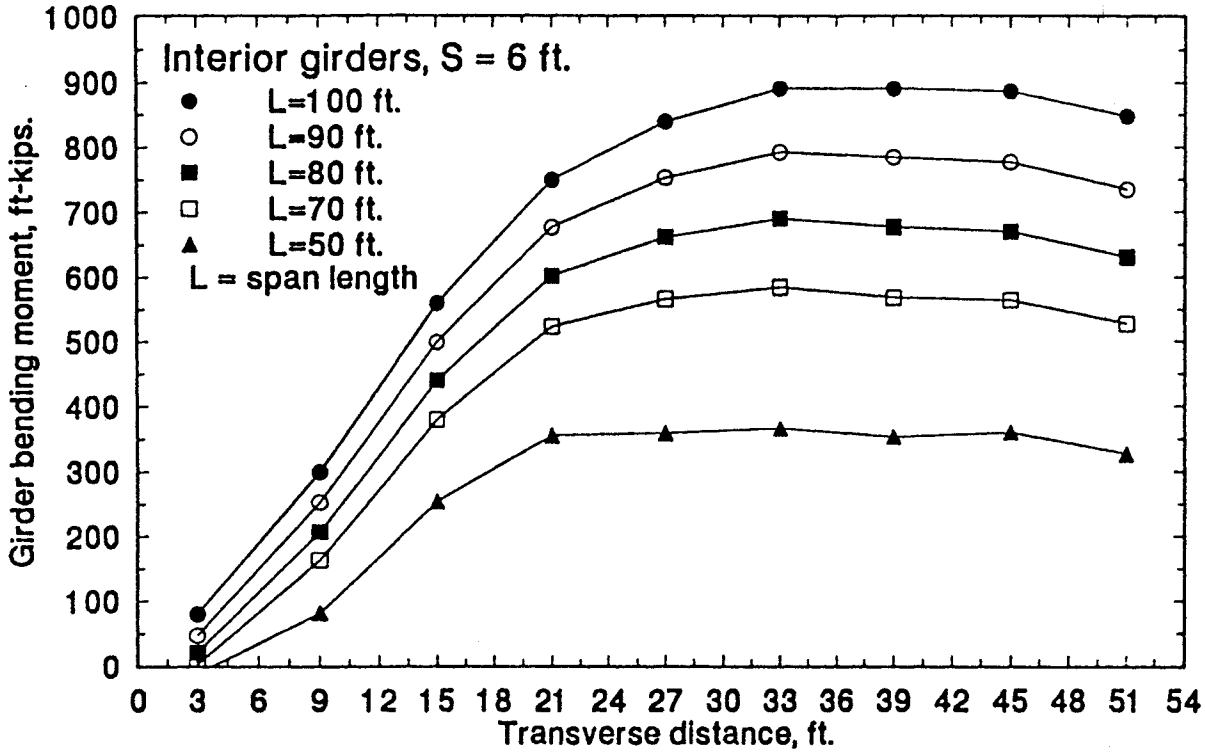

Fig. 5.5 Effect of span length on interior girder bending moment distribution

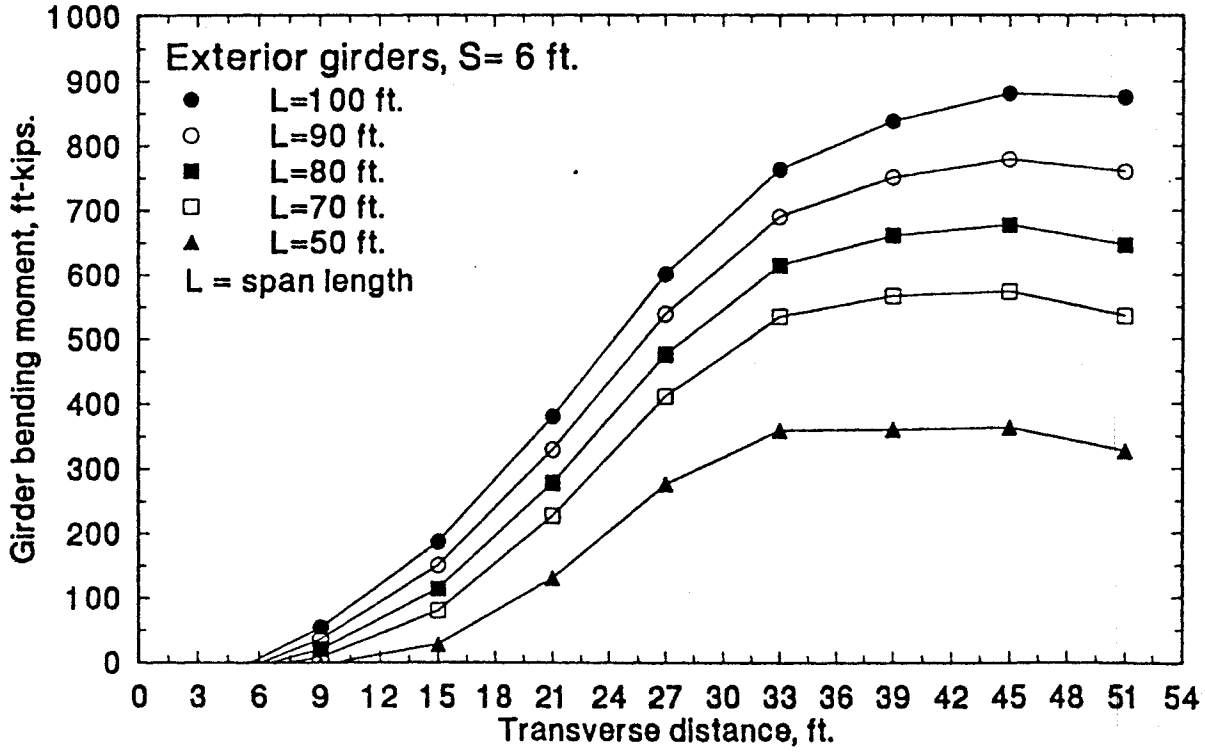

Fig. 5.6 Effect of span length on exterior girder bending moment distribution

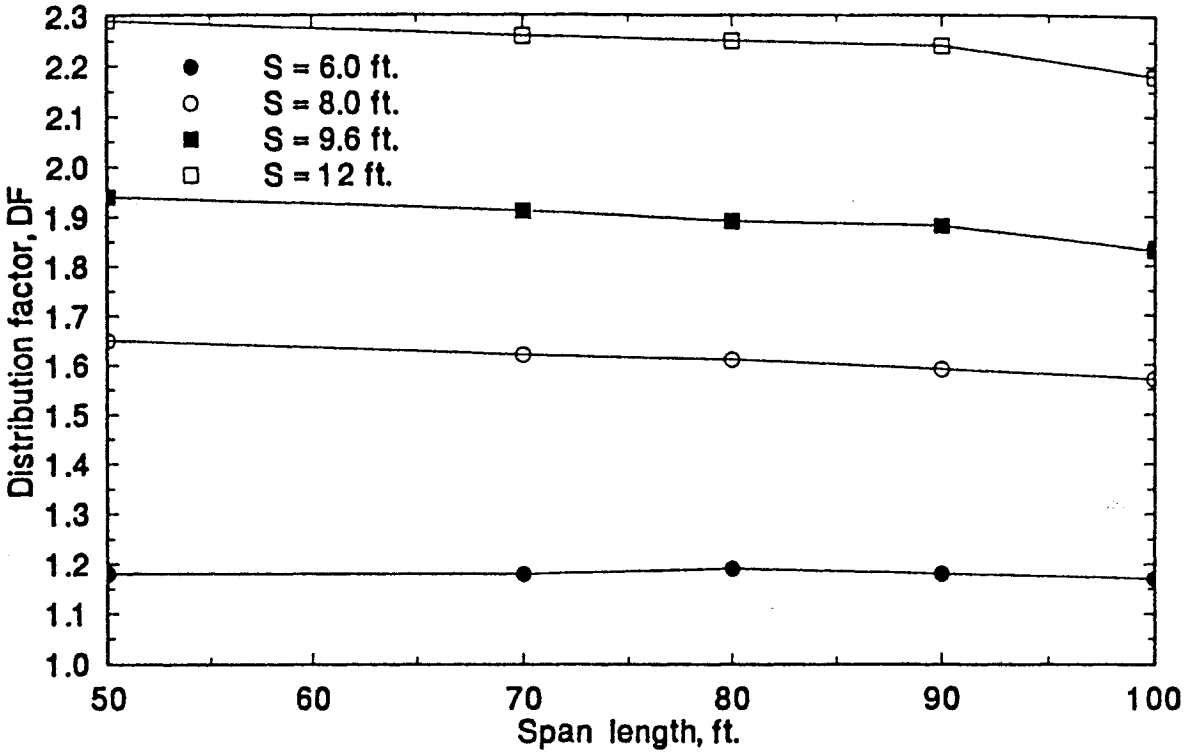

Fig. 5.7 Effect of span length variation on load distribution of slab-on-girder bridges (interior girders)

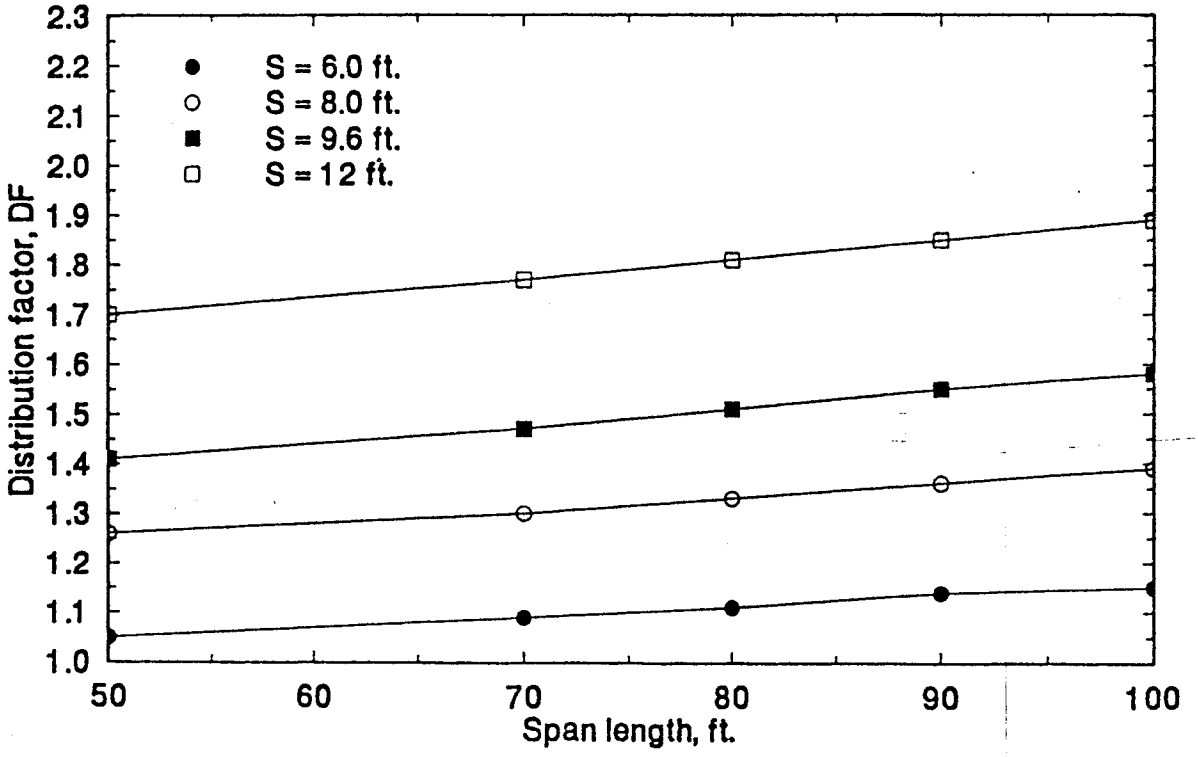

Fig. 5.8 Effect of span length variation on load distribution of slab-on-girder bridges (exterior girders)

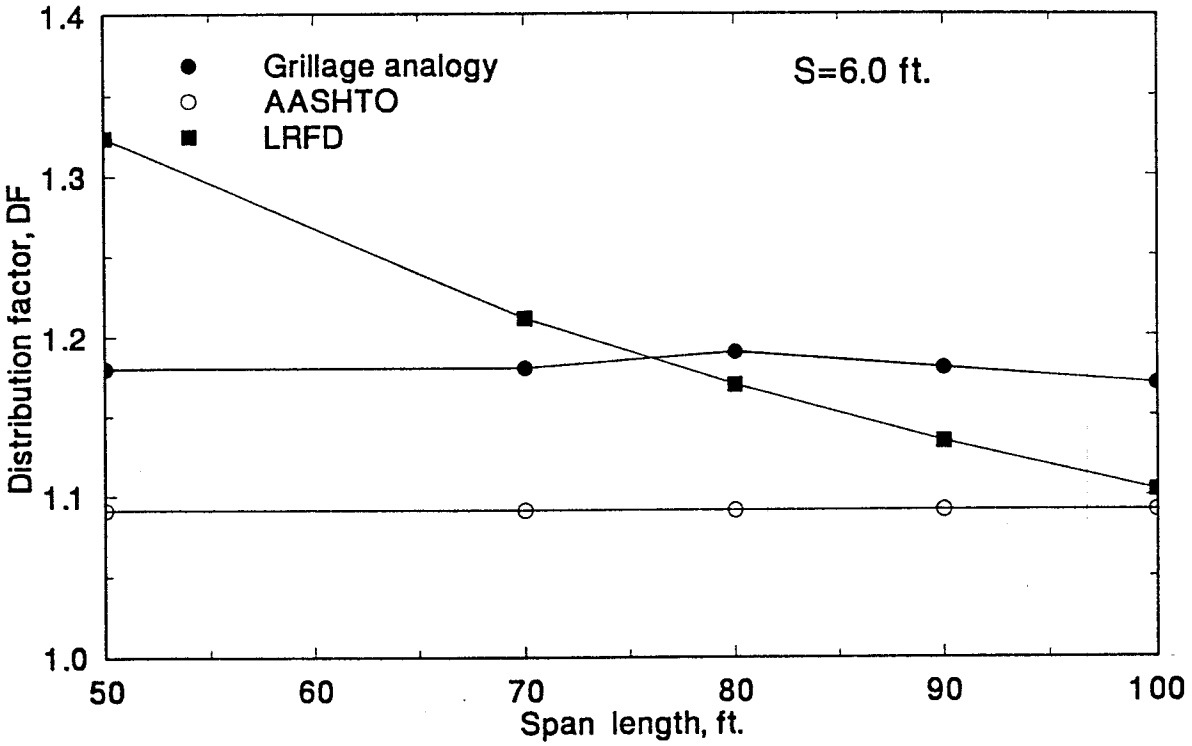

Fig. 5.9 Span length variation effect on load distribution based on grillage analogy, AASHTO and LRFD codes (interior girders)

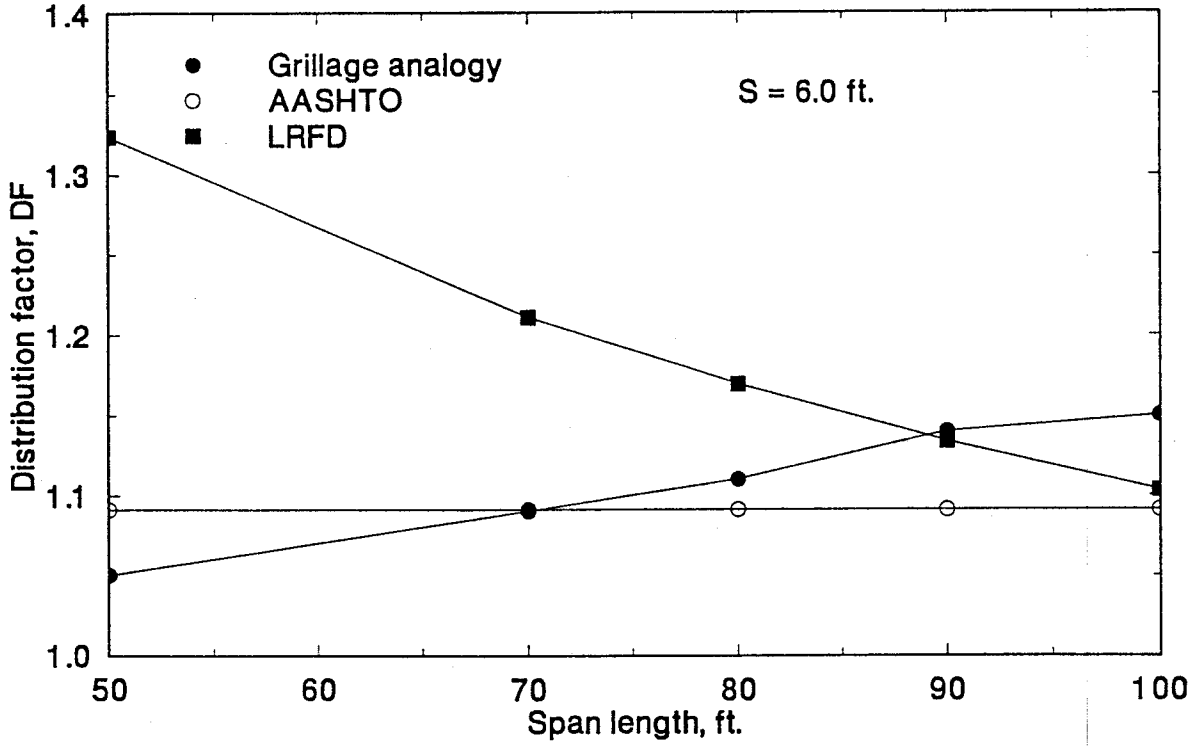

Fig. 5.10 Span length variation effect on load distribution based on grillage analogy, AASHTO and LRFD codes (exterior girders)

spans. However, The AASHTO and LRFD load distribution factors are accurate for longer spans (90 and 100 ft) which are more commonly used in bridges.

5.3.3 Bridge Width

AASHTO and LRFD codes ignore the bridge width as a parameter in load distribution of trucks. To study the effect of bridge width variation, two bridges with widths 54 ft. and 36 ft. were studied (Table 5.1). Figure 5.11 shows the variation of interior girder load distribution factors calculated using grillage analogy, AASHTO and LRFD codes for the two bridges. It is shown in Fig. 5.11 that the DF for the 54 ft. wide bridge is slightly higher than the 36 ft. wide bridge (2% to 4%) and this can be considered to be insignificant. This establishes that AASHTO and LRFD codes are realistic in neglecting the bridge width as a parameter in load distribution.

5.3.4 AASHTO Girder Types

The proposed LRFD code introduces the girder stiffness as a parameter in load distribution. The longitudinal stiffness parameter, K_g is used in the flexural load distribution factor equation (Eqn. 5.2). Twelve cases were investigated using grillage analogy method as shown in Table 5.1. The span length of 100 ft. with a bridge width of 54 ft. was kept constant in all the cases. Three types of AASHTO girders (Types 4, 5 and 6) were studied to determine the effect of girder type on the load distribution. The longitudinal stiffness parameter, K_g was computed to be 1,108,026.7, 1,729,700.8 and 2,393,776.2 for AASHTO girder types IV, V and VI respectively.

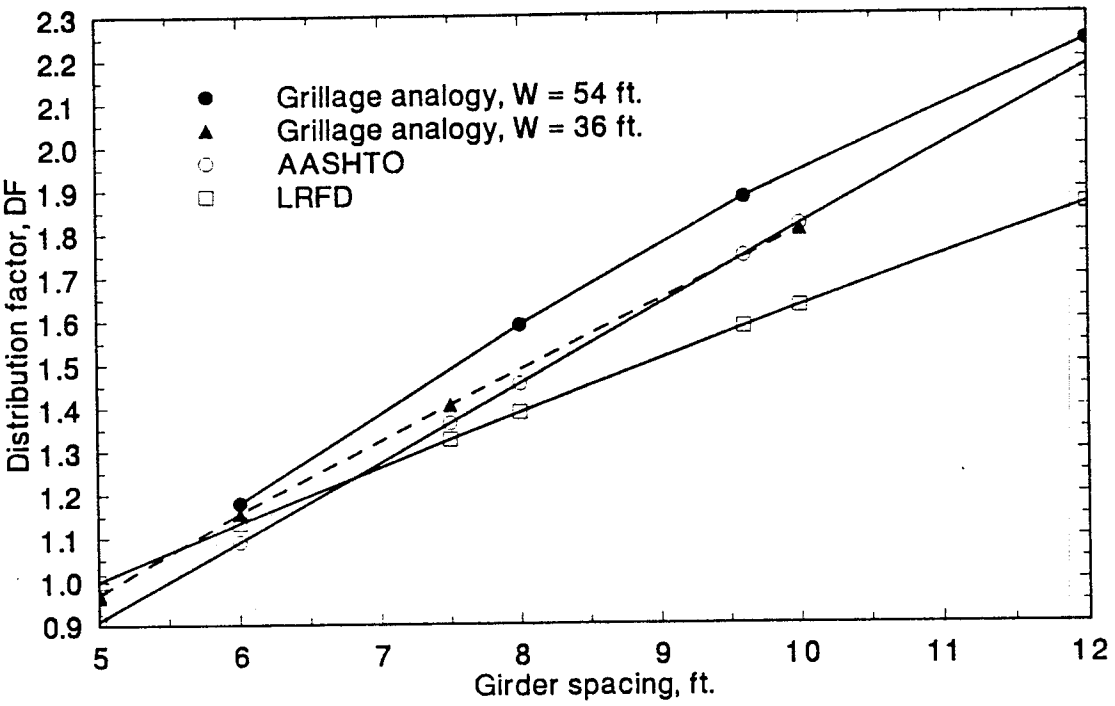

Fig. 5.11 Effect of bridge width variation on load distribution of slab-on-girder bridges (interior girders)

Figures 5.12 and 5.13 show the effect of variations in the longitudinal stiffness parameter, K_g on load distribution factor of slab-on-girder bridges for the interior and exterior girders respectively. As K_g increases, the load distribution factors increase only marginally (2 to 3%) for interior girders and slightly decrease (3 to 5 %) for exterior girders. For a given spacing, the LRFD load distribution equation overestimates the effect of K_g as shown in Figures 5.14 and 5.15 for interior and exterior girders respectively. This is more evident in case of exterior girders shown in Fig. 5.15.

5.4 SLAB-ON-AASHTO GIRDER SHEAR LOAD DISTRIBUTION FACTORS: PARAMETRIC STUDIES

The current AASHTO code assumes that the transverse distribution patterns of various load effects (moment, shear, etc..) are similar. This means the load distribution factors for bending moment and shear are the same along the span. This assumption is discussed in section 5.2.2 and shown that this concept is difficult to justify. The proposed LRFD code has two different sets of equations for flexural and shear load distribution factors as explained in section 5.2.

It is important to understand the effect of various parameters on shear load distribution. Several parameters affect the load distribution of slab-on-girder bridges. Girder spacing, span length, bridge width and girder type are the main parameters, which are considered in this section. Bridge parameters are varied one at a time in a typical bridge. Variation of wheel load

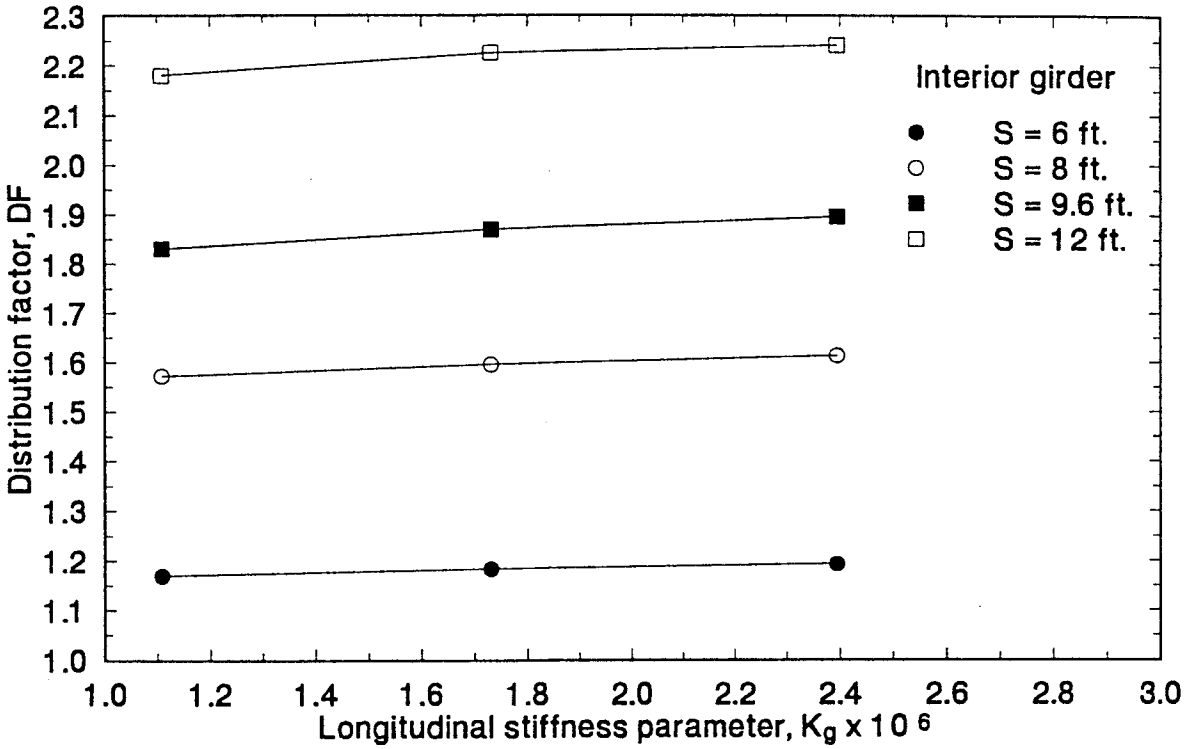

Fig. 5.12 Effect of longitudinal stiffness parameter, K_g on load distribution of slab-on-girder bridges (interior girders)

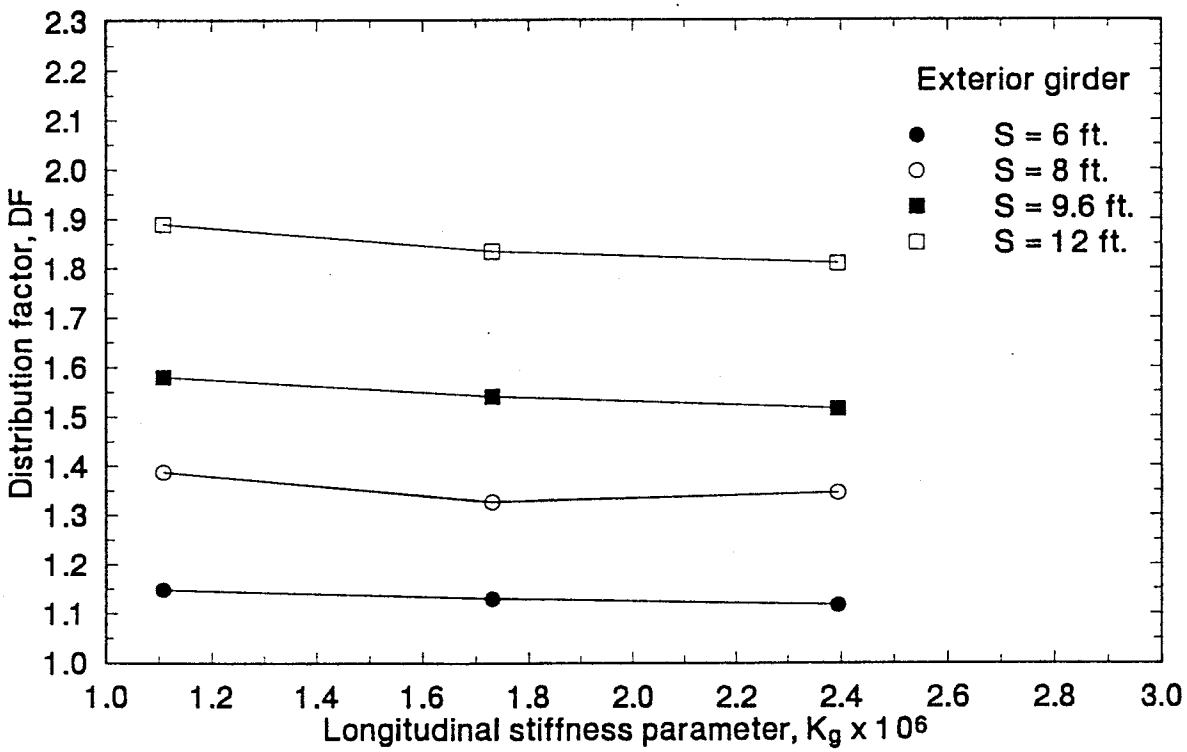

Fig. 5.13 Effect of longitudinal stiffness parameter, K_g on load distribution of slab-on-girder bridges (exterior girders)

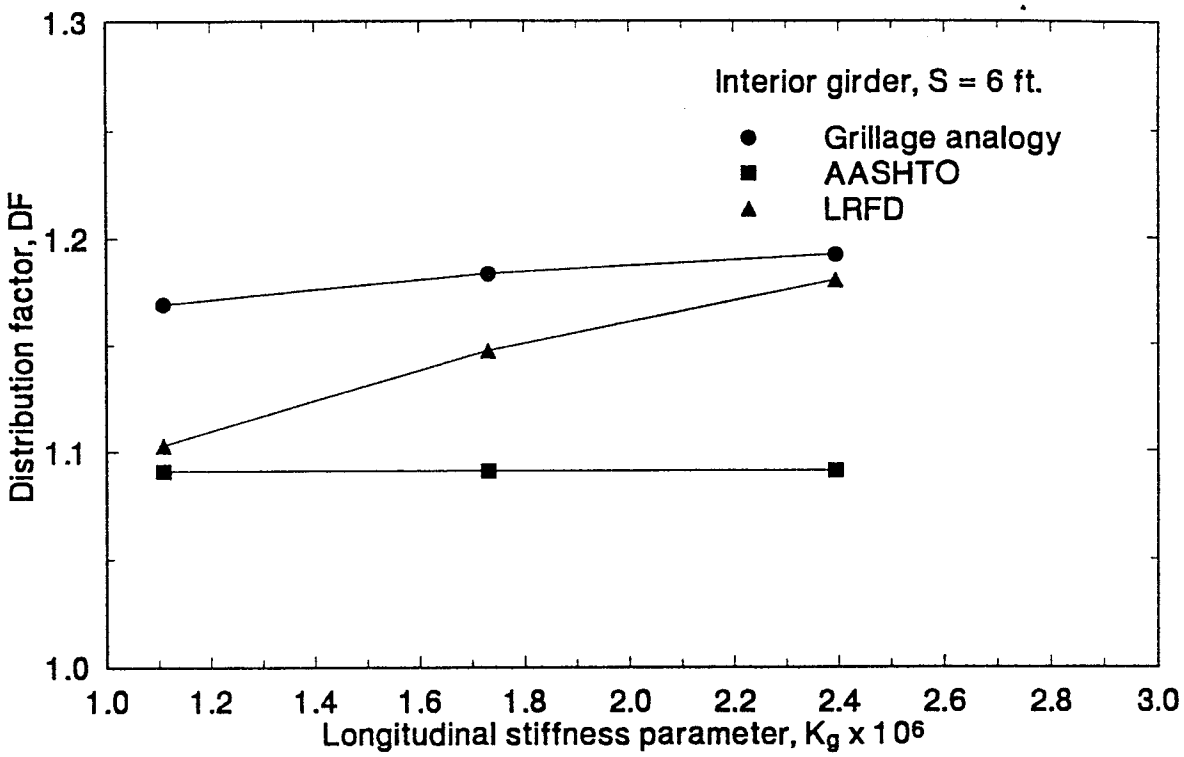

Fig. 5.14 Longitudinal stiffness parameter, K_g effect on load distribution based on grillage analogy, AASHTO and LRFD codes (interior girders)

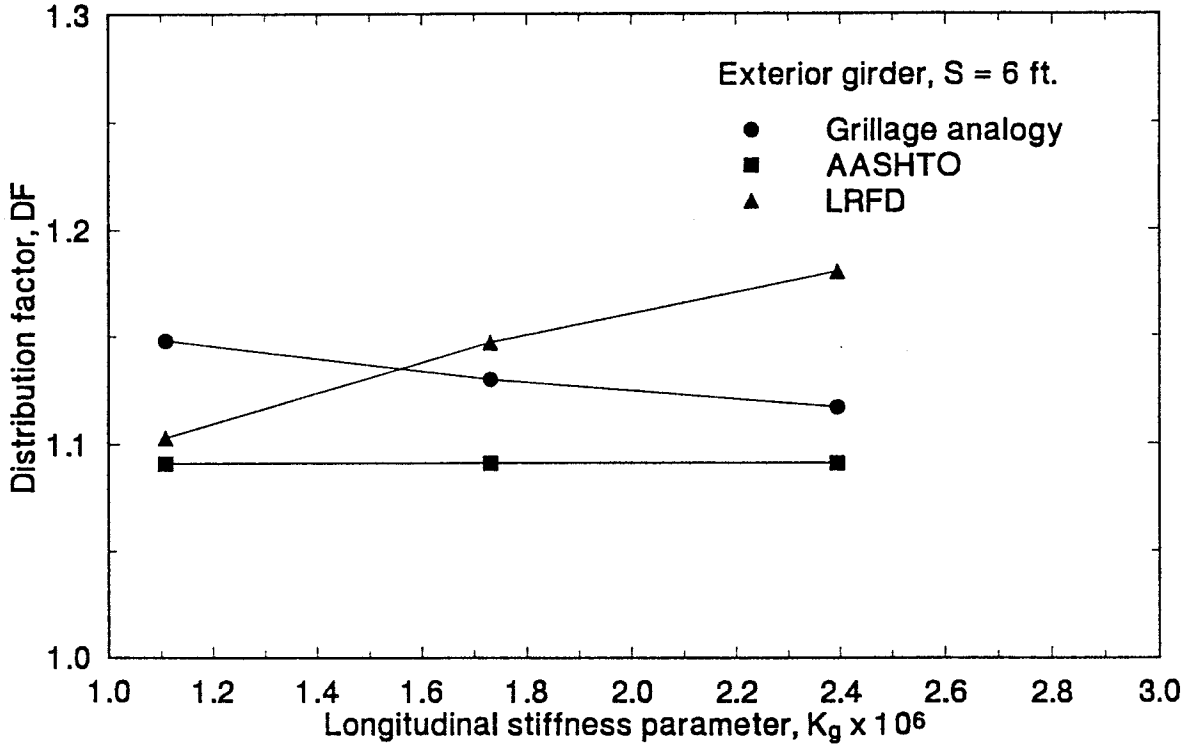

Fig. 5.15 Longitudinal stiffness parameter, K_g effect on load distribution based on grillage analogy, AASHTO and LRFD codes (exterior girders)

distribution factors with each parameter shows the relative importance of the parameters. Figure 5.1 shows the typical slab-on girder bridge cross section used in the analysis. The typical slab-on-girder bridge has span length equal to 90 ft. with a bridge width of 54 ft. It has prestressed AASHTO type IV girders with a slab thickness of 7 in. The concrete strengths of both the girder and slab are taken equal to 5000 psi.

The typical slab-on-girder bridge shown in Figure 5.1 are divided into elements in the longitudinal and transverse directions shown in Figure 5.2. Eight longitudinal elements coincide with each girder center line in addition to elements in the transverse direction through the longitudinal nodes.

Truck Load Position

The AASHTO HS-20 truck was used in this parametric study. The truck position in the longitudinal direction (span direction) was located to give the maximum shear forces. To get the maximum shear in the bridges, two, three or four trucks were positioned in the transverse direction. The transverse distance between each truck varied from 4 to 6 ft. and in the most cases, it was selected to be 4 ft. The first axle of the first truck was at 3 ft. from the bridge edge, i.e., directly over the exterior girder as shown in Fig. 5.3.

Table 5.2 summarizes sixty four cases considered for the shear distribution factors of AASHTO girders. The parameters include girder spacing, span length, bridge width, girder type, etc.

Table 5.2 Slab-on-girder bridges for AASHTO girders: shear load distribution

Parameter	Spacing, ft.	Span length, ft.	Bridge width, ft.	Girder type	Load cases
Spacing (8 cases)	6.0 8.0 9.6 12.0	90 90 90 90	54 54 54 54	IV IV IV IV	3 trucks and 4 trucks
Bridge width (8 cases)	5.0 6.0 7.5 10.0	90 90 90 90	36 36 36 36	IV IV IV IV	2 trucks and 3 trucks
Span length (32 cases)	6.0 8.0 9.6 12.0	50 50 50 50	54 54 54 54	IV IV IV IV	3 trucks and 4 trucks
	6.0 8.0 9.6 12.0	70 70 70 70	54 54 54 54	IV IV IV IV	
	6.0 8.0 9.6 12.0	80 80 80 80	54 54 54 54	IV IV IV IV	
	6.0 8.0 9.6 12.0	100 100 100 100	54 54 54 54	IV IV IV IV	
Girder type (16 cases)	6.0 8.0 9.6 12.0	100 100 100 100	54 54 54 54	V V V V	3 trucks and 4 trucks
	6.0 8.0 9.6 12.0	100 100 100 100	54 54 54 54	VI VI VI VI	

5.4.1 Girder Spacing

Girder spacing is an important factor in load distribution of slab-on-girder bridge and it is the only parameter considered in the current AASHTO code. The spacing between AASHTO girders was varied between 5 ft. and 10 ft. for three lane bridges and between 6 ft. and 12 ft. for four lane bridges as shown in Table 5.2. Figures 5.16 and 5.17 show that the shear distribution factor, DF increases with increasing girder spacing for interior and exterior girders respectively. The shear DF calculated using grillage analogy ranges from 0.61 to 1.17 for interior girders and from 0.54 to 0.885 for exterior girders. In general, the shear load distribution factors are smaller than the flexural load distribution factors.

The current AASHTO code requires that the lateral load distribution of the wheel loads at ends of the beams shall be that produced by assuming the flooring to act as a simple span between beams. For wheels in other positions on the span, the distribution for shear shall be determined by the same method as that for moment (S/5.5). Figures 5.16 and 5.17 show that the AASHTO code distribution factors are much larger than those calculated using grillage analogy for interior and exterior girders respectively. It is obvious that the AASHTO code sometimes overestimates the shear load distribution factors by more than 100 percent. When the value of d_e in Eqn. 5.6 is assumed equal to about 2 ft., the LRFD code distribution factors are the same for interior and exterior girders. The LRFD code distribution factors are larger than those calculated using grillage analogy particularly for larger spacing (S = 12 ft). For spacing S, equal to 12 ft., the LRFD code overestimates the shear load distribution factor by 30 % for interior girders and

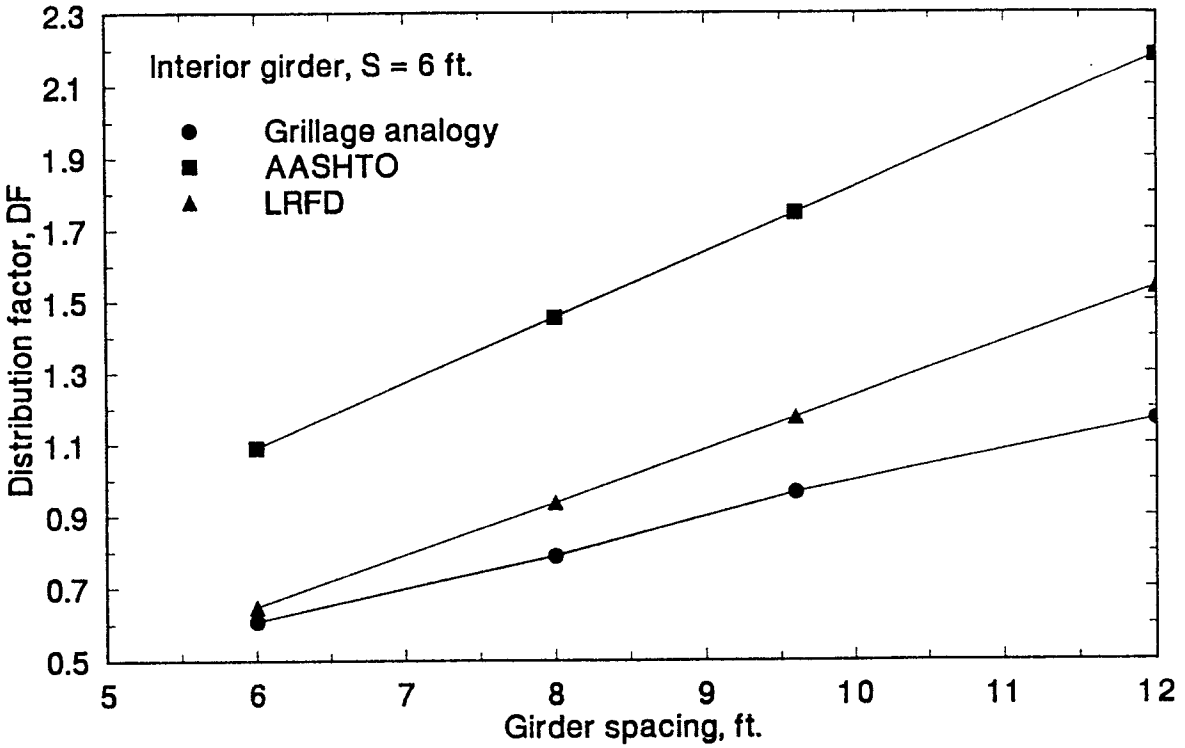

Fig. 5.16 Effect of girder spacing variations on load distribution of slab-on-girder

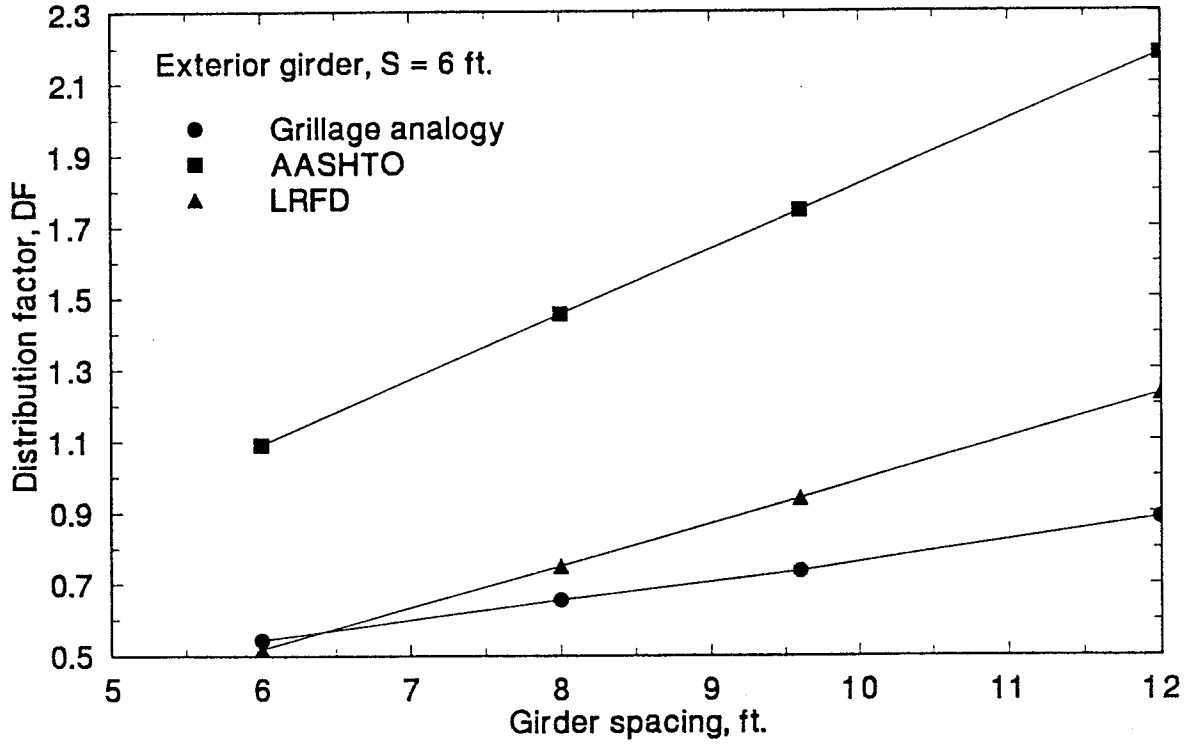

Fig. 5.17 Effect of girder spacing variations on load distribution of slab-on-girder bridges (exterior girder)

39% for exterior girders. It is shown in Fig. 5.16 that the distribution factor based on LRFD code is within 7 percent of those from the grillage analogy for smaller spans (S = 6 ft).

5.4.2 Span Length

Span length is one of the main factors in flexural load distribution of slab-on-girder bridges. The current AASHTO and the proposed LRFD codes ignore span length effect on shear load distribution. Spans of slab-on-AASHTO girder bridges vary from 50 ft. to 100 ft. as shown in Table 5.2. The slab thickness was 7 in. for all bridges.

Four AASHTO HS-20 trucks were positioned in the transverse direction to calculate the maximum shear for interior girders, while three HS-20 trucks were positioned to calculate the maximum shear for exterior girders. The bending moment distributions of each girder were calculated using grillage analogy. These bending moment distributions were used to calculate the shear force distributions along the span. The shear load distribution factor was calculated by dividing the maximum shear in the girder by the maximum shear force in the bridge idealized as a one-dimensional beam subjected to one set of wheel loads.

Figures 5.18 and 5.20 show the changes in load distribution factors based on grillage analogy with increasing span for interior and exterior girders respectively. The load distribution factor of the interior girders decreases marginally with increasing span (1% to 3%) and the load distribution factor of exterior girders increases with increase in the span (4% to 6%). It is clear that the load distribution factor for interior and exterior girders are independent of span length.

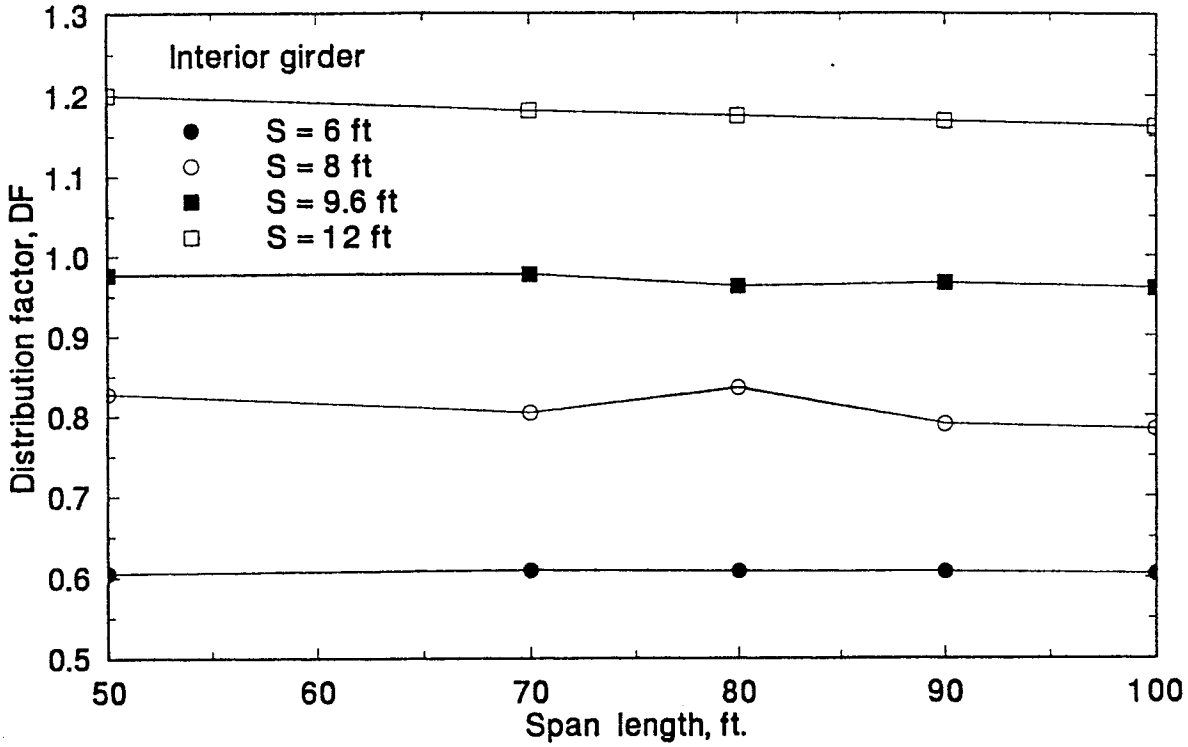

Fig. 5.18 Effect of span length variation on shear load distribution of slab-on-girder bridges (interior girders)

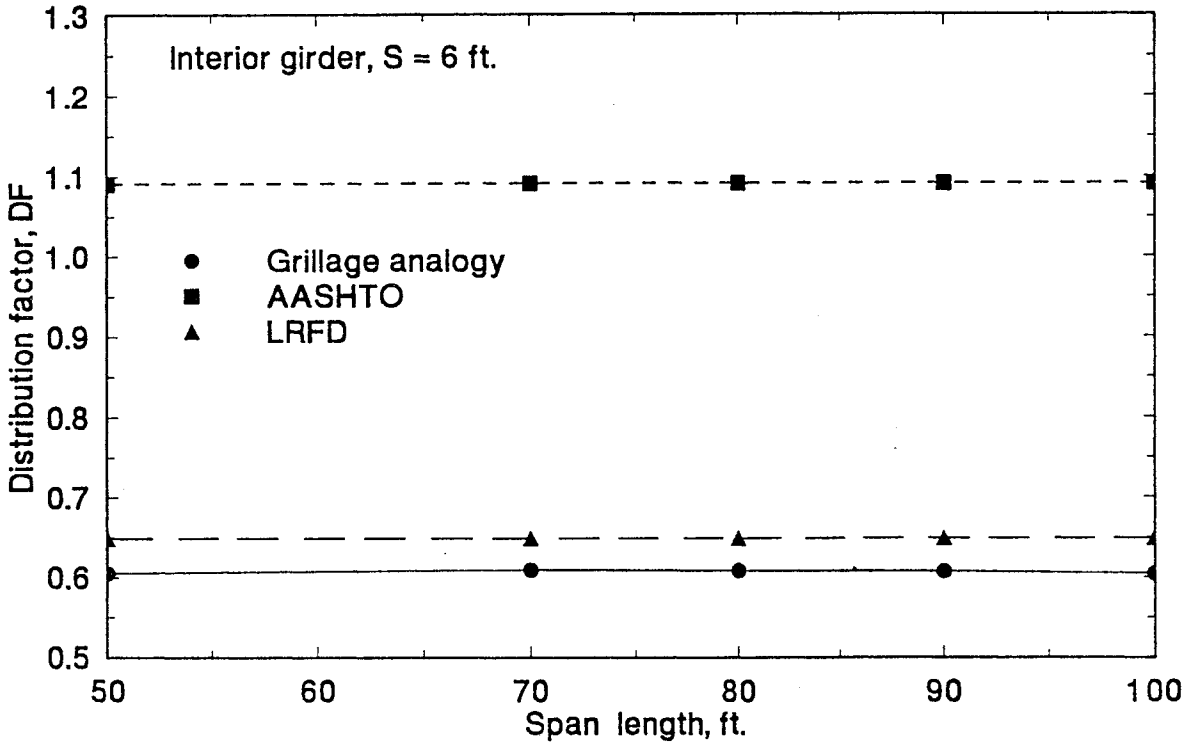

Fig. 5.19 Effect of span length variation on shear load distribution of slab-on-girder bridges (exterior girders)

This is consistent with the assumptions implied in the AASHTO and LRFD codes that the span length does not affect the shear load distribution.

The distribution factors calculated using grillage analogy are smaller than those calculated using AASHTO and LRFD codes as shown in Figures 5.19 and 5.21 for interior and exterior girders respectively. It is also clear that the current AASHTO code gives very conservative estimate of the shear distribution factor, DF.

5.4.3 Bridge Width

Both AASHTO and LRFD codes ignore the bridge width as a parameter in load distribution of trucks. To study the effect of bridge width variation of slab-on girder bridges, two bridges with widths of 54 ft. and 36 ft. were considered in the analysis. Figures 5.22 and 5.23 show the shear distribution factors calculated using grillage analogy method, AASHTO and LRFD codes for the interior and exterior girders respectively. The DFs for the 54 ft. width bridge is slightly higher than those of 36 ft. bridge, which could be considered insignificant. This shows that both AASHTO and LRFD codes are realistic in neglecting the bridge width as a parameter in shear load distribution.

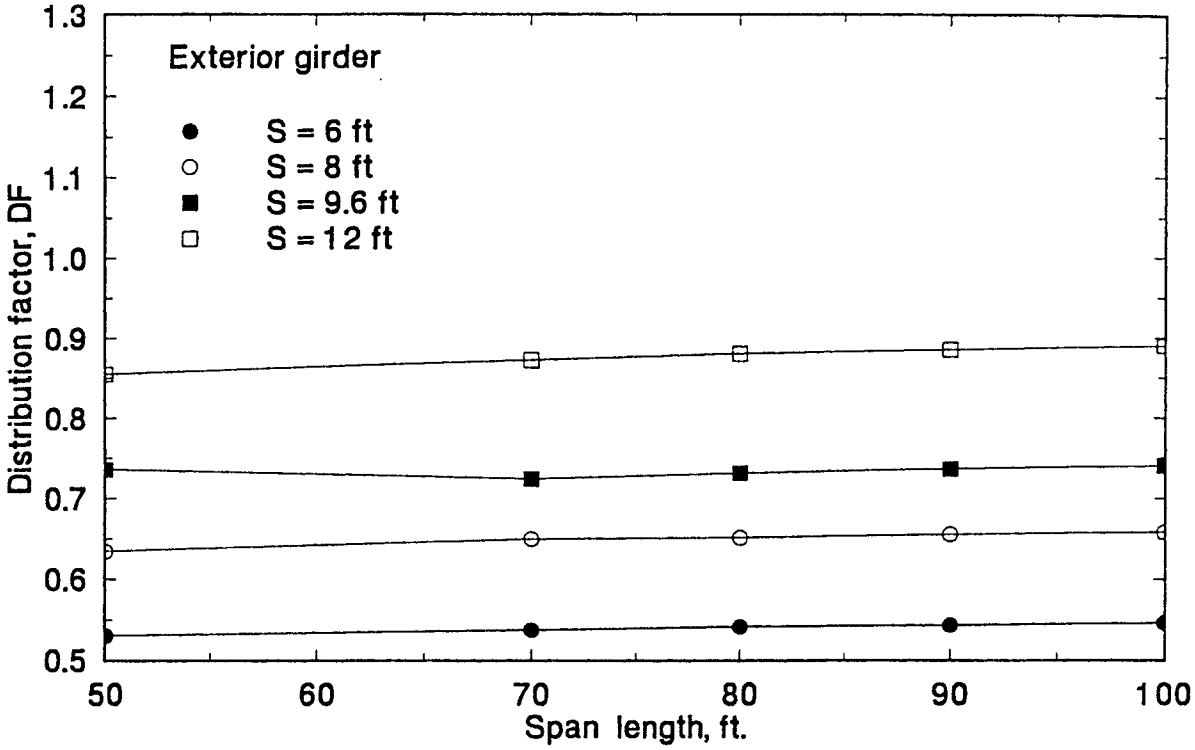

Fig. 5.20 Span length variation effect on shear load distribution based on grillage analogy, AASHTO and LRFD codes (interior girders)

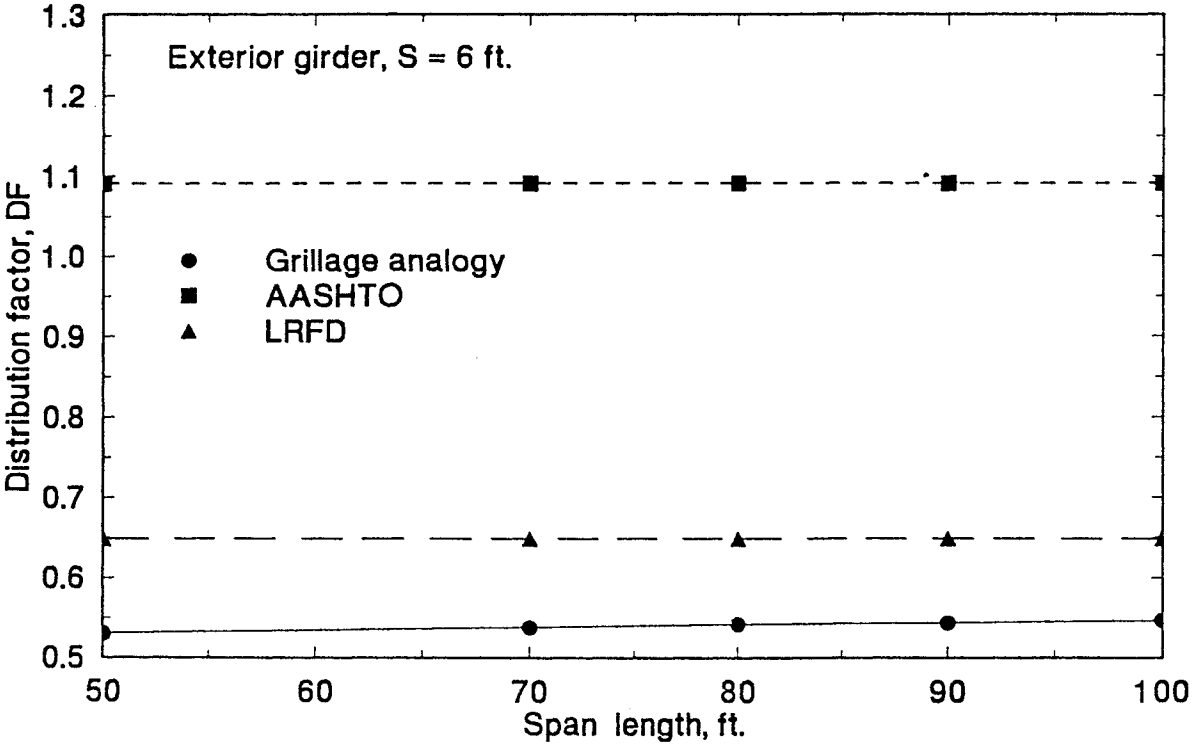

Fig. 5.21 Span length variation effect on shear load distribution based on grillage analogy, AASHTO and LRFD codes (exterior girders)

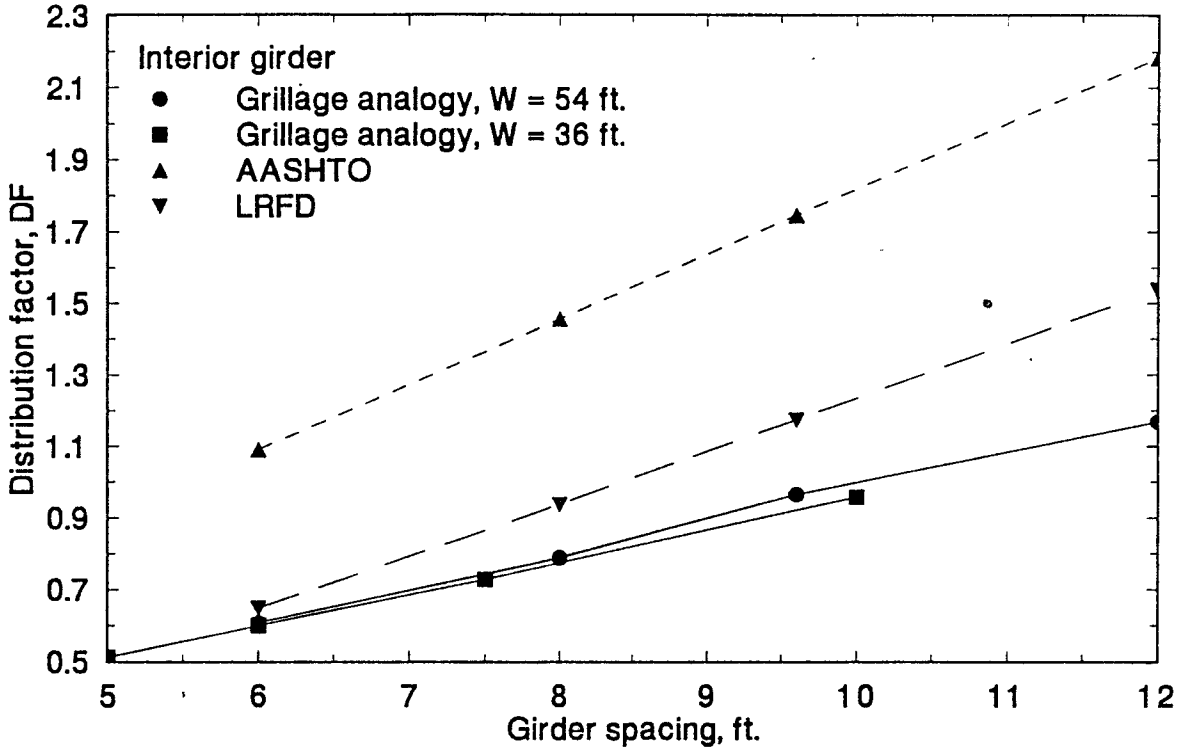

Fig. 5.22 Effect of bridge width variation on shear load distribution of slab-on-girder bridges (interior girders)

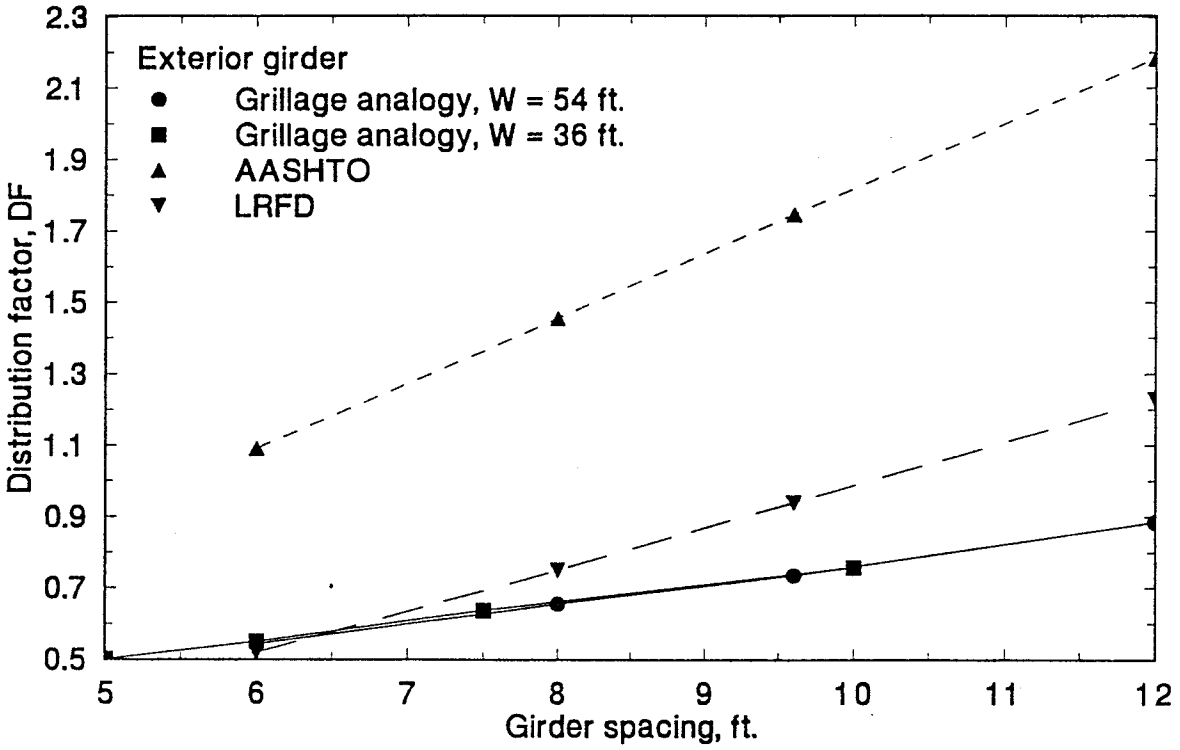

Fig. 5.23 Effect of bridge width variation on shear load distribution of slab-on-girder bridges (exterior girders)

5.4.4 AASHTO Girder Types

The proposed LRFD code introduces the girder stiffness as a parameter in flexural load distribution, but ignores this parameter in shear load distribution. Twelve cases were investigated using grillage analogy method as shown in Table 5.2 to study the effect of girder stiffness in shear load distribution. In all the cases, the span length and bridge width were kept constant at 100 ft. and 54 ft. respectively. Three types of AASHTO girders (Types 4, 5 and 6) were studied to determine the effect of girder type on the shear load distribution.

Figures 5.24 and 5.25 show the effect of K_g variations on shear load distribution factor for the interior and exterior girders respectively. As K_g increases, the shear load distribution factor increases only slightly for interior girders and decreases marginally for exterior girders. It is shown that the LRFD code is realistic in neglecting the girder stiffness in shear load distribution.

5.5 SLAB-ON-AASHTO GIRDER: SIMPLIFIED EQUATION FOR SHEAR LOAD DISTRIBUTION

It can be concluded from the detailed parametric studies in section 5.4, that the spacing between girders is the dominant parameter in shear load distribution. Parameters such as span length, bridge width and girder stiffness have little effect on shear load distribution for AASHTO girders. Figure 5.26 shows the effect of girder spacing variation on load distribution factors for

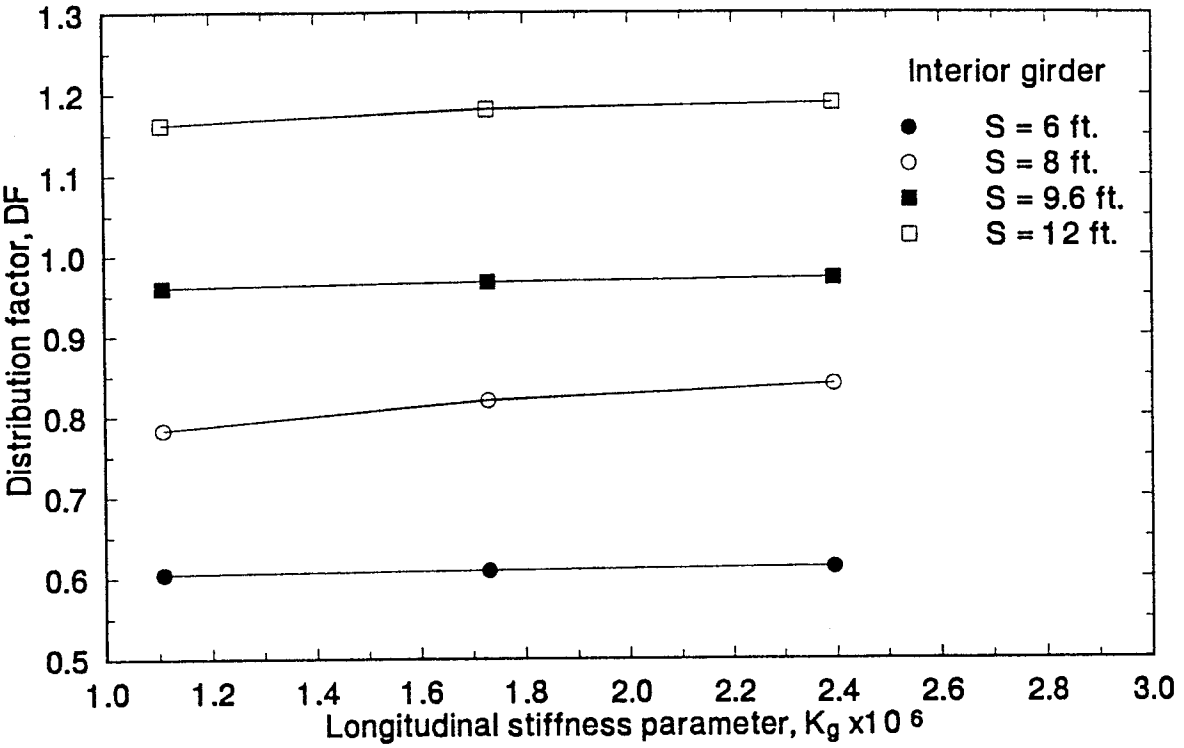

Fig. 5.24 Effect of longitudinal stiffness parameter, K_g on shear load distribution of slab-on-girder bridges (interior girders)

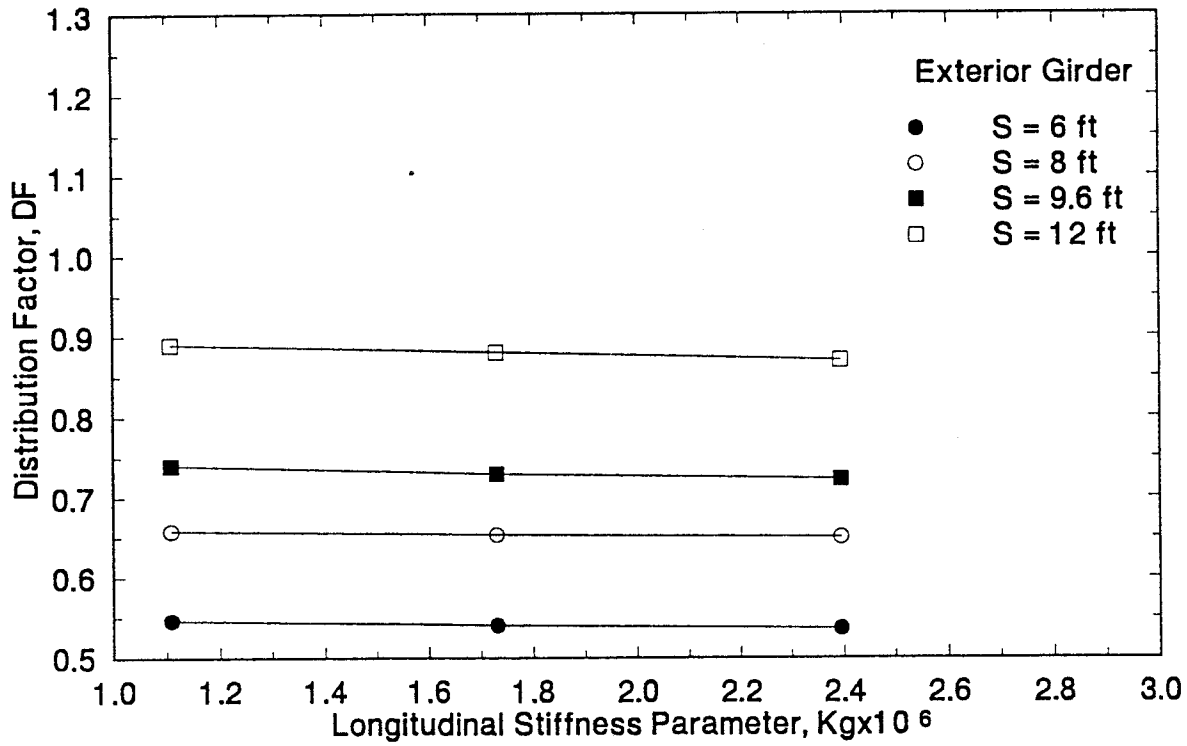

Fig. 5.25 Effect of longitudinal stiffness parameter, K_g on shear load distribution of slab-on-girder bridges (exterior girders)

all the cases calculated using grillage analogy method for interior girders. The best linear fit for shear load distribution of AASHTO interior girders is given by

$$\textbf{Shear DF} = 0.04 + 0.1\,S \qquad (5.7)$$

Figure 5.27 shows the effect of girder spacing variation on load distribution factors for all the cases calculated using grillage analogy method for exterior girders. The best linear fit for shear load distribution of AASHTO exterior girders is given as

$$\textbf{Shear DF} = 0.21 + 0.055\,S \qquad (5.8)$$

Equations 5.8 and 5.9 are simple and gives better accuracy than those based on LRFD code.

5.6 SLAB-ON-BULB TEE GIRDER FLEXURAL LOAD DISTRIBUTION FACTORS: PARAMETRIC STUDIES

In all the states surveyed by FHWA in 1982, the most economical bridges for spans of approximately 70 ft. to 130 ft. are constructed with pretensioned concrete girders. When compared with other sections, AASHTO standard bridge girders are not the most structurally efficient or cost-effective for spans of 80 ft. to 140 ft. (Helm, 1989). For girders with 6-inch thick webs, most effective sections are modified bulb-tees. For spans of 80 ft. to 120 ft., modified bulb-tees have 17% less in-place cost of girder and deck compared to AASHTO girders. Figures 5.28 summarizes the section properties for three common bulb tee girders which

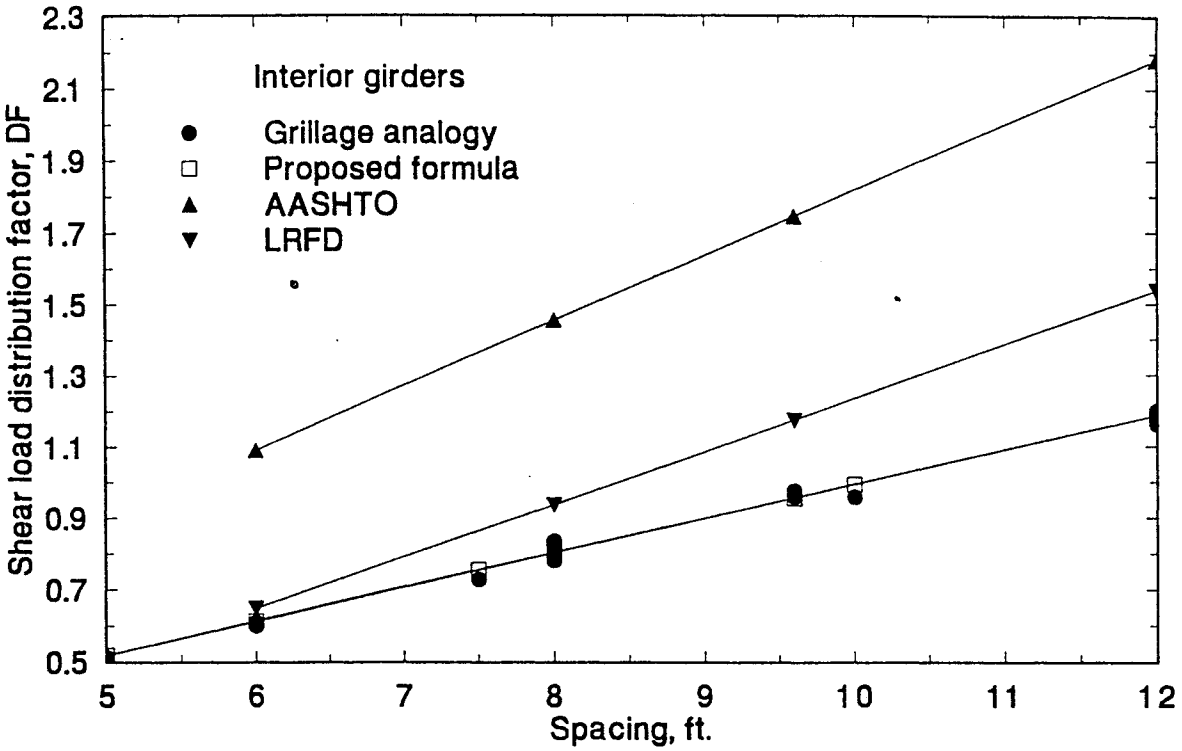

Fig. 5.26 Shear load distribution simplified formula (interior girder)

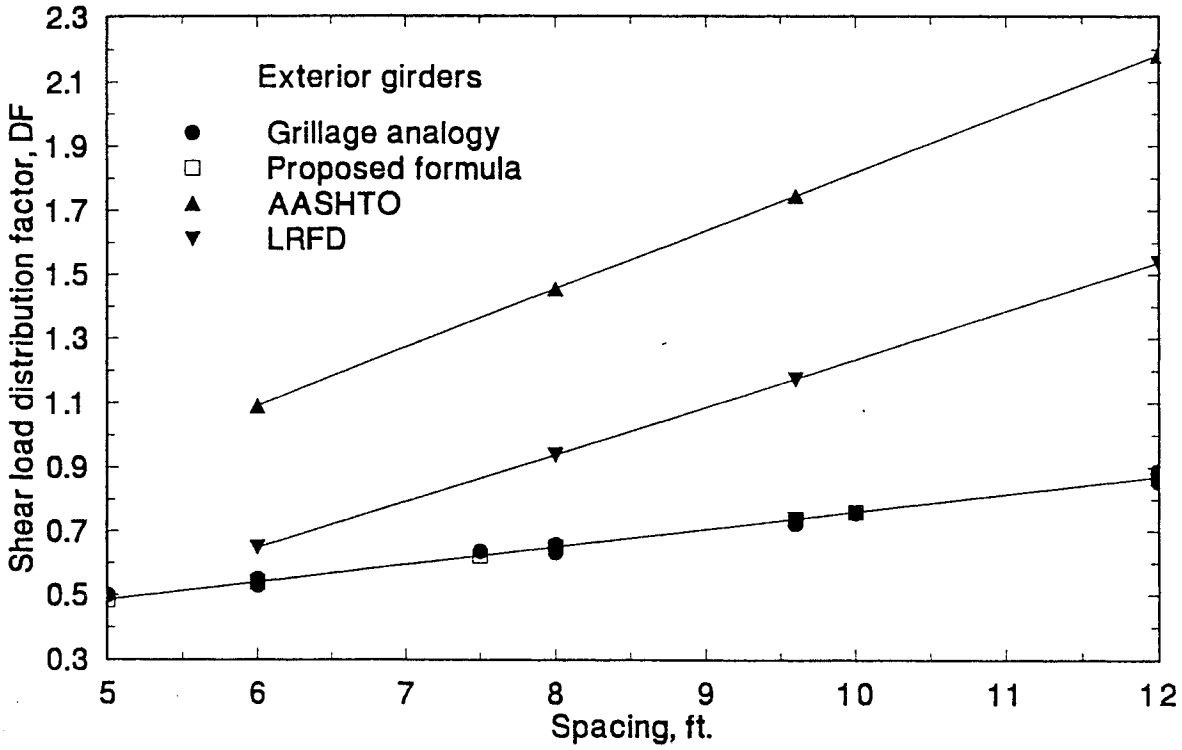

Fig. 5.27 Shear load distribution simplified formula (exterior girder)

are used in this study. These sections are 54 in., 63 in. and 72 in. bulb-tees. Figures 5.29 and 5.30 show comparison between standard AASHTO girders and bulb-tee girders. For the same height, the bulb-tee girders are lighter and stiffer than the standard AASHTO girders.

Several parameters affect the load distribution of slab-on-bulb tee girder bridges. Girder spacing, span length and girder type are the main parameters which are considered in this section. Bridge parameters are varied one at a time in a typical bridge. Variation of wheel load distribution factors with each parameter shows the importance of that parameter. Figure 5.1 shows the typical slab-on-bulb-tee girder bridge cross section used in the analysis. The typical slab-on-girder bridge has a span length equal to 100 ft with a bridge width of 42 ft. It has prestressed bulb Tee girder 54 in. with a slab thickness of 7 in. The concrete strengths of both the girder and slab were taken equal to 5000 psi.

Grillage Analysis

The typical slab-on-bulb-Tee girder bridge is divided into elements in the longitudinal and transverse directions similar to the slab-on-AASHTO girder shown in Figure 5.2. Eight longitudinal elements coincide with each girder center line in addition to elements in the transverse direction along the longitudinal nodes.

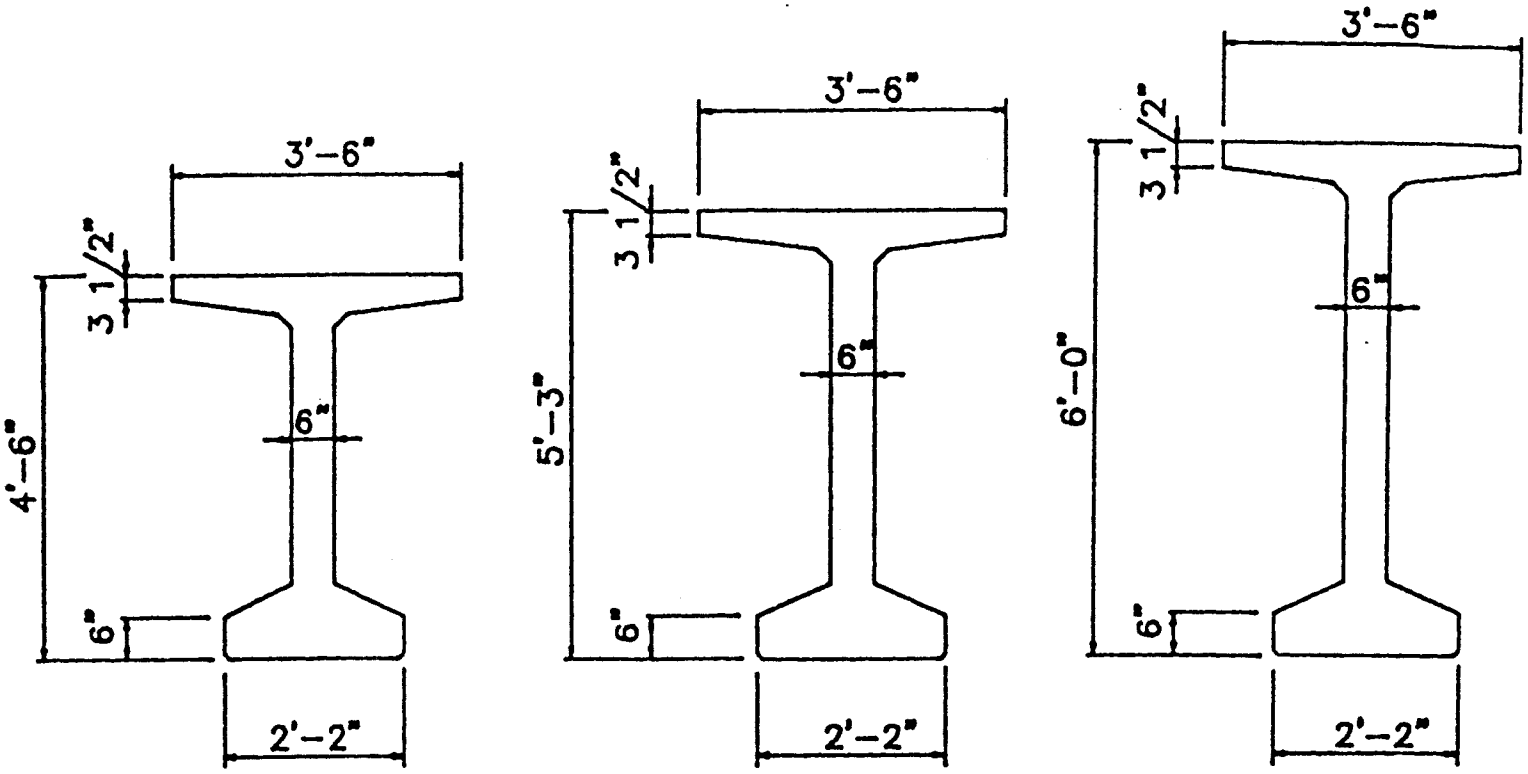

54" Bulb Tee **63" Bulb Tee** **72" Bulb Tee**

Section Properties						
Designation	A ($in.^2$)	I ($in.^4$)	Y_b (in.)	Z_b ($in.^3$)	Z_t ($in.^3$)	Wt (plf)
54" Bulb Tee	659	268,045	27.63	9,701	10,165	686
63" Bulb Tee	713	392,509	32.12	12,220	12,711	743
72" Bulb Tee	767	545,850	36.60	14,914	15,419	799

	Typical Span							
Designation	80'	90'	100'	110'	120'	130'	140'	150'
54" Bulb Tee	80 — 100							
63" Bulb Tee			100 — 125					
72" Bulb Tee					120 — 150			

Fig. 5.28 Typical bulb tee girder cross sections

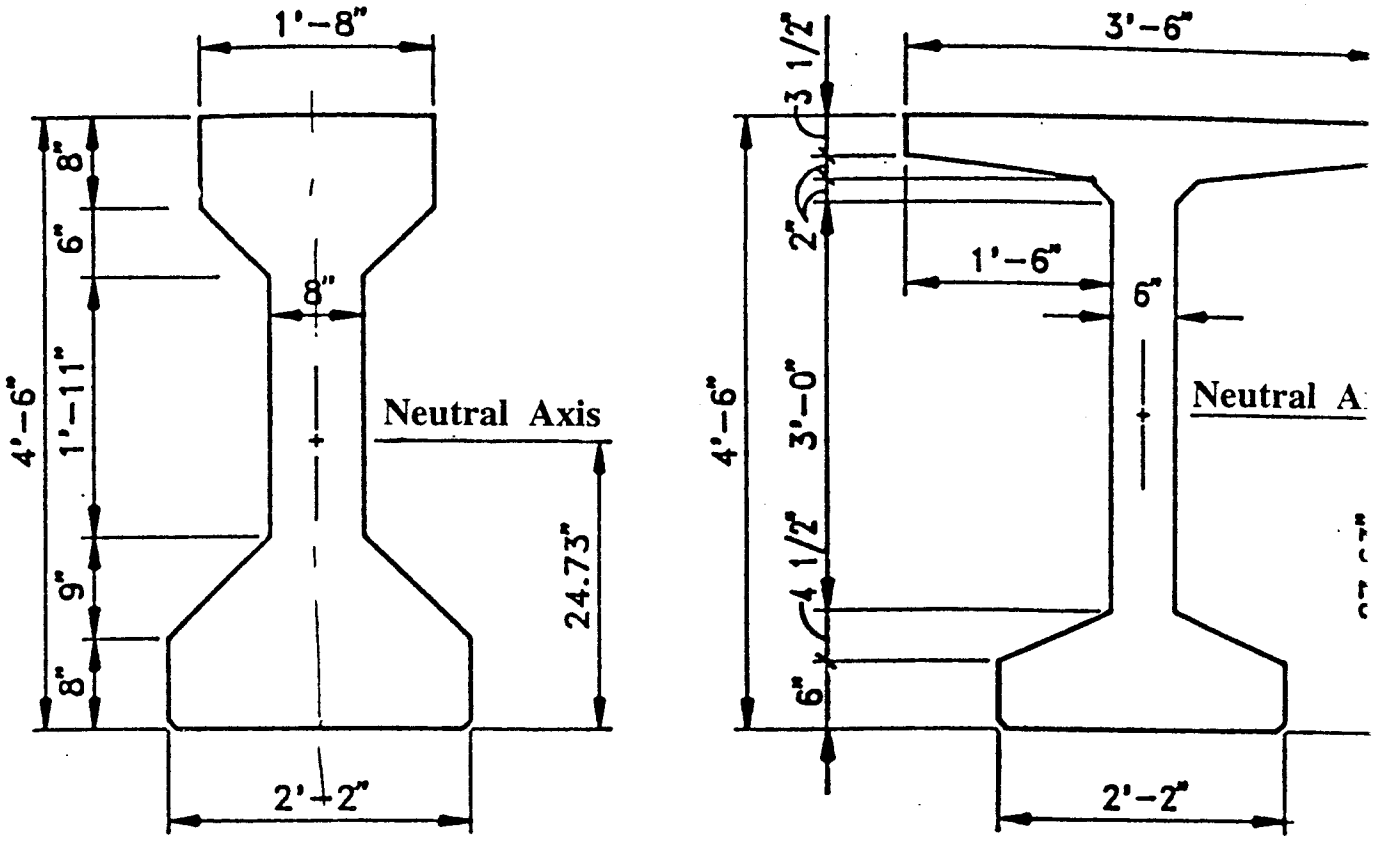

AASHTO Type IV I - Girder **54" Bulb Tee**

Type	Area (in^2)	Wt. (lb/ft)	I_x (in^4)	Y_b (in)	S_b (in^3)	S_t (in^3)
Type IV (Modified)	909	947	369,500	28.99	12,746	11,916
54" Bt	713	743	392,509	32.12	12,220	12,711

Fig. 5.29 Bridge girder comparison (AASHTO type IV and 54 in. bulb tee)

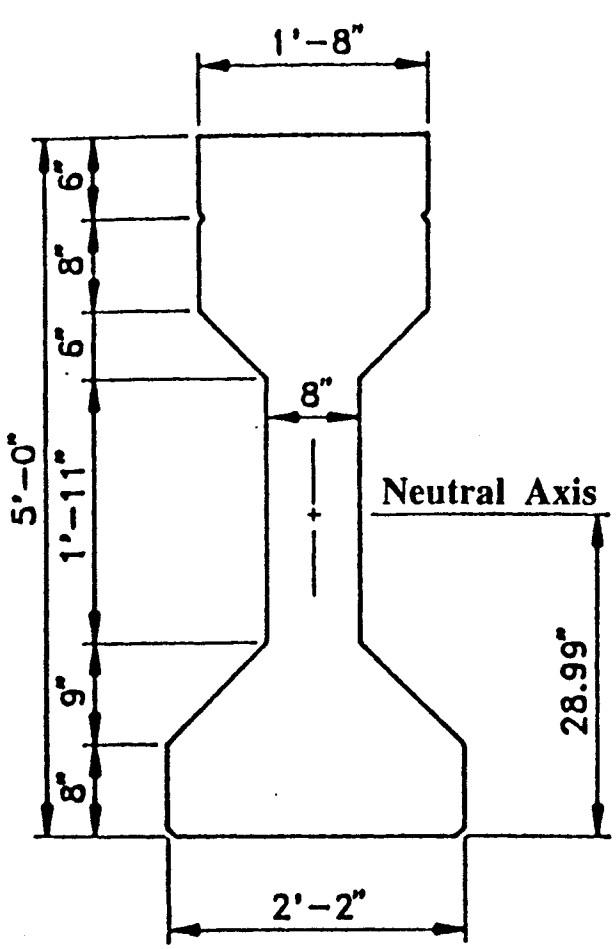

AASHTO Type IV I - Girder (Modified)

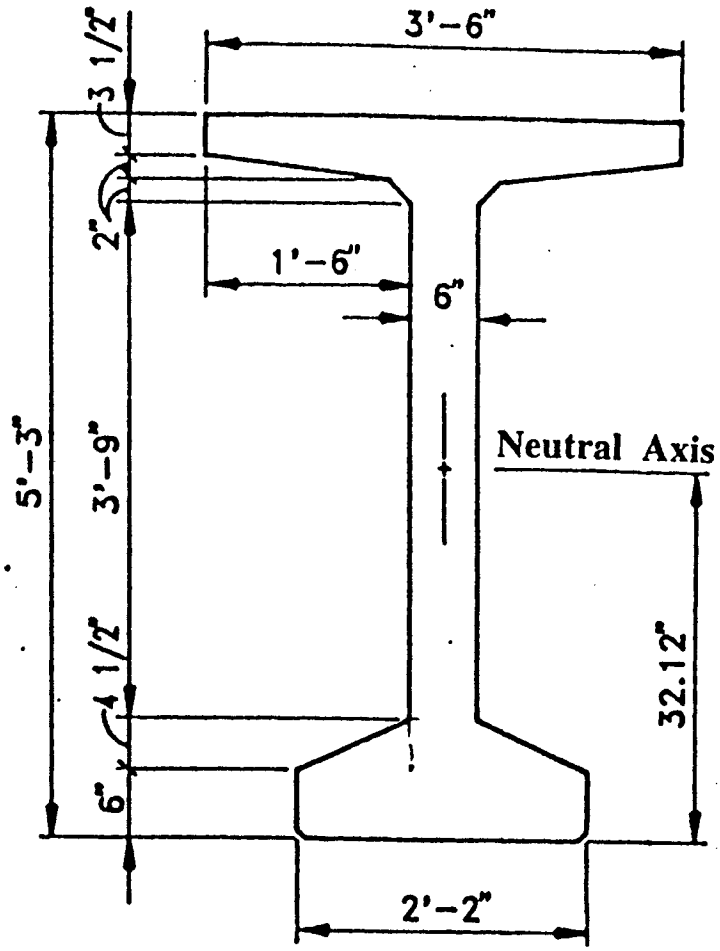

63" Bulb Tee

Type	Area (in^2)	Wt. (lb/ft)	I_x (in^4)	Y_b (in)	S_b (in^3)	S_t (in^3)
Type IV	789	822	260730	24.73	10543	8908
63" Bt	659	686	268045	27.63	9701	10165

Fig. 5.30 Bridge girder comparison (AASHTO type IV and 63 in. bulb tee)

Truck Load Position

The AASHTO HS-20 truck was used in this parametric study. The truck position in the longitudinal direction (span direction) was located to produce the maximum bending moments. To get the maximum bending moments in the bridges, two, three or four trucks were positioned in the transverse direction. The transverse distance between each truck varied from 4 to 6 ft. and in the most cases, it was selected to be 4 ft. The first axle of the first truck was at 3 ft. from the bridge edge, i.e., exactly over the exterior girder as shown in Fig. 5.3.

Table 5.3 summarizes thirty two cases for the flexural distribution factors of bulb-Tee girders. Several parameters were studied such as spacing, span length and girder type, etc.

5.6.1 Girder Spacing

The spacing between bulb-Tee girders was varied between 4.5 ft. and 9.0 ft. for three lane bridges with a width of 42 ft. as shown in Table 5.3. Figures 5.31 and 5.32 show that the distribution factor, DF increases with increasing girder spacing for interior and exterior girders respectively of a typical bulb-Tee bridge. The DF calculated using grillage analogy method ranges from 0.9 to 1.67 for interior girder and from 0.986 to 1.53 for exterior girders. In general, the girder spacing is very important factor in determining load distribution of bulb-Tee girders.

Table 5.3 Slab-on-bulb-Tee girders: flexural load distribution study cases

Parameter	Spacing, ft.	Span length,ft.	Girder type	Load cases
Spacing (8 cases)	4.5 6.0 7.2 9.0	100 100 100 100	54 in. 54 in. 54 in. 54 in.	3 trucks and 4 trucks
Span length (16 cases)	4.5 9.0	80 80	54 in. 54 in.	3 trucks and 4 trucks
	4.5 9.0	120 120	63 in. 63 in.	
	4.5 9.0	120 120	72 in. 72 in.	
	4.5 9.0	150 150	72 in. 72 in.	
Girder type (8 cases)	4.5 6.0 7.2 9.0	100 100 100 100	63 in. 63 in. 63 in. 63 in.	3 trucks and 4 trucks

When the value of d_e in Eqn. 5.3 is taken as 2 ft., the LRFD code distribution factors are the same for interior and exterior girders. Figure 5.31 shows that the distribution factors based on AASHTO and LRFD codes are in general smaller than those calculated using grillage analogy for interior girders (7 % for AASHTO and 2 % for LRFD). This is also valid for exterior girders (7 % for AASHTO and 6 % for LRFD) as shown in Fig. 5.32.

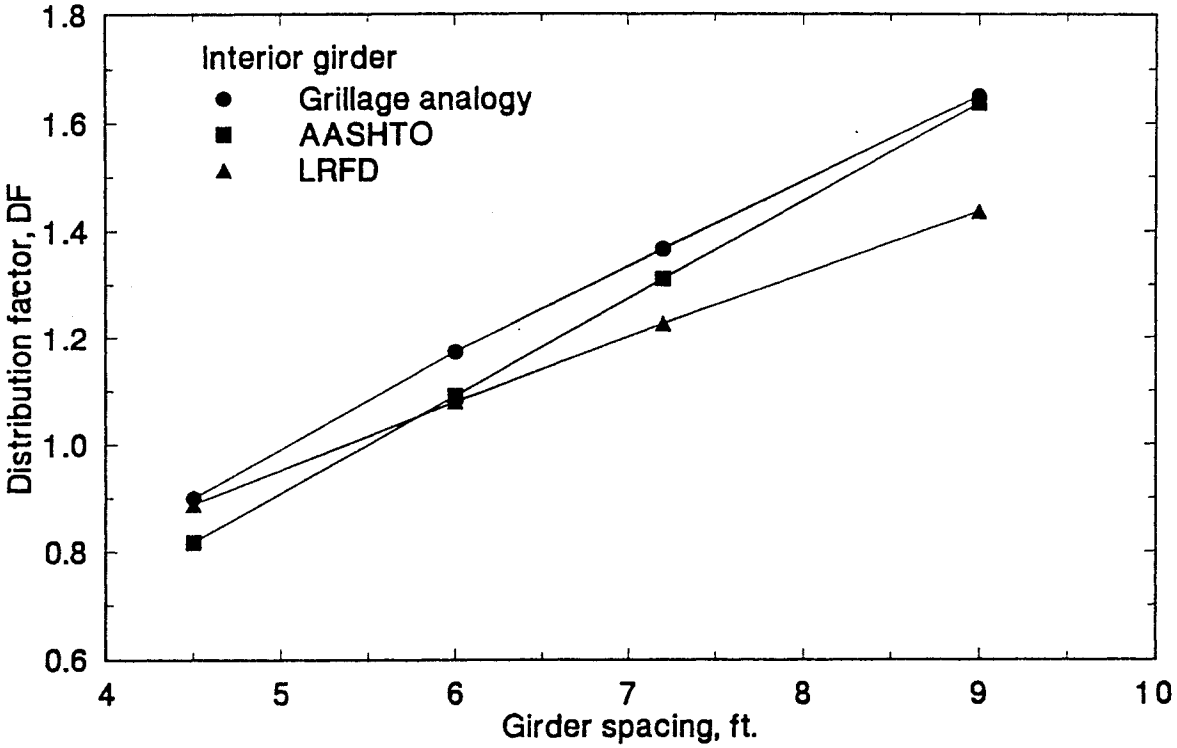

Fig. 5.31 Effect of girder spacing variations on load distribution of slab-on-bulb Tee bridges (interior girder)

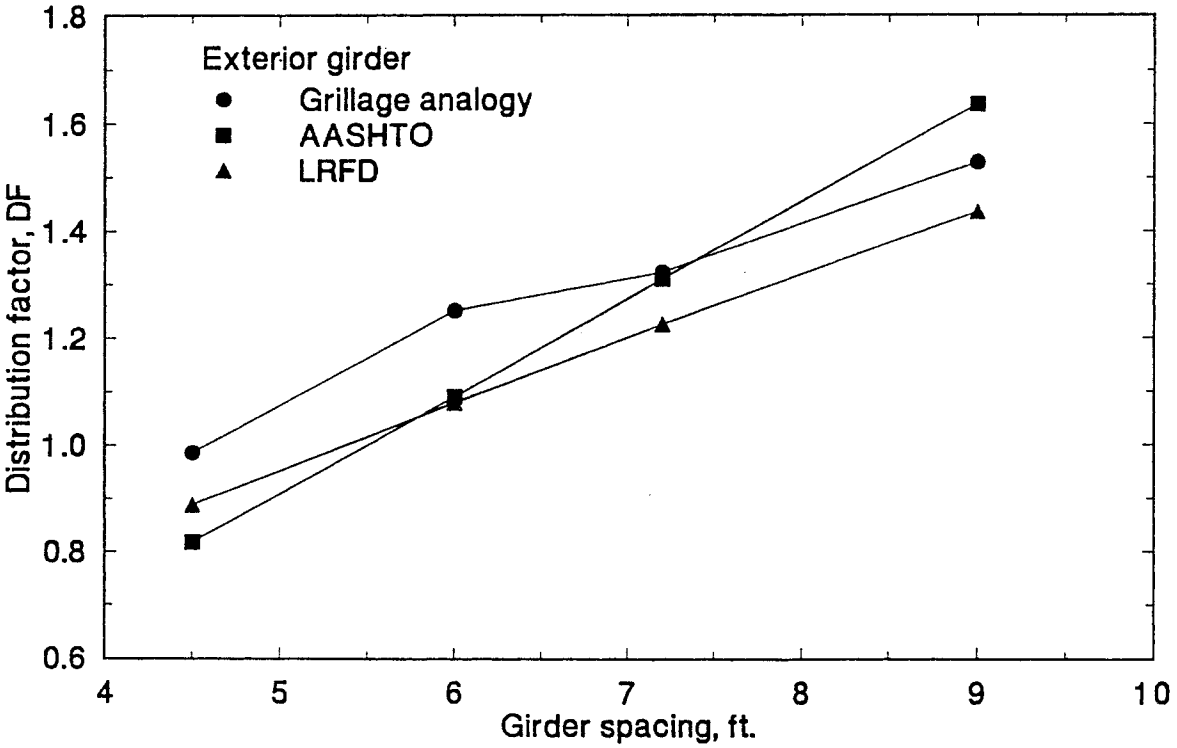

Fig. 5.32 Effect of girder spacing variations on load distribution of slab-on-bulb Tee bridges (exterior girder)

5.6.2 Span Length

The current AASHTO code ignores span length effect on load distribution, while the proposed LRFD code considers the span length as an important factor in wheel load distribution. Slab-on-bulb-Tee girder have spans varying from 80 ft. to 150 ft. as shown in Table 5.3. These bridges are investigated in this section to study the importance of the span length in calculating the load distribution. Two girder spacings were chosen for span length study (S = 4.5 ft. and S = 9.0 ft.). The slab thickness was 7 in. for all the bridges.

Three AASHTO HS-20 trucks were positioned in the transverse direction to calculate the maximum bending moment for interior girders, while two HS-20 trucks were positioned to calculate the maximum bending moment for exterior girders. In this section, bulb-tee girder 54 in. was selected for spans 80 ft. and 100 ft., bulb-Tee girder 63 in. was selected for spans 100 ft. and 120 ft.; whereas bulb-Tee girder 72 in. was selected for spans 120 ft. and 150 ft. (Refer to Fig. 5.28). The bending moment distributions of each bridge were used to calculate the distribution factors as mentioned in section 5.2.1.

Figures 5.33 and 5.34 show the changes in load distribution factors with increasing span for interior and exterior girders respectively. The sudden changes in the load distribution factors are due to changes in cross section mentioned before. In general, the load distribution factor decreases with increasing span for interior and exterior girders as shown in Table 5.4. The effect

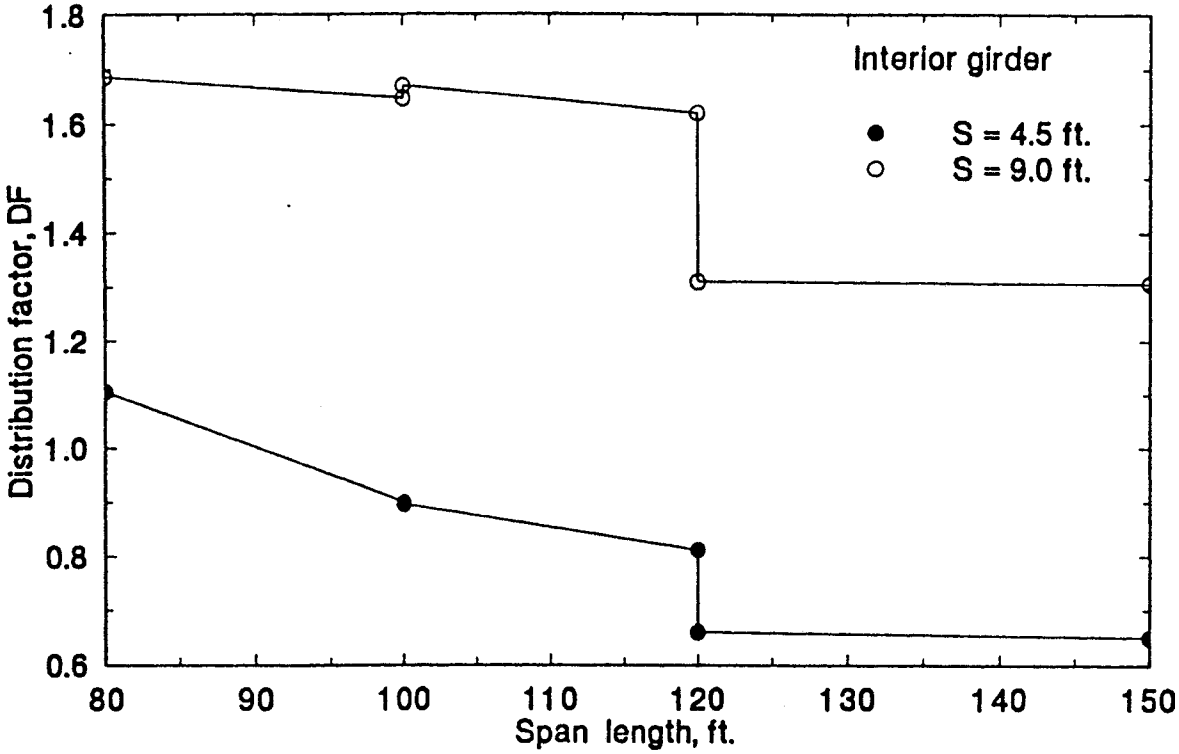

Fig. 5.33 Effect of span length variation on load distribution of slab-on-bulb Tee girders (interior girders)

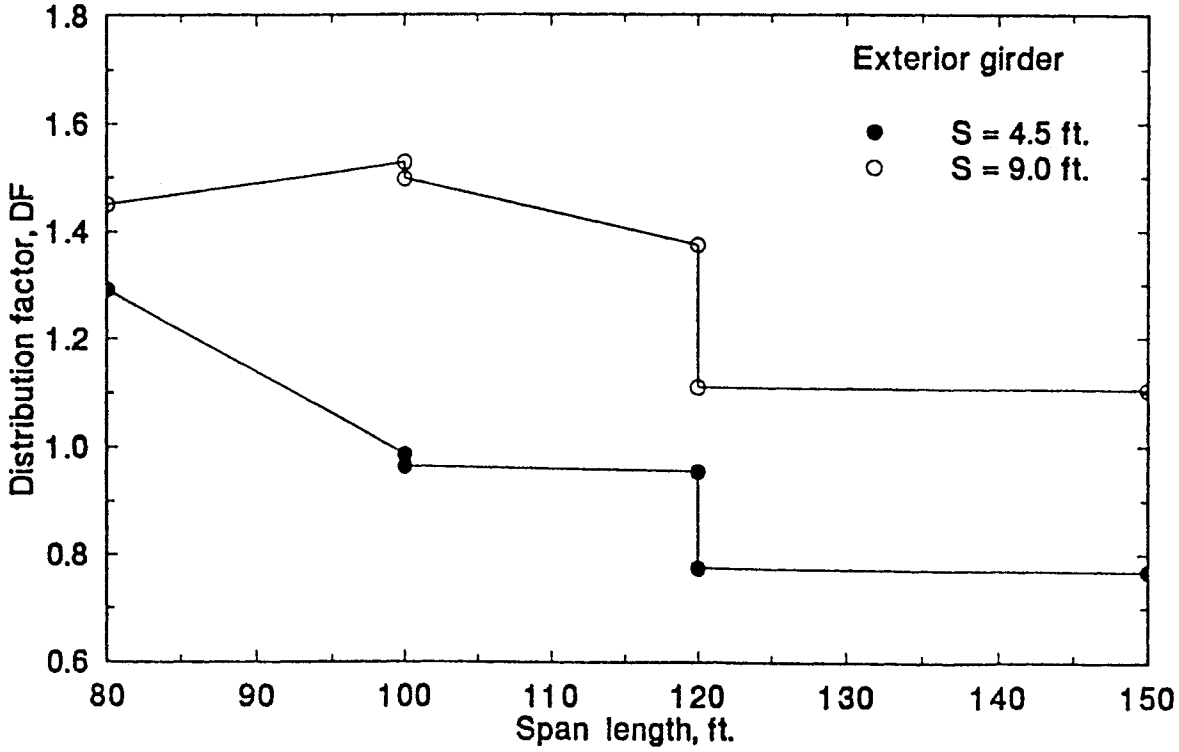

Fig. 5.34 Effect of span length variation on load distribution of slab-on-bulb Tee girders (exterior girders)

of span length in distribution factors of bulb-Tee girder requires more studies including field test data to quantify its importance.

Table 5.4 Effect of span length variation on flexural distribution factors of slab-on-bulb Tee girder bridges

Span length and girder type	Interior girder		Exterior girder	
	S = 4.5 ft.	S = 9.0 ft.	S = 4.5 ft.	S= 9.0 ft.
80 ft., 54 in.	1.105	1.686	1.291	1.45
100 ft., 54 in.	0.9	1.647	0.986	1.528
100 ft., 63 in.	0.896	1.67	0.954	1.498
120 ft., 63 in.	0.812	1.62	0.954	1.374
120 ft., 72 in.	0.66	1.31	0.774	1.11
150 ft., 72 in.	0.654	1.307	0.768	1.104

5.6.3 Bulb-Tee Girder Types

The proposed LRFD code introduced the girder stiffness as a parameter in load distribution. The longitudinal stiffness parameter, K_g, is used in the flexural load distribution

factor equation (Eqn. 5.2). Sixteen study cases were investigated using grillage analogy method as shown in Table 5.3. In all the cases, the span length of 100 ft. and bridge width of 42 ft. were kept constant. Two types of bulb_Tee girders (54 in. and 63 in.) were studied to determine the effect of girder type on the load distribution. The longitudinal stiffness parameter, K_g was computed to be 856,015.9, 1,235,263.9 and 1,706,482.1 for bulb-Tee girders type 54 in., 63 in. and 72 in. respectively.

Figures 5.35 and 5.36 show comparisons between the load distribution factors of 54 in. and 63 in. bulb-Tee girders for interior and exterior girders respectively. Figures 5.35 and 5.36 show the distribution factors of the 54 in. and 63 in. are almost equal for interior girders and exterior girders respectively. The girder stiffness effect was insignifcant in bulb-Tee flexural load distribution.

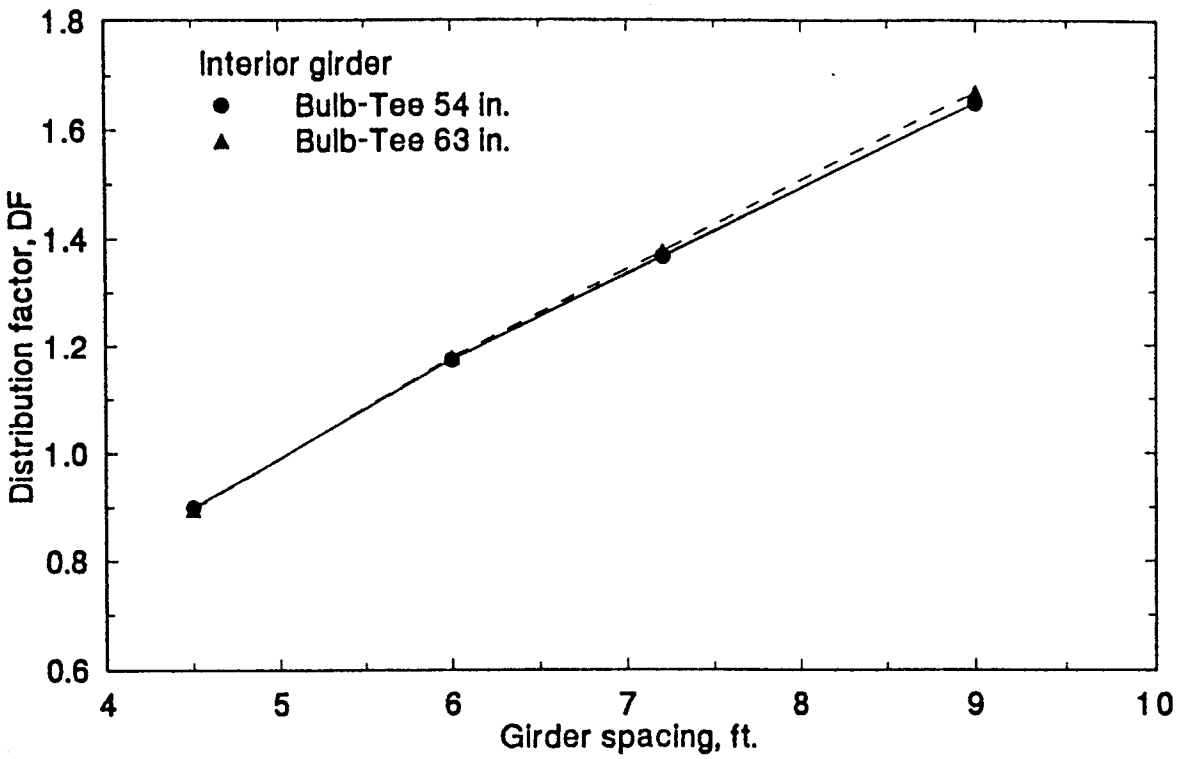

Fig. 5.35 Comparison of load distribution factors for the interior girders

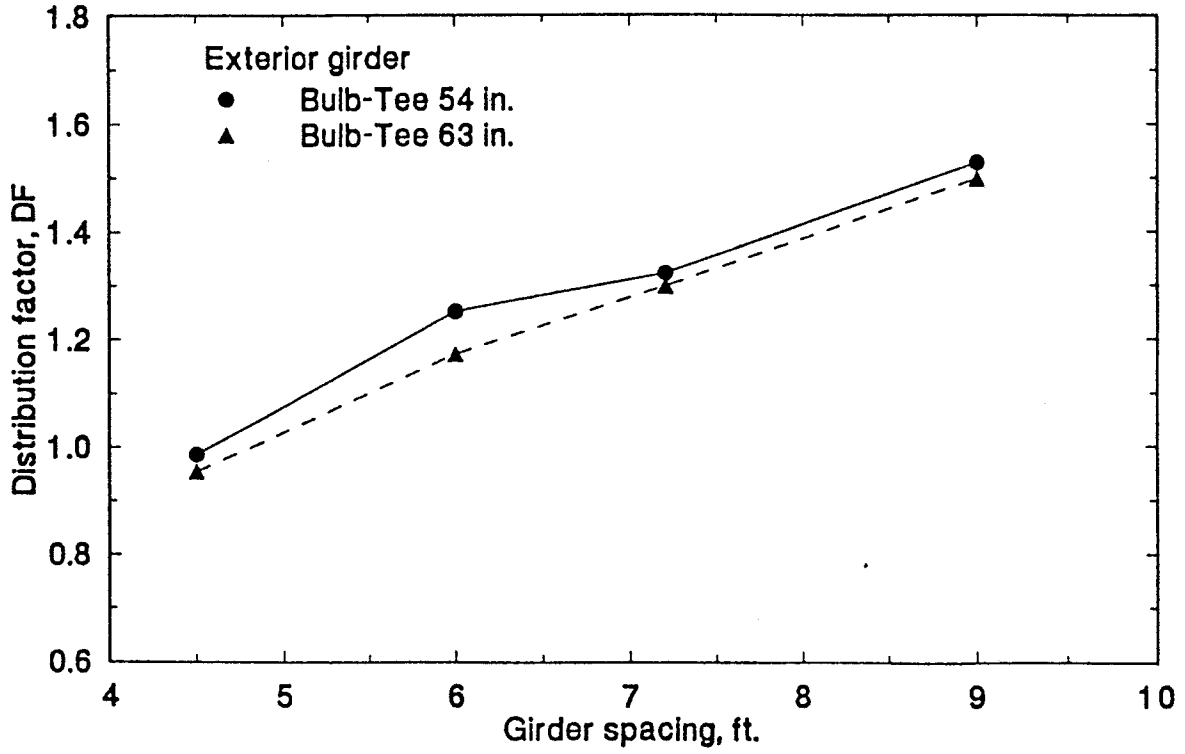

Fig. 5.36 Comparison of load distribution factors for the exterior girders

5.7 SLAB-ON-AASHTO GIRDER BRIDGES: FIELD TESTS

Florida Department of Transportation (FDOT) have tested many bridges to check the strength and establish bridge ratings. The strength of bridge elements is generally determined by first placing strain or deflection transducer gages at the bridge critical locations along the girders, and then incrementally loading the bridge to induce maximum effects. The data collected can then be analyzed and used to establish the strength of each component as well as the **load distribution**.

The FDOT's bridge load testing apparatus consists of two test vehicles, a mobile data acquisition system and a mobile machine shop. The two test vehicles have been designed to deliver the ultimate live loads specified by AASHTO code. Detailed dimensions of the test vehicles are shown in Figure 3.13. Each vehicle can carry maximum of 72 concrete blocks, each weighing approximately 2,150 pounds. Incremental loading is achieved by adding blocks with a self-contained hydraulic crane mounted on each truck.

The test vehicles are initially loaded with a number of concrete blocks, established from the preliminary analysis of the existing structure. The vehicles are then driven and placed on the critical locations of the bridge. After each load step, if the results compare favorably with the theoretical prediction, additional blocks are added to the vehicles and the test repeated until the ultimate AASHTO load is achieved. The data gathered can then be analyzed and a report of the findings prepared.

Data from certain slab-on-AASHTO girder bridge test reports are used for load distribution analyses. The typical report contains transverse strain distributions in the maximum bending moment section for several load stages. The report also contains the applied moment vs. strain curves for several load stages.

One method for use of test results in rating calculations is to use test data to calculate wheel load distribution factors. This measured wheel load distribution factor can be used in bridge-rating calculations in the place of those based on AASHTO. AASHTO (Guide specifications 1989) has also presented a refined bridge-rating methodology in which measured wheel load distribution factors can be used.

The girder bending moment can be calculated from the measured strains as follows:

$$M = \varepsilon E S \qquad (5.9)$$

where

ε = the strain measured at the extreme fibers of the bottom flange

E = the modulus of elasticity

S = the section modulus.

The ACI equation was used to calculate the elastic modulus of concrete which is based on f'_c = 5000 psi. Many bridges exhibit some degree of composite action even when they were not constructed with shear studs or other devices for transferring shear between girders and deck.

The composite and non-composite section modulus were used to calculate the measured bending moments. The use of composite section modulus overestimated the measured bending moments. The use of cracked section modulus may be more realistic in the calculation of the bending moment based on the measured strains. Limited information about the girder prestress force, prestress losses and loading history made the calculation of the cracked section modulus very difficult. The uncracked non-composite section modulus was used for its simplicity and this is consistent with Stallings and Yoo (1993) analysis of steel-I bridges. The sum of the bending moments calculated from girder strains based on the non-composite section modulus was about 85-95% of the total moment applied during the field test. This indicates that the use of uncracked non-composite section is realistic. The difference may be due to bearing restraint, curbs and railings effects.

For tests where all traffic lanes are loaded with equal-weight trucks, the measured wheel load distribution factor for the *i*th girder was given by Stallings and Yoo (1993) as

$$DF_i = \frac{n\varepsilon_i}{\sum_{j=1\rightarrow k} \varepsilon_j w_j} \qquad (5.10)$$

where

ε_i = the bottom flange strain at the ith girder,

w_j = the ratio of the section modulus of the ith girder to the section modulus of a typical interior girder

k = number of girders,

n = the number of wheel lines of applied loading.

The parameter, n is required to make the measured wheel load distribution factor compatible with AASHTO definition. In this chapter, similar approach was used to calculate the measured load distribution factor based on the calculated bending moments. The measured distribution factor is compared with those based on AASHTO, LRFD and grillage analysis.

5.7.1 Manatee County Bridge (# 130119)

The bridge is located on I-275 in Manatee County (Bartow, Florida). It consists of 4 simply supported spans with span lengths of 33'-6", 87'-9", 87'-9" and 29 ft. respectively. The overall length of the bridge is 238 ft. and the total width is 42'-9", 40 ft. curb to curb as shown in Figure 5.37. Spans 1 and 4 consist of two exterior type IV and 3 interior type II prestressed beams, while spans 2 and 3 consist of five type IV prestressed beams. The load test was carried out on the second span of the bridge going east, which consists of 5 prestressed type IV girders spaced at 9'-3" center-to-center with slab thickness of 7.5 in. Prior to load testing, an inspection of the bridge was conducted. The slabs, piles and pile caps along the entire length of the bridge appeared to be in excellent condition with no noticeable cracking or spalling of concrete.

The measured strain distribution along the bridge width is shown in Figure 5.38 for different load stages. The maximum strain in the transverse direction was found to occur at the central girder. Figure 5.39 shows the moment distribution along the transverse direction calculated from the maximum measured strains and those using grillage analogy. The grillage analogy predicted more uniform bending moment distribution than the results from the field tests. Table 5.5 summarizes the results of the bridge analyses using the measured strain, grillage analogy, AASHTO and LRFD wheel load distribution factor for bridges #130119 and #720408. The measured wheel load distribution factor, DF, was equal to 1.29, which is higher by about 40% than that from grillage analogy DF, which equals 0.92. This difference may be attributed to variation in concrete strength and section modulus which are used on calculating the measured DF. Both DF calculated using AASHTO and LRFD were higher than the DF calculated using the measured strains and grillage analogy method. This confirms that AASHTO code and to a lesser extent, the proposed LRFD code give conservative values for wheel load distribution factor for slab-on-girder bridges.

5.7.2 Duval County Bridge # 720408

The bridge is located on I-295 over S.C.L.R.R. and U.S. 90 , in Duval County (Jacksonville, Florida). It consists of seven simply supported spans with span lengths of 56', 104.15', 62.13', 64.21', 64.23', 79.56', and 60.50 ft. respectively. The 104.15 ft. span consists of eight type IV prestressed concrete girders, spaced at 5.30 ft. center to center. The total width is 42'-9", 40 ft. curb to curb as shown in Figure 5.40. The superstructure is supported by concrete

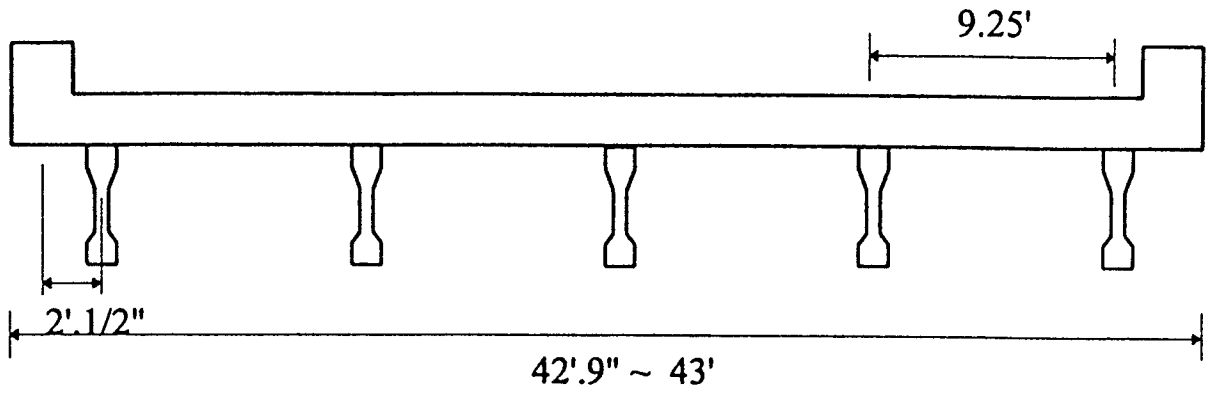

Fig. 5.37 Typical cross-section of slab-on-girder bridge # 130119

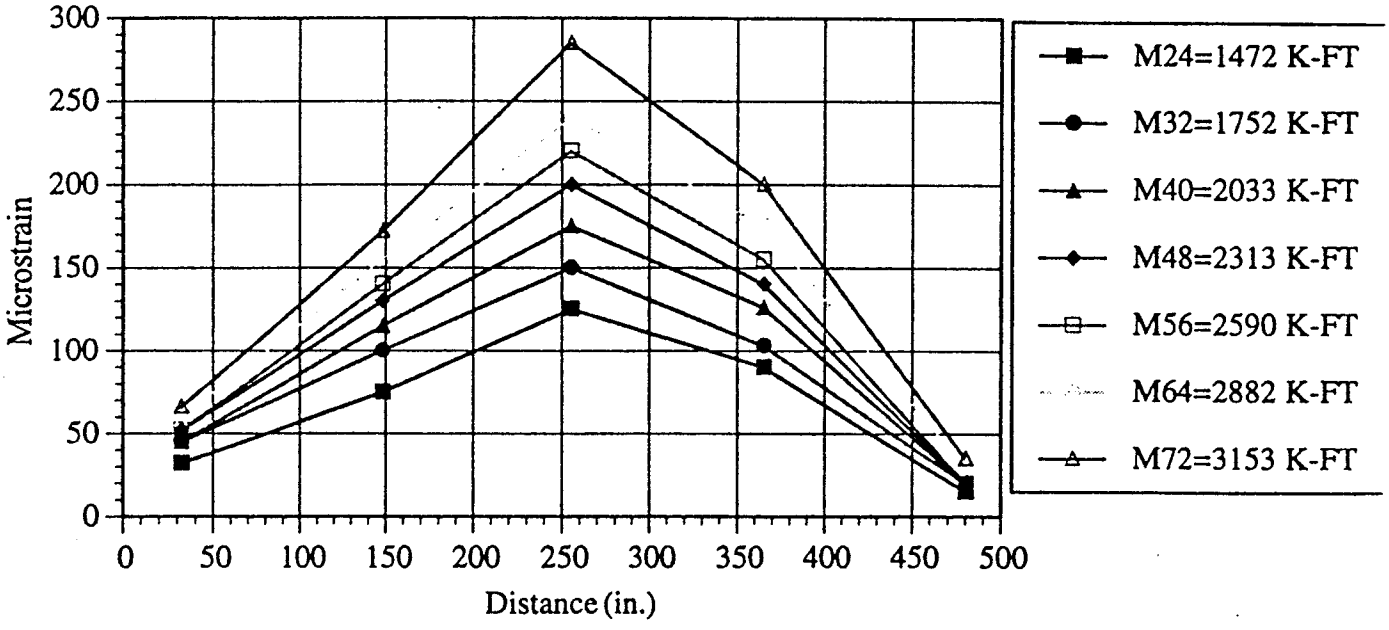

Fig. 5.38 Measured girder strains for different applied loads (slab-on-girder bridge # 130119)

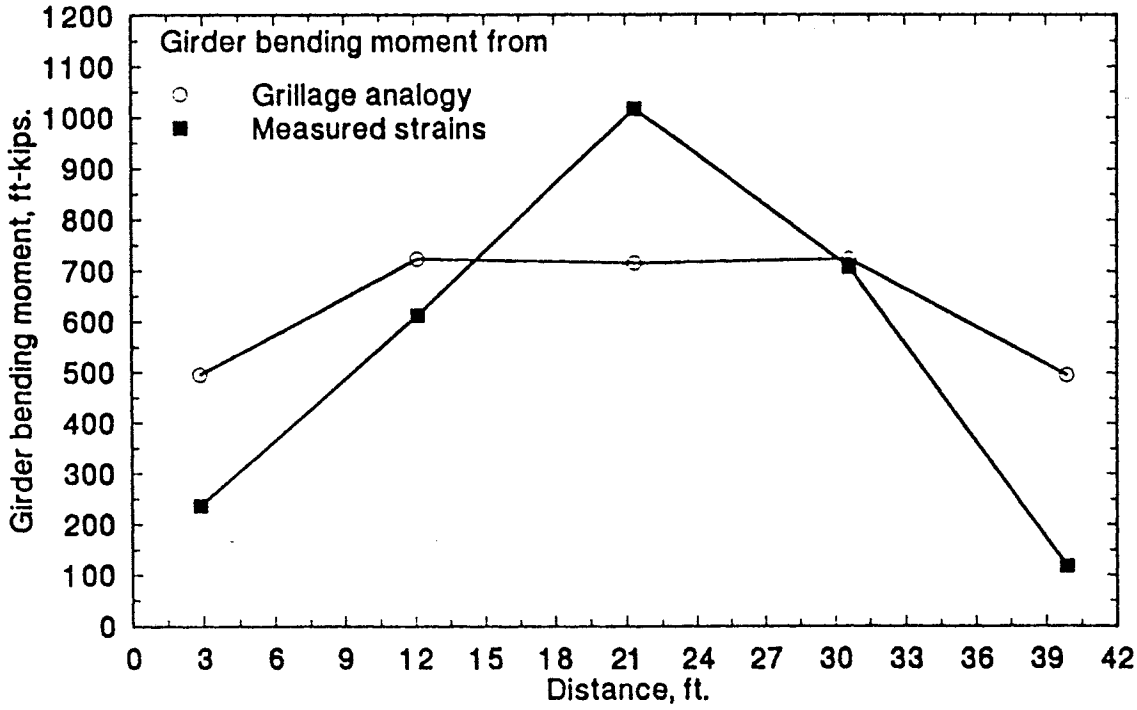

Fig. 5.39 **Girder bending moment based on field test and grillage analogy (slab-on-girder bridge # 130119)**

piles and pier caps, with a slab thickness of 7 in. Prior to load testing, an inspection of the bridge was conducted. The slabs, piles and pile caps along the entire length of the bridge appeared to be in good condition.

The measured strain distribution along the bridge width is shown in Figure 5.41 for maximum load stage. The maximum strain in the transverse direction occurred at girder number 4. Figure 5.42 shows the moment distribution along the transverse direction calculated from the maximum measured strains and those from grillage analogy. In this bridge, the grillage analogy bending moments were consistent with those based on measured strains. This may be due to smaller spacing of this bridge than the Manatee County bridge (this bridge spacing = 5.3 ft. and Manatee County bridge = 9.25 ft.). Consequently, the DF from measured strains and grillage analogy are very close as shown in Table 5.5. Both DF calculated from grillage analogy and measured strains are smaller than those based on AASHTO and LRFD values as shown in Table 5.5. This again confirms that both AASHTO and the proposed LRFD codes give conservative estimates for wheel load distribution factors. .

Table 5.5 Summary of load distribution factors, DF.

Bridge	Measured strains	Grillage analogy	AASHTO code	LRFD code
#130119	1.29	0.92	1.68	1.52
#720408	0.68	0.71	0.96	1.00

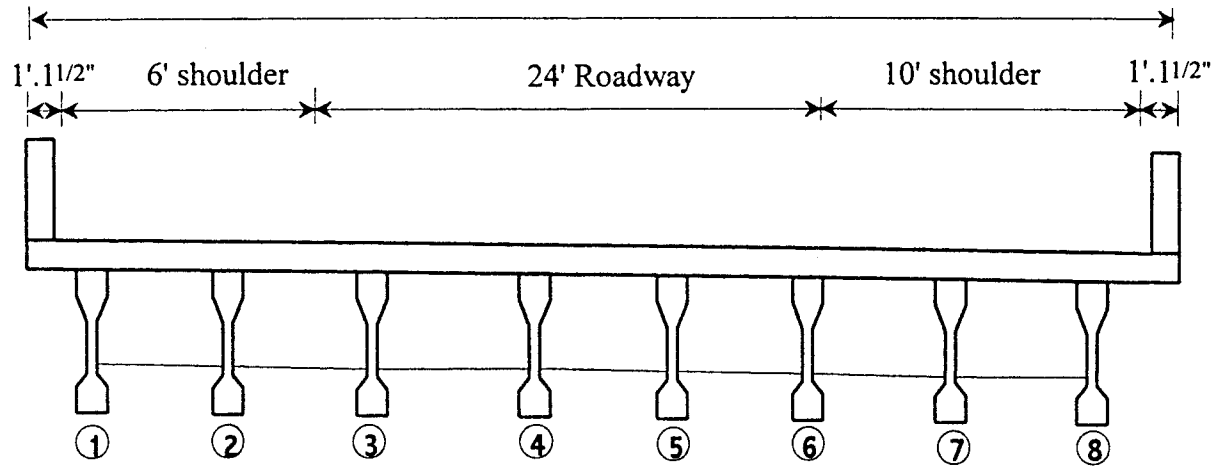

Fig. 5.40 Typical cross-section of slab-on-girder bridge # 720408

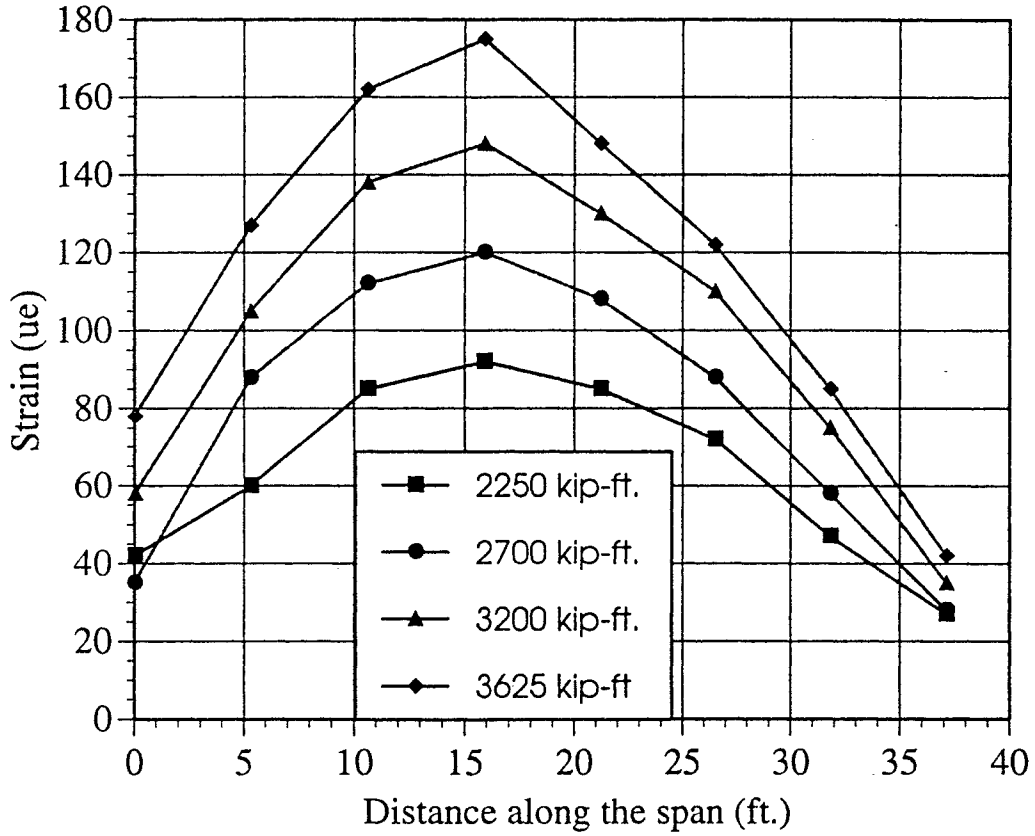

Fig. 5.41 Measured girder strains for different applied loads (slab-on-girder bridge # 720408)

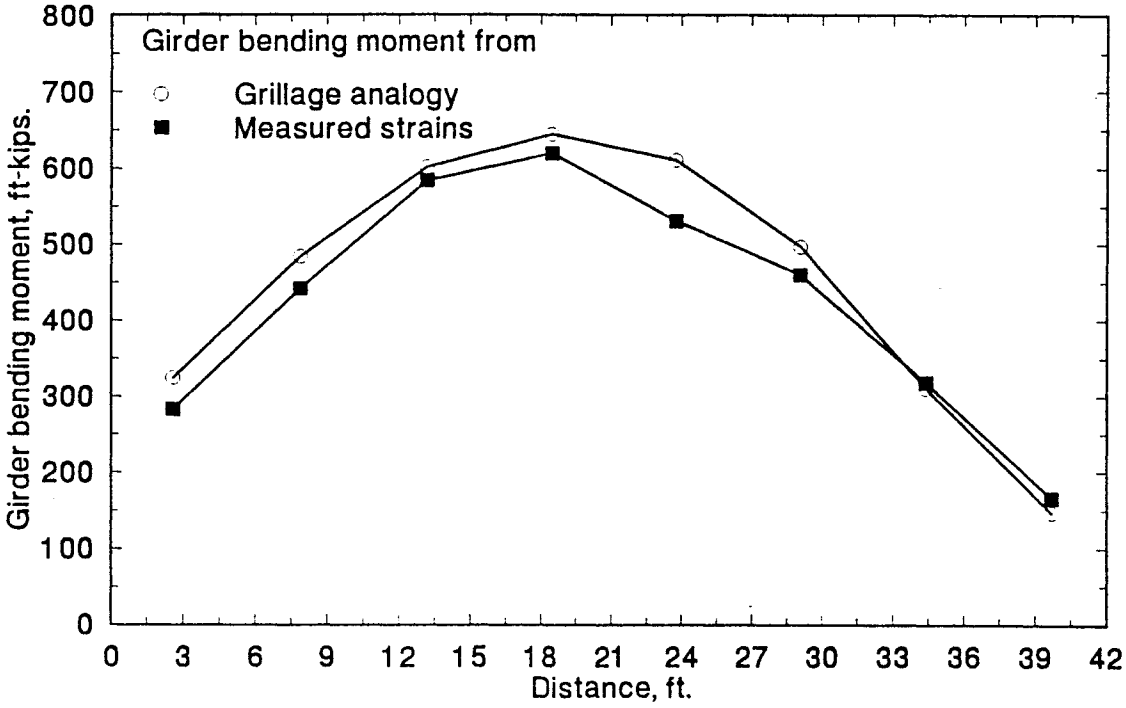

Fig. 5.42 Girder bending moment based on field test and grillage analogy (slab-on-girder bridge # 720408)

CHAPTER 6

LOAD DISTRIBUTION ANALYSIS OF DOUBLE TEE BRIDGES

6.1 INTRODUCTION

The need to replace the large number of deteriorated highway bridges in the United States has stimulated the efforts to intensify the search for more economical and durable bridge systems. Standardization in bridge construction might provide a practical and economical solution. Standardized cross sections such as precast AASHTO I-girders, bulb-Tee girders and double-Tee girders are produced in large numbers, yet customized by varying the length of each element. Excellent quality control and optimum use of labor and materials are achieved in the production of these precast components. AASHTO and bulb-Tee girders are discussed in Chapter 5. Double Tee girders are discussed in this chapter.

Double tee beams have been used in the past for rural and secondary roads; however they can be used at state and interstate highways with spans up to 80 ft. The precast double-Tee beams are arranged longitudinally side by side forming a simple "V" joint and tied together by transverse post-tensioning. The elimination of cast-in-place elements is associated with speed of construction and reduction in labor costs. El Shahawy [1987 and 1990] investigated experimentally and

analytically the feasibility of transversely prestressed double tee bridges. Following this investigation, the FDOT performed field load testing of two double tee bridges in Tallahassee, Florida. Based on the tests, the performance of double tee bridges was found to be satisfactory.

In studying the load distribution of double tee bridges, Stanton (1983) assumed that flange connectors could only transmit vertical shear, and no moments. Jones and Boaz (1986) assumed the flange connectors can transmit shear forces in three directions as well as a moment along the axis parallel to that of the beams. El-Moussa (1988) studied this type of bridges using finite-element analysis and assumed that the connector can transmit only vertical forces. Bishara (1993) studied this type of bridges using three-dimensional finite element method.

In the present study, grillage analogy method is used to analyze a double tee simply supported bridge and calculate the corresponding load distribution factors. The results obtained are compared with those based on AASHTO (1989) and proposed LRFD (1993) codes. Field tests of double tee bridges performed by FDOT are analyzed to investigate the load distribution factors of double tee bridges.

6.2 LOAD DISTRIBUTION BASED ON AASHTO AND THE PROPOSED LRFD CODES

The current AASHTO method of load distribution reduces the complex analysis of a bridge subjected to one or more vehicles to the simple analysis of a beam. According to this method, the

maximum bending moment in a girder is obtained by treating a girder as a one-dimensional beam. This beam is subjected to a loading, which is obtained by multiplying one line of wheels of the design vehicle by a load fraction (S/D) where S is average beam spacing in feet. The quantity D for concrete floor supported by double tee beams is 6.5 for one lane bridges and 6.0 for multi-lane bridges. If S exceeds 6.0 ft. for one lane bridges and 10 ft. for multi-lane bridges, the load in each beam shall be the reaction of the wheel loads, assuming the flooring between the girders to act as a simple beam. The D values for double tee beams are smaller than those for I-girders and this implies that AASHTO code assumes that the bending moment due to the truck loads is more localized in double tee girders than I-girders.

The proposed LRFD approach is similar to AASHTO method, but considers more parameters such as span length, bridge width, slab thickness and number of lanes. The proposed LRFD approach for double tee bridges gives different distribution factors for bending and shear in the interior and exterior girders. The distribution of live loads on precast concrete double tee section is categorized under the category "i" in the proposed LRFD code.

The category "i" has the same equations for load distribution as for I-girders (Eqns. 5.1 to 5.6) if sufficiently connected to act as a unit. If the double tee sections are connected so as to prevent relative vertical displacement at the interface, the following for (S/D) is specified (regardless of number of loaded lanes) for the flexural distribution factor of interior girders:

S/D **(6.1)**

where

$D = 11.5 - N_L + 1.4\ N_L\ (1\text{-}0.2\ C)^2$ when $C < 5$

$D = 11.5 - N_L$ when $C > 5$

$C = 2.0\ (W/L)$

N_L = number of design lanes

L = span of beam, ft.

W = edge to edge width of bridge, ft.

For exterior girders, the lever rule is specified in the proposed LRFD code to calculate the load distribution factor. The lever rule is defined as the statical summations of moments about one point to calculate the reaction at the second point.

6.3 DOUBLE TEE GIRDERS FLEXURAL LOAD DISTRIBUTION FACTORS: PARAMETRIC STUDY

Several parameters affect the load distribution of double tee bridges. Girder spacing, span length and girder type are the main parameters which should be considered. One type of cross section of double tee girders (limited number of sections are available) is used in the parametric study. The girder spacing is established in the previous sections as a very important parameter in load distribution and hence there is no need to investigate the girder spacing effect on double tee load distribution. The span length is the only parameter which need to be investigated to determine its effect on double tee load distribution.

Figure 6.1 shows the typical double tee bridge cross section used in the analysis. The double tee bridge has a bridge width equal to 42 ft. 9 in. Six precast prestressed double tee beams with identical dimensions as shown in Fig. 6.2 are used in the bridge. The concrete strength of both the girder and slab was taken equal to 5000 psi. In this bridge, it is assumed that the beams are connected together by transverse post-tensioning to act as an integral unit.

The double tee bridge shown in Figure 6.1 is divided into elements in the longitudinal and transverse directions as shown in Figure 6.3. The double tee was idealized as an equivalent single T-beam. This single T beam has the same area, moment of inertia and depth of centroid as that of the actual double tee beam shown in Fig. 6.3. Eight longitudinal elements were considered with each girder center line in addition to elements in the transverse direction along the longitudinal nodes.

The AASHTO HS-20 truck was used in this parametric study. The truck position in the longitudinal direction (span direction) was determined so as to produce the maximum bending moments. To get the maximum bending moments in the bridges, two / three trucks were positioned in the transverse direction. The transverse distance between each truck varied from 4 to 6 ft. and in most cases, it was selected to be 4 ft. The first axle of the first truck was at 6.5 ft. from the bridge edge (shoulder is 5 ft. and parapet is 16.5 in.).

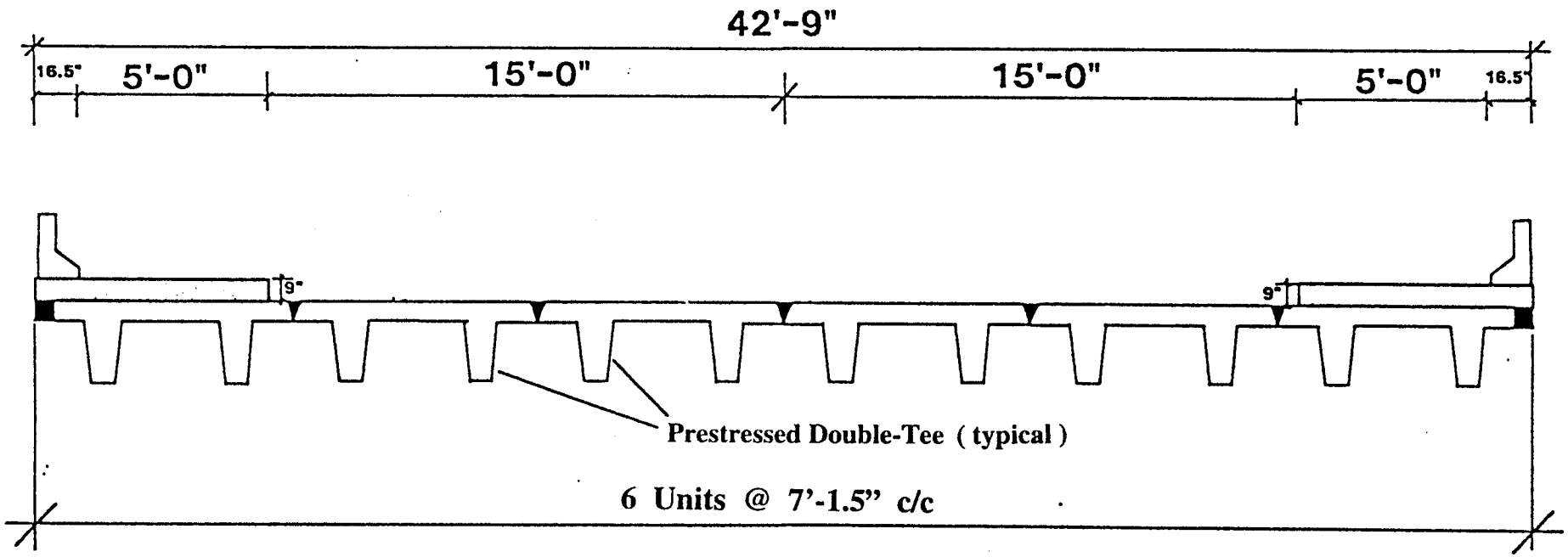

Fig. 6.1 Typical double tee bridge cross-section

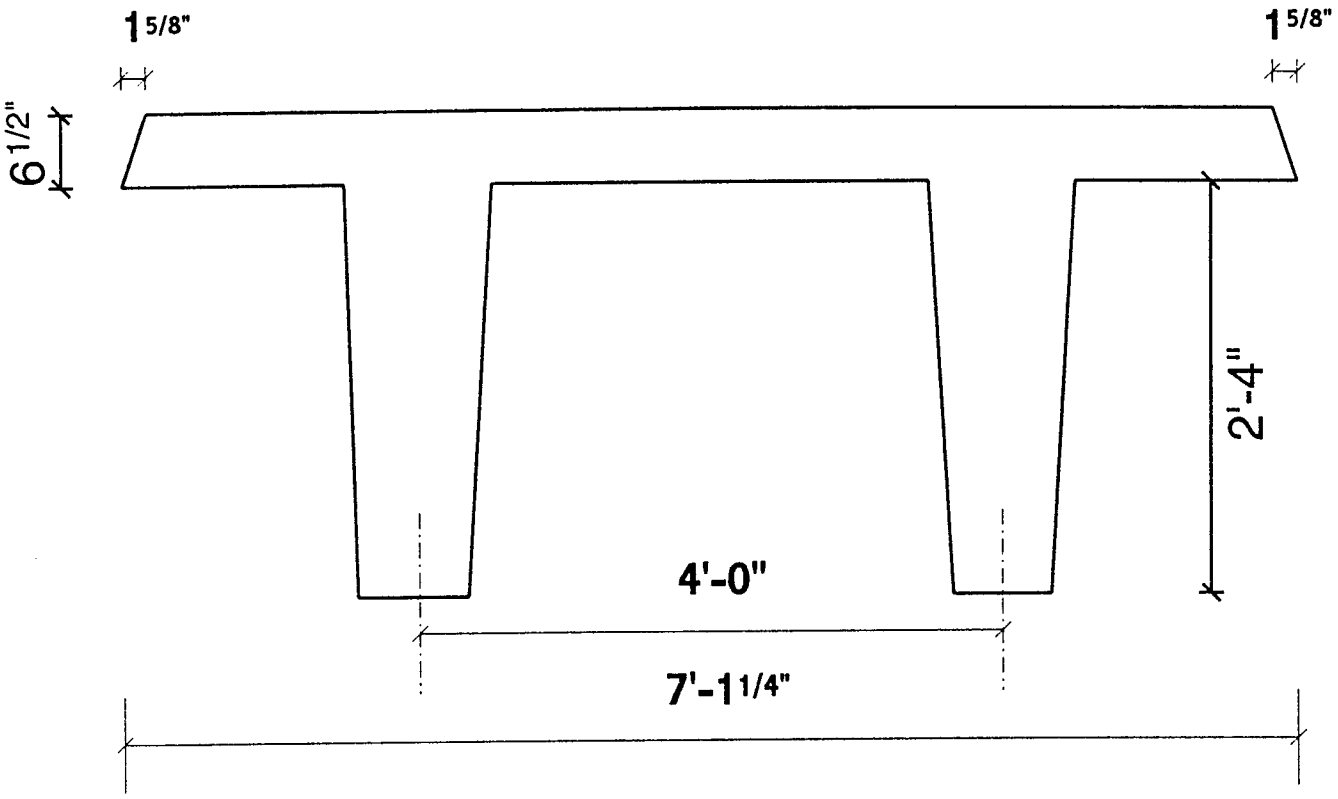

Fig. 6.2 Typical double tee beam cross-section

(a) Double-T Girder

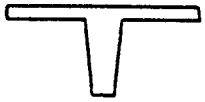

(b) Combining the two webs of Double-T into a single T-Beam

Fig. 6.3 Idealization of double tee beam into a single beam

6.3.1 Span Length

The current AASHTO code does not take into account the span length effect on load distribution, whereas the proposed LRFD code considers the span length as an important factor in truck load distribution. Double Tee beam bridges with spans varying from 40 ft. up to 80 ft. were investigated in this section.

Figure 6.4 shows the bending moment distributions for different span lengths of an interior double tee beam. The bending moment increases with the increase in the span length and the moment distribution tends to be more uniform for shorter spans. These bending moment distributions were used to calculate the distribution factors as mentioned in section 5.2.1.

Figures 6.5 and 6.6 show the changes in load distribution factor with increasing span for interior and exterior girders respectively. The load distribution factor for the interior girders decreases with increasing span (about 35%) and the load distribution factor of exterior girders increases with span increase (about 50%). It is clear that the load distribution factor of the exterior girders is more dependent on the span than the interior girders. This is consistent with the results of slab-on-AASHTO girders discussed in Chapter 5. The proposed LRFD code does not consider that exterior girders are more dependent on span length than interior girders. The distribution factor for interior girders calculated using grillage analogy is larger (about 8% to 14%) than those using LRFD as shown in Figure 6.5. Figure 6.6 shows that the LRFD load distribution factors are

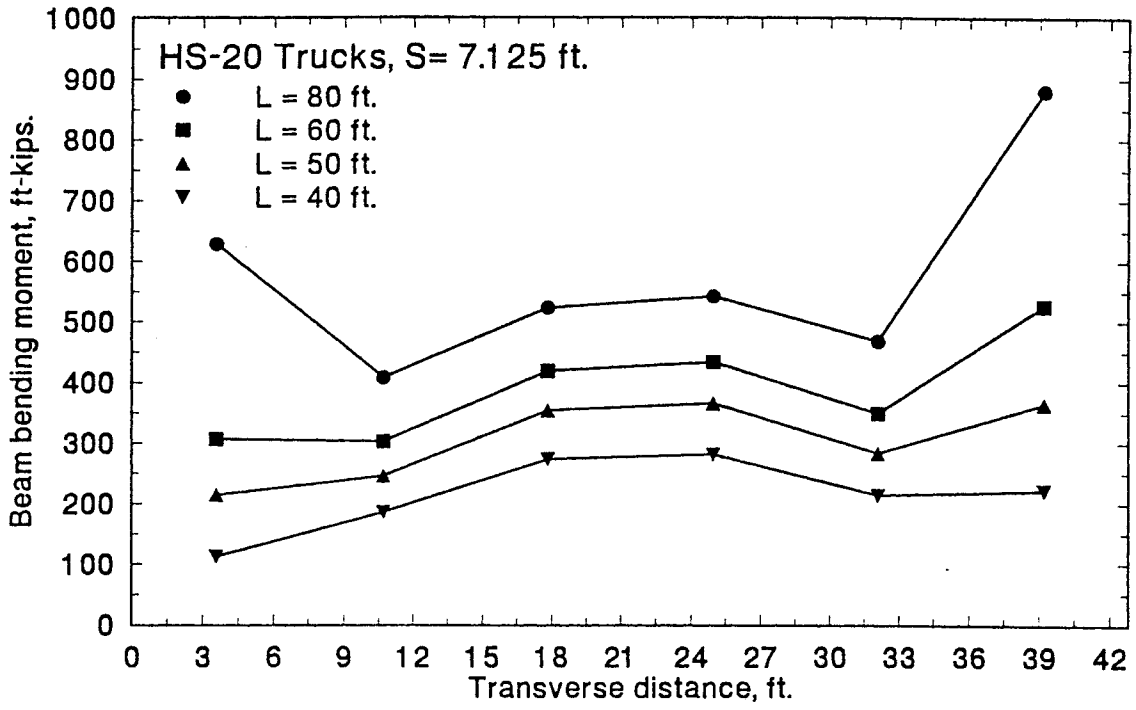

Fig. 6.4 Double tee bending moments for different span lengths

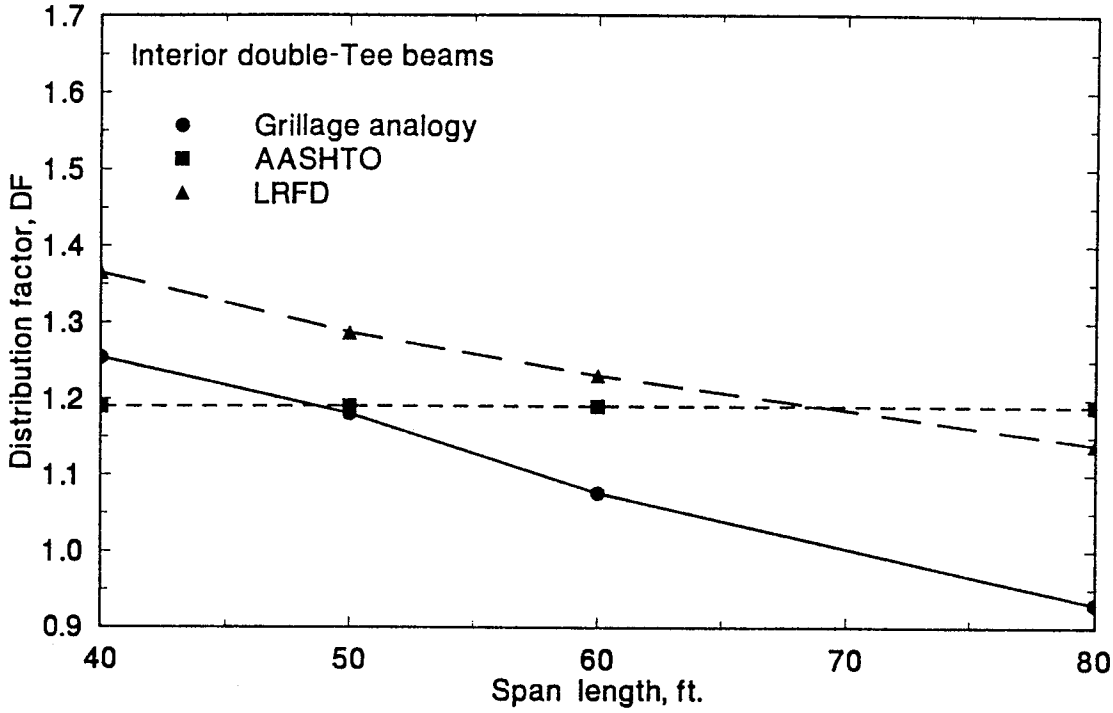

Fig. 6.5 **Load distribution factor variation with span length for interior double tee beam**

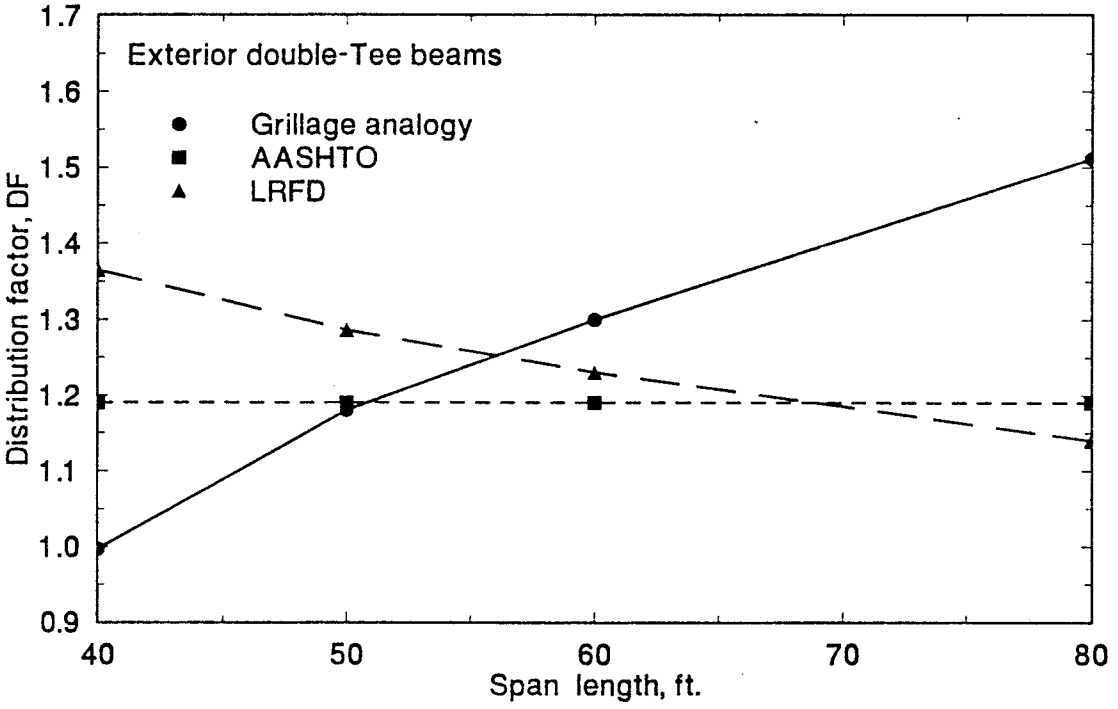

Fig. 6.6 **Load distribution factor variation with span length for exterior double tee beam**

inaccurate in calculating the load distribution factor for exterior double tee beams. This observation needs further research on more double tee cross section types.

6.4 DOUBLE TEE BEAM BRIDGE FIELD TEST

Florida Department of Transportation (FDOT) tested limited number of double tee bridges to check their strength and establish bridge ratings. The strength of bridge elements is generally determined by first placing strain or deflection transducer gages at the bridge critical locations along the elements, and then incrementally loading the bridge to induce the maximum effects. The data collected can then be analyzed and used to establish the strength of each component as well as the load distribution.

The test vehicles are initially loaded with a number of concrete blocks, established from the preliminary analysis of the existing structure. After each load step, if the results compare favorably with the theoretical prediction, additional blocks are added to the vehicles and the test repeated until the ultimate AASHTO load is achieved. The data can then be analyzed and a report of the finding prepared.

Data from a double tee bridge test report are used in the load distribution analysis. The report contains transverse deflection distributions in the mid-span for several load stages. One method for use of test results in rating calculations is to use test data to calculate wheel-load

distribution factors. The measured wheel load distribution factors can be used in bridge-rating in the place of wheel load distribution factor defined by AASHTO.

For tests where all traffic lanes are loaded with equal-weight trucks, the measured wheel-load distribution factor for the *i*th girder may be given as:

$$DF_i = \frac{n\delta_i}{\sum_{j=1\rightarrow k} \delta_j}$$

where

δ_i = the deflection at the ith double tee beam;

k = number of double tee beams;

n = the number of wheel lines of applied loading.

The parameter n is required to make the measured wheel-load distribution factor compatible with AASHTO definition. In this chapter, this approach is used to calculate the measured load distribution factor for double tee beams. The measured distribution factor is compared with this based on AASHTO , LRFD and grillage analysis.

6.4.1 Tallahassee Double-Tee Bridge

The bridge is located in the city of Tallahassee, Florida. The bridge has two lanes and consists of six precast prestressed double tee beams. A cross section of the bridge is shown in Fig. 6.1. The cross section of a typical double tee beam is shown in Figure 6.2. The bridge has a span of 60 ft. with a width equal to 42' 9", 30 ft. curb to curb.

Vertical deflections were measured with linear variable displacement transducers (LVDT's) placed at center line, 1/4 points of each double tee beams. Deflection measurements were taken in all four load positions. Figure 6.7 summarizes the deflection measurements at center line for different load stages.

Figure 6.8 shows the deflection measurements of the double tee beams at mid-span and the corresponding deflections calculated using grillage analogy method. Figure 6.9 shows the bending moment distribution along the transverse direction calculated using grillage analogy method. These bending moments are used to calculate the load distribution factor based on grillage analogy method. Table 6.1 summarizes the wheel-load distribution factors based on measured deflections, grillage analogy, AASHTO and LRFD for the field test bridge. The measured load distribution factor is calculated based on the deflection instead of the bending moments. The measured DF was smaller than the DF calculated based on grillage analogy, LRFD and AASHTO codes.

Table 6.1 Field test: load distribution factor, DF.

Bridge	Measured deflections	Grillage analogy	AASHTO code	LRFD code
Double-Tee	0.94	1.23	1.2	1.23

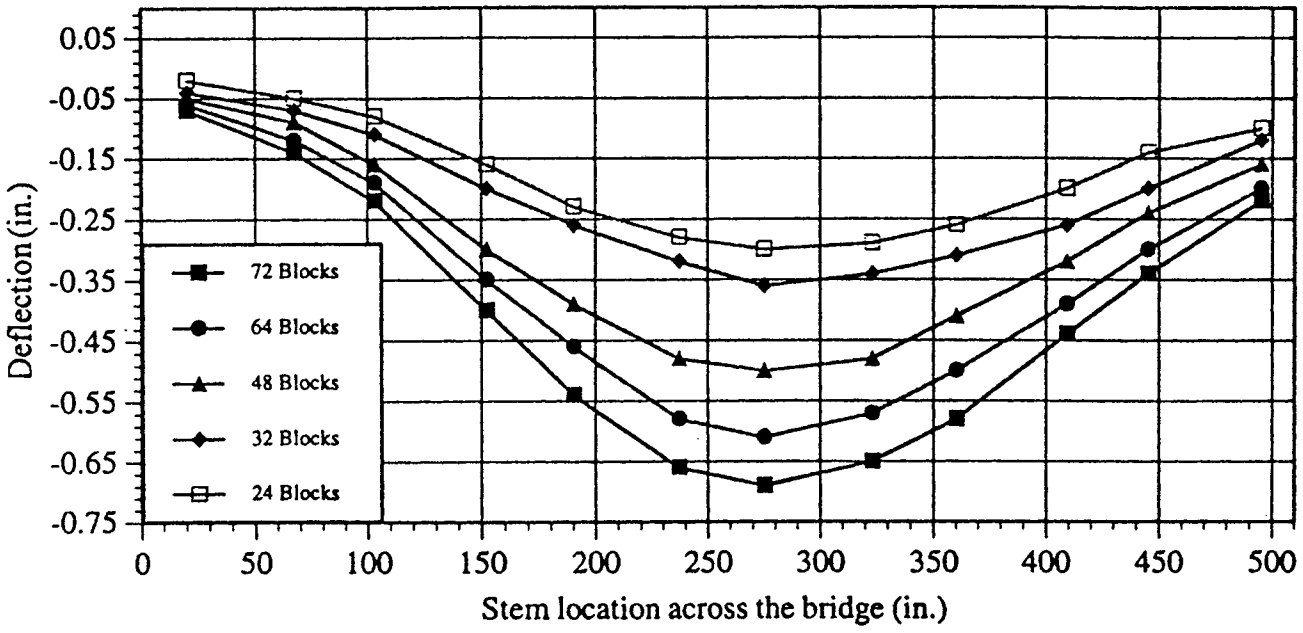

Fig. 6.7 Measured deflections at mid-span for different applied loads (double tee beam bridge)

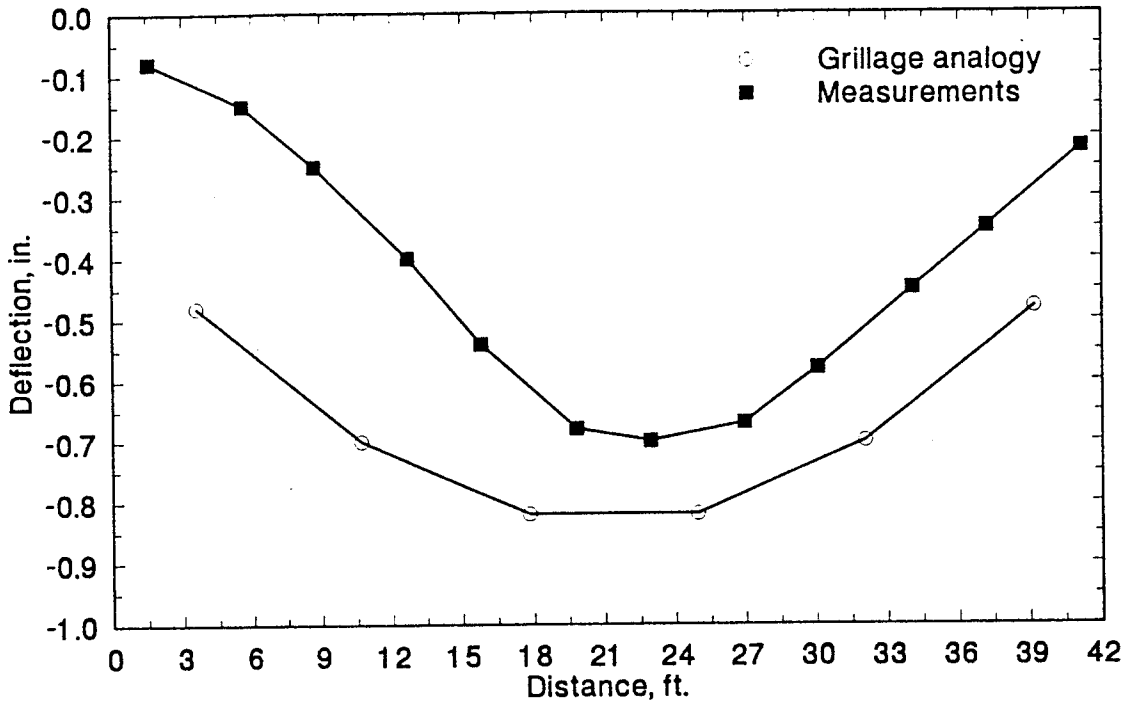

Fig. 6.8 Deflections from field test and grillage analogy (double tee beam bridge)

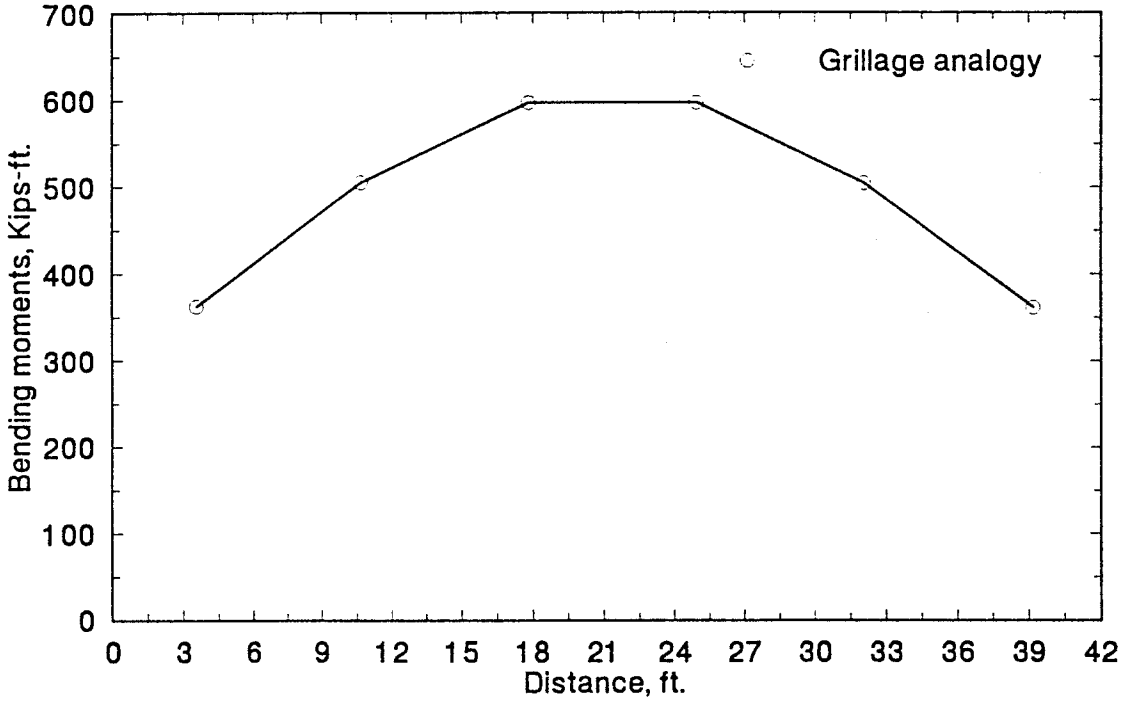

Fig. 6.9 Bending moments based on grillage analogy (double tee beam bridge)

CHAPTER 7

SUMMARY AND CONCLUSIONS

7.1 SUMMARY

The present study on wheel load distribution is focused on the more commonly used bridge types in Florida viz., slab-on-girder, solid slab, voided slab and double Tee bridges. Chapter 2 reviews the existing different analytical and field load distribution methods for different bridge types. Chapter 3 discusses the grillage analogy concepts, the cross sectional properties of different bridge types for grillage analogy idealization, field test procedures and methodologies.

In Chapter 4, both analytical and field studies on the wheel load distribution of solid and voided slab bridges are presented. Grillage analogy is used as an analytical tool to study the various parameters affecting load distribution and suggest which parameters should be considered. In addition to the analytical study, data from field tests performed by Structures Research Center, FDOT, are compared with those based on the grillage analogy, AASHTO and LRFD codes. Several parameters such as span length, bridge width, slab thickness, edge beam and number of lanes are considered in the parametric studies.

Both analytical and field studies on the truck load distribution of slab-on-girder bridges are presented in Chapter 5. Grillage analogy is used to study the various parameters affecting load

distribution and suggest which parameters must be considered (160 study cases were performed). In addition to the analytical study, data from field tests performed by Structures Research Center, FDOT, are used to verify the analytical results.

In Chapter 6, grillage analogy method is used to analyze double Tee simply supported bridges and calculate the corresponding load distribution factors. The analytical results obtained are compared with those based on AASHTO (1989) and the proposed LRFD (1993) codes. Field test of double Tee bridges are analyzed to investigate the load distribution factors.

The current AASHTO code does not take into account the span length effect on load distribution, whereas the proposed LRFD code considers the span length as an important factor in truck load distribution. Double Tee beam bridges with spans varying from 40 ft. up to 80 ft. were investigated in this study.

7.2 CONCLUSIONS

7.2.1 Solid and Voided Slab Bridges

7.2.1.1 Solid slab bridges

i) The effective widths calculated using grillage analogy are larger than those calculated using AASHTO and LRFD codes, which indicate that both AASHTO and LRFD codes give conservative estimate of effective width, E for solid slab bridges.

ii) Based on this limited study, the bridge width can be neglected as a parameter in calculating the effective widths of solid slab bridges.

iii) The variation of slab thickness has very little effect in the effective width. This confirms the approaches adopted by AASHTO and LRFD codes in neglecting the thickness as a parameter in effective width calculation.

iv) The edge beam moment increases with increase in moment of inertia, i.e. increase in edge beam depth or width. The edge beam depth significantly affects the value of E. Slab bridges without edge beams or with hidden edge beams have greater maximum moment than similar slab bridges with edge beam and hence the resulting effective width is smaller. These results suggest that the edge beam size should be taken into account in wheel load distribution. Neither current AASHTO specifications nor the proposed LRFD code considers the edge beam effect in the effective width equation.

v) Based on the solid slab parametric studies, the span length and the edge beam depth are the main parameters, which significantly affect the effective width calculations. Effective width equations are proposed for solid slab bridges without edge beams and with edge beams.

vi) Effective widths calculated from grillage analogy and measured strains are higher than the AASHTO and LRFD values. The effective widths based on the AASHTO and LRFD codes are more conservative.

vii) The bridge rating based on effective widths calculated from measured strains seems to give satisfactory results.

viii) The effective width based on measured strains are inaccurate for the slab bridges with preexisting of cracks as shown in the analysis of Nassau County bridge.

7.2.1.2 Voided slab bridges

Comparisons between similar solid and voided slab bridges were made to examine the assumption that both solid and voided slab bridges have the same effective width. The results from the grillage analogy method was used in making the comparisons. It is clear that the maximum bending moment for solid slab is smaller than that for voided slab, which means the solid slab has larger effective width than voided slab bridges. The difference in effective widths of solid and voided bridges may be attributed to the relative vertical movements between the voided slab precast units. This can be observed from the presence of longitudinal cracks in the bridge.

7.2.2 Slab-on-Girder Bridges

i) Girder spacing is a very important factor in determining flexural and shear wheel load distributions of slab-on girder bridges.

ii) The flexural distribution factors based on LRFD are in general slightly smaller than those calculated using grillage analogy particularly for larger girder spacings. It is shown that the

distribution factors based on LRFD code are in better agreement with those calculated using grillage analogy for smaller girder spacings which are more commonly used.

iii) The distribution factor calculated using grillage analogy is slightly larger than those based on AASHTO and LRFD codes particularly for shorter spans. However, the AASHTO and LRFD load distribution factors are more accurate for longer spans (90 and 100 ft) which are commonly used in bridges.

iv) The DF for the 54 ft. wide bridge is slightly higher than that for the 36 ft. wide bridge (2% to 4%) and this can be considered to be insignificant. This establishes that AASHTO and LRFD codes are realistic in neglecting the bridge width as a parameter in load distribution.

v) For a given girder spacing, the LRFD load distribution equation overestimates the effect of K_g on wheel load distribution and this is more evident for exterior girders.

vi) The detailed parametric studies on shear load distribution indicate that the spacing between girders is a dominant parameter in shear load distribution. Parameters such as span length, bridge width and girder stiffness have little effect on shear load distribution for AASHTO girders.

vii) Simplified equation for shear load distribution of slab-on-AASHTO girders is suggested for interior and exterior girders (section 5.5)

viii) In general the load distribution factor decreases with increasing span for interior and exterior bulb-tee girders; but this decrease is more than that for AASHTO girders. The effect of span length in distribution factors of bulb-Tee girder requires more studies including field test data to quantify its importance.

ix) The girder stiffness effect was insignificant in bulb-Tee flexural load distribution.

x) For Manatee county bridge, the measured wheel load distribution factor, DF was equal to 1.29, which is higher by about 40% than the DF of 0.92 obtained from grillage analogy. This difference may be attributed to the variations in concrete strength and section modulus, which are used in calculating the measured DF. Both DFs based on AASHTO and LRFD were higher than those calculated using the measured strains and grillage analogy method. This confirms that AASHTO code and to a lesser extent, the proposed LRFD code give conservative values for wheel load distribution factor for slab-on-girder bridges.

xi) For Duval County bridge, the bending moments computed from the grillage analogy were consistent with those based on measured strains. This may be due to smaller girder spacing in the bridge than the Manatee County bridge (this bridge spacing = 5.3 ft. and Manatee County bridge = 9.25 ft.). Consequently, the DFs from measured strains and grillage analogy were very close. Both DFs calculated from grillage analogy and measured strains are smaller than those based on AASHTO and LRFD values. This again confirms that both AASHTO and the proposed LRFD codes give conservative estimates for wheel load distribution factors.

7.2.3 Double-Tee Bridges

i) The load distribution factors for the interior girders decrease with increasing span and the load distribution factors of exterior girders increase with span increase. It is clear that the load distribution factor of the exterior girders is more dependent on the span than the interior girders. This is consistent with the results of analysis of slab-on-AASHTO girders. The proposed LRFD code does not consider that exterior girders are more dependent on span length than interior girders. This observation needs further research on more double tee cross section types.

ii) The measured DF was smaller than that based on grillage analogy, LRFD and AASHTO codes.

REFERENCES

1. AASHTO," Guide Specifications for Strength Evaluation of Existing Steel and Concrete Bridges", Washington, D.C., 1989.

2. AASHTO," Manual for Maintenance Inspection of Bridges", Washington, D.C., 1982.

3. Bakht, B., and Csagoly, P.F.," Diagnostic Testing of a Bridge", Journal Structural Division, ASCE, Vol. 106, July, 1980.

4. Bakht, B., and Jaeger, L.G.," Bridge testing--A surprise every time", Journal Structural Engineering, ASCE, Vol. 116, May, 1990.

5. Bakht, B., and Jaeger, L.G. (1985), "Bridge Analysis Simplified", McGraw-Hill Book Co., New York, N.Y., 1985.

6. Bakht, B., and Moses, F., "Lateral Distribution Factors for Highway Bridges", Journal of Structural Engineering, ASCE, Vol. 114, No. 8, August, 1988.

7. Bishara, A.G, " Analysis for design of bearings at skew bridge support", Report ODOT 14346, Ohio Department Transportation, Columbus, Ohio.

8. Bishara, A.G., and Soeglarso, R.," Load Distribution in Multibeam Precast Pretopped Prestressed Bridges", Journal of Structural Engineering, ASCE, Vol. 119, No. 3, March, 1993.

9. Cope, R.J., and Clark, L.A.," Concrete Slabs: Analysis and Design", Elsevier Applied Science Publishers, 1984.

10. Darlow, M.S., and Bettigole, N.H." Instrumentation and Testing of Bridge Rehabilitated with Exodermic Deck", Journal Structural Engineering, ASCE, Vol. 115, October, 1989.

11. Ghosen, M., Moses, F., and Gogieski, J.," Structural Design of Bridges", Transportation Research Record, 1072, 1986.

12. Harrison, H.B.," Computer Methods in Structural Analysis", Prentice-Hall, 1973.

13. Hays, C. O., Sessions, L., and Berry, A.," Further Studies on Lateral Load Distribution Using a Finite Element Method", Transportation Research Record No. 1072, Structural Design of Bridges, 1986.

14. Imbsen, R.A., and Nutt, R.V.," Load Distribution Study on Highway Bridges using STRUDL F.E.A. Capabilities." Conference on Computing in Civil Engineering, ASCE, New York, N.Y.

15. Jaeger, L.G., and Bakht, B. (1982), "The grillage analogy in bridge analysis", Canadian Journal of Civil Engineering.

16. Jaeger, L.G., and Bakht, B. (1982), "Bridge Analysis by Microcomputer", McGraw-Hill Book Co., New York, N.Y., 1989.

17. Newmark, N.M. (1948)," Design of I-beam bridges", Highway Bridge Floor Symp., Journal of Structural Division, ASCE, 74(2), 141-161.

18. O'Connor, C., and Pritchard, R.W.," Impact Studies on small Composite girder Bridge", Journal Structural Engineering, ASCE, Vol. 111, March, 1985.

19. Sanders, W.W., and Elleby, H.A. (1970),"Distribution of wheel loads on highway bridges", National Co-operative Highway Research Program Report 83, Transportation Research Board, Washington, D.C.

20. Stallings, J.M. and Yoo, C.H.," Tests and Ratings of Short Span Steel Bridges", Journal of Structural Engineering, Vol. 119, No. 7, July, 1993.

21. Tarhini, K., and Frederick, G.R.,"Wheel Load Distribution in I-girder Highway Bridges", Journal of Structural Engineering, Vol.118, No. 5, May, 1992.

22. Tiedeman, J., Albrecht, P., and Cayes, L.," Behavior of Two-Span Continuous Bridge Under Truck Axle Loading", Journal of Structural Engineering, Vol. 119, No. 4, April, 1993.

23. Warren, G., and Malvar, L.J.," Lateral Distribution of Loads in One-Way Continuous Navy Pier Decks", Journal of Structural Engineering, Vol. 119, No. 8, August, 1993.

24. Zokaie, T., Imbsen, R.A., and Osterkamp, T.A., "Distribution of Wheel Loads on Highway Bridges", Transportation Research Record No. 1290, Vol. 1, Bridges and Structures, 1191.

25. Zokaie, T.," Distribution of Wheel Loads on Highway Bridges", Final Report NCHRP Project 12-26, NCHRP Research Results Digest, May 1992, No. 187.

26. Standard specification for highway bridges (1989).13th Ed., American Association of State Highway and Transportation Officials, Washington, D.C.

27. Conrad P. Heins and Richard A. Lawrie, "Design of Modern Concrete Highway Bridges", John Wiley & Sons, Inc., 1984.

28. Warren, G. and Malvar, L.J., "Lateral Distribution of Loads in One-way Continuous Navy Pier Decks", Journal of Structural Engineering, Vol. 119, No. 8, August, 1993, pp 2332-2348.

29. Westergaard, H.M., "Computation of Stresses in Bridge Slabs Due to Wheel Loads," Public Roads, March 1930.

30. "Distribution of Wheel Loads on Highway Bridges," National Cooperative Highway Research Program (NCHRP), Transportation Research Board (TRB) No. 187, May 1992, pp 1-31.

31. "Distribution of Wheel Loads on Highway Bridges," National Cooperative Highway Research Program (NCHRP), Transportation Research Board (TRB) No. 187, May 1992, pp 1-31.

32. Bakht, B. and Moses, F., "Lateral Distribution Factors for Highway Bridges", Journal of Structural Engineering, ASCE, Vol. 114, No. 8, August, 1988, pp 1785-1803.

33. Stallings, J.M. and Yoo, C.H., "Analysis of Slab-on-Girder Bridges", Computers and Structures, Vol. 45, No.5/6,1992, pp 875-880.

34. Walker, W.H., "Lateral Load Distribution in Multigirder Bridges", Engineering Journal, AISC, 24, 1987, pp 21-28.

35. Newmark, N.M., "Design of I-beam Bridges", Proceedings, ASCE, March 1948.

36. Arockiasamy, M., "Load Distribution on Highway Bridges Based on Field Test Data", Progress Report, State Job No. 99500-3512-119, March 1994.